U.PORTO

MESTRADO EM ONCOLOGIA

ONCOLOGIA LABORATORIAL

Mitochondrial Dynamics in Thyroid Cancer: Unravelling the Role of DRP1

SARA AEXANDRA DE SOUSA BARRAMBANA

M

2019

U.PORTO

Sara Sousa Barrambana. Mitochondrial Dynamics in Thyroid Cancer: Unravelling the Role of DRP1

M.ICBAS **2019**

Mitochondrial Dynamics in Thyroid Cancer: Unravelling the Role of DRP1

SARA AEXANDRA DE SOUSA BARRAMBANA

INSTITUTO DE CIÊNCIAS BIOMÉDICAS ABEL SALAZAR

Sara Alexandra de Sousa Barrambana

Mitochondrial Dynamics in Thyroid Cancer: Unravelling the Role of DRP1

Dissertação de Candidatura ao grau de Mestre em Oncologia submetida ao Instituto de Ciências Biomédicas Abel Salazar da Universidade do Porto

Orientador – Doutor Valdemar Máximo

Categoria – Professor Auxiliar

Afiliação – Faculdade de Medicina da Universidade do Porto (FMUP), Instituto de Patologia e Imunologia Molecular da Universidade do Porto (Ipatimup), Instituto de Investigação e Inovação em Saúde (i3S)

Co-orientador – Doutor Marcelo Correia

Categoria – Investigador Júnior

Afiliação – Instituto de Patologia e Imunologia Molecular da Universidade do Porto (Ipatimup), Instituto de Investigação e Inovação em Saúde (i3S)

“Rien dans la vie n’est à caindre, tout doit être compris. C’est maintenant le moment de comprendre d’avantage, afin de craindre moins.”

Marie Curie

Agradecimentos

Gostaria de começar por agradecer ao Instituto de Ciências Biomédicas Abel Salazar (ICBAS) da Universidade do Porto e ao Instituto Português de Oncologia do Porto (IPOP) por me terem recebido como aluna e por unirem a investigação à clínica, permitindo que cada aluno compreenda o impacto que o seu trabalho pode ter em cada pessoa. Ao IPATIMUP/I3S, por criarem investigação de excelência e por defenderem a investigação e os investigadores.

Agradeço à Doutora Paula Soares por me ter aceite no grupo e por reconhecer o trabalho de todos os seus alunos. Ao meu orientador, o Doutor Valdemar Máximo, agradeço por me ter aceite para trabalhar com ele, por me ter oferecido a oportunidade de integrar este projeto e por permitir que o projeto fosse também meu, focando-se acima de tudo no meu crescimento. A todo o grupo, Cancer Signaling and Metabolism, agradeço por me ensinarem, corrigirem e motivarem. Agradeço, sobretudo, à Raquel Lima e à Ana Pestana que estiveram por perto sempre que precisei e à Rita Lima por trabalhar lado a lado comigo.

Marcelo… Acredito que neste momento já me conheces bastante bem... Como tal, sabes que te sou eternamente grata. Ninguém perdeu o controlo e a paciência não se esgotou, apesar de as bobagens serem incontáveis. Serás sempre uma referência para mim. Foste meu co-orientador e, em muitos momentos, meu amigo. Acreditaste em mim e fizeste com que eu acreditasse também! Obrigada!

Ao meu gang Ana Júlia, Mary Jane, Bela, Ana Riquinha e Mila todos os momentos com vocês foram únicos e repletos de alegria. Nem acredito na sorte que tive em vos encontrar. Obrigada por cada abraço e por cada gargalhada!

Rita, Márcia, Silvana e Rute, a minha "Oncoteam", a minha família no Norte, fizeram com que me sentisse em casa desde o primeiro dia, foram o meu abrigo em muitos momentos, sem vocês nada faria sentido. Obrigada por serem amigas incríveis!

Madeirense, eu sei que foste para o laboratório ao lado só para ficares por perto… Obrigada por dramatizares e desdramatizares comigo, por tudo o que nos rimos e pelo que ainda havemos de nos rir!

A todos os meus amigos de Évora… Obrigada por me confortarem à distância, só amigos tão únicos como vocês sabem como fazê-lo!

Por fim, quero agradecer a toda a minha família a quem devo todas as minhas conquistas, vocês são o meu apoio incondicional e a minha fonte de amor e inspiração! Obrigada tia Mali e tio Luís por todo o carinho. Obrigada Ana e Nuno por todos os conselhos a horas tardias que fazem com que seja realista e perca o medo. Obrigada Sónia e Miguel por me inspirarem. Meus bebés, Afonso, Inês, Rodrigo e Carolina os vossos abraços e brincadeiras, a vossa genuinidade, são a minha alegria…

Paulo, quando penso no significado de família penso em ti, obrigada por me ofereceres o mundo!

Mãe, pai, eu sei que as minhas aventuras são mais difíceis para vocês do que para mim. Obrigada por sentirem cada frustração, cada preocupação, cada conquista e cada sorriso como se fosse vosso… Obrigada sonharem comigo! Mana, estamos juntas em tudo, sempre. Obrigada por esse olhar sempre atento e cauteloso!

Avó, foi contigo que aprendi que o impossível também é possível! Quero dedicar-te esta conquista por nunca desistires! A ti, agradeço todo o amor e toda a felicidade! Sempre que puder, irei a correr para os teus braços! Adoro-te!

Abstract

Cancer cells prefer to metabolise glucose by glycolysis instead of OXPHOS, even in the presence of O_2. Mitochondria produce energy through OXPHOS and adapt their structure and function by mitochondrial fission and fusion. Mitochondrial fission provides an adequate number of mitochondria to support growing and dividing cells, DRP1 is the mitochondrial fission key component. Our group demonstrated that DRP1 is overexpressed in Hürthle cell tumours.

MAPK signalling is frequently activated in thyroid cancer, BRAF (one main protein of MAPK signalling) was related with higher expression of DRP1 in melanoma – suggesting a synergistic effect of both pathways.

We aim to assess the functional relevance of DRP1 and to understand the interaction between mitochondrial fission and MAPK signalling, in thyroid cancer.

We assessed the effects of Mitochondrial division related protein 1 inhibitor (Mdivi-1) and Dabrafenib - BRAF inhibitor – on cell viability (Presto Blue and SRB assay), apoptosis (Annexin V/PI staining) and cell cycle (PI DNA staining) in four thyroid cancer cell lines – TPC1, C643, 8505C and XTC-1. Moreover, we evaluated their effects on downstream signalling targets through Western Blot and RQ-PCR. Colony assay formation has, also, been performed.

Our results show that Mdivi-1 decreases cell viability and cell proliferation, as well as cells colonic potential, in all cell lines. Also, the DRP1 inhibitor induces cells to death. The drug increases the number cells in G1. Mdivi-1 effect is dose-dependent, but it is not time-dependent. and is verified in all cell lines, except in the oncocytic cell line XTC-1. Dabrafenib, in its turn, has an effect in cell viability that is not dose-dependent, except for TPC1 cell line, but it is time-dependent. The BRAF inhibitor induces cell death, however its effect is less accentuated. Dabrafenib increases the number of cells in G1 and decreases the number of cells in G2. The combined treatment seems to have a synergistic effect on cells colonic potential and cell death. In 8505C cell line, Mdivi-1 and Dabrafenib decrease the proteins expression. In XTC-1 cell line, Dabrafenib seems to increase TSHR and NIS mRNA expression.

Concluding, mitochondrial dynamics and DRP1 are relevant for thyroid cancer. Moreover, DRP1 interacts with signaling pathways, as MAPK pathway, altering the behavior of cancer cells. Mdivi-1 and Dabrafenib are promisor drugs as

a complement treatment to the conventional treatments of thyroid cancer, especially for oncocytomas.

Keywords: mitochondrial fission, DRP1, thyroid cancer, oncocytomas, MAPK signaling, BRAF

Resumo

As mitocôndrias, através do sistema de fosforilação oxidativa, dependente de oxigénio, produzem a maior parte da energia das células. Assim, as mitocôndrias adaptam a sua função e estrutura, com a cooperação de proteínas reguladoras dos processos de divisão e fusão mitocondriais, de forma a suprir as necessidades energéticas da célula e a manter a homeostasia celular. Porém, as células cancerígenas obtêm a maior parte da energia de que necessitam pela metabolização da glucose através da glicólise, mesmo na presença de oxigénio. O nosso grupo demonstrou que a proteína DRP1 – responsável pela divisão mitocondrial - se encontra sobre expressa em tumores oncocíticos da tiróide.

A via de sinalização MAPK encontra-se frequentemente ativa em tumores, e a ativação da proteína BRAF (pertencente a esta via) está relacionada com a sobre expressão da DRP1 em melanoma, sugerindo um efeito sinergético das duas vias.

O objetivo deste projeto é compreender a relevância funcional da proteína DRP1 e a interação entre a divisão mitocondrial e a via de sinalização MAPK no cancro da tiróide.

Para tal, foram estudados os efeitos de dois fármacos – um inibidor da proteína DRP1 (Mdivi-1) e um inibidor da proteína BRAF (Dabrafenib) – na viabilidade, crescimento, divisão e apoptose celulares em quatro linhas celulares – TPC1, C643, 8505C e XTC-1 - de cancro da tiróide. Os efeitos dos fármacos em alvos moleculares relevantes foram, também, avaliados através das técnicas de *Western Blot* e *RQ-PCR*. Finalmente, foi estudada a capacidade para as células formarem colónias.

Os resultados demonstram que o Mdivi-1 diminui a viabilidade e proliferação celulares, bem como a capacidade de formação de colónias e aumenta o número de células em apoptose. Este efeito depende da dose, mas não do tempo de exposição à droga, e é verificado em todas as linhas celulares, exceto na linha celular oncocítica, XTC-1. Já o Dabrafenib, tem um efeito na viabilidade celular que parece não depender da dose, exceto para a linha celular TPC1, mas que depende do tempo de exposição, diminuindo a proliferação celular e aumentando o número de células apoptóticas, sendo o efeito menor que o do Mdivi-1. O tratamento simultâneo com os dois fármacos tem um efeito sinergético. Na linha celular 8505C, o Mdivi-1 e o Dabrafenib diminuem a expressão de proteínas. Na linha celular XTC-1, o Mdivi-1 e o Dabrafenib aumentam a expressão do mRNA TSHR e NIS.

O Mdivi-1 parece ter efeito sobre as capacidades de proliferação, colonização e sobrevivência das células de cancro da tiróide, demonstrando a relevância da dinâmica mitocondrial e da proteína DRP1 na doença. A proteína DRP1 interage com vias de sinalização, o que influencia o comportamento das células cancerígenas. O Mdivi-1 e o Dabrafenib poderão ser usados como terapia adicional às terapias convencionais de cancro da tiróide, sobretudo no tratamento de oncocitomas.

Palavras-chave: divisão mitocondrial, DRP1, cancro da tiróide, oncocitomas, sinalização MAPK, BRAF

List of Contents

List of Tables

List of Figures

List of Abbreviations

AKT: Akt serine/threonine kinase

ATC: anaplastic thyroid cancer

ATP: adenosine-5'-triphosphate

BAK: bcl-2 homologous antagonist killer

BAX: bcl-2-associated X protein

BRAF: B-type Raf kinase

Ca^{2+}: calcium

CAMK-α: Ca^{2+} calmodulin depend protein kinase

CCDC6: coiled-coil domain-containing 6

cDNA: complementary deoxyribonucleic acid

CH_3OH: methanol

Ci: Curie

COI: cytochrome c oxidase subunit I

CO_2: carbon dioxide

CytB: cytochrome B

CytC: cytochrome C

dH_20: destilated water

DMEM: Dulbecco's modified Eagle's medium

DNA: deoxyribonucleic acid

DRP1: dynamin-related protein 1

EBRT: external beam radiotherapy

EMT: epithelial-mesenchymal transition

ER: endoplasmic reticulum

ERK: extracellular regulated kinase

FBS: fetal bovine serum

FIS1: mitochondrial fission 1 protein

FNA: fine needle aspiration

FOXO: forkhead box 3

FTC: follicular thyroid cancer

GDAP: ganglioside-induced differentiation associated protein

GSK3β: glycogen synthase 3β

GTP: guanosine-5´-triphosphate

Gy: gray

HCT: Hürthle cell tumour

HIF: hypoxia-inducible factor

^{131}I: iodine-131

IARC: international agency for research on cancer

IMM: inner mitochondrial membrane

IMS: intermembrane space

l: long

LB: loading buffer

MARCH5: membrane associated ring-CH-type finger 5

MAPK: mitogen-activated protein kinase

MCU: mitochondrial calcium uniporter

Mdivi-1: mitochondrial division inhibitor-1

MEK: mitogen-activated protein kinase

MFF: mitochondrial fission factor

MFN: mitofusin

MiD49: mitochondrial dynamics protein of 49kDa

MTC: medullary thyroid cancer

mtDNA: mitochondrial DNA

mTOR: mammalian target of rapamycin

MTP18: mitochondrial protein 18kDa

Myc: MYC proto-oncogene

NADH: nicotinamide adenine nucleotide

NADPH: adenine dinucleotide phosphate

NCO4: non-crossover 4

ND1: ubiquinone oxireductase chain 1

NIS: sodium iodide symporter

O_2: oxygen

OCT4: octamer-binding transcription factor 4

OMM: outer mitochondrial membrane

OPA1: OPA1 mitochondrial dynamin like GTPase

OXPHOS: oxidative phosphorylation

p53: tumour protein p53

PAGE: polyacrylamide gel electrophoresis

PB: presto blue

PBS: phosphate buffered saline

PI: propidium iodine

PI3K: phosphoinositide 3-kinase

PIK3CA: phosphatidylinositol-4,5-bisphosphate 3-kinase catalytic subunit alpha

PKA: protein kinase A

PKC: protein kinase C

PTC: papillary thyroid cancer

PTEN: phosphatidylinositol-3,4,5-triphosphate 3-phosphatase

RAS: rat sarcoma virus

RET: ret proto-oncogene

RET/PTC: ret proto-oncogene rearrangement

RIPA: reagent-based cell lysis using radioimmunoprecipitation

ROCK: rho-associated coiled coil kinase

ROS: reactive oxygen species

RPMI: Roswell Park Memorial Institute

RQ-PCR: real-time quantitative polymerase chain reaction

s: short

SD: standard deviation

SDS: sodium dodecyl sulfate

Ser: serine residues

SRB: sulforhodamine b

T_3: triiodothyronine

T_4: thyroxine

TBS-T: tris-buffered saline - Tween

TC: thyroid cancer

TKI: tyrosine kinase inhibitor

TSH: thyroid stimulating hormone

TSHR: thyroid stimulating hormone receptor

Chapter 1: Introduction

The thyroid gland is in the front side of the neck below the thyroid cartilage. The endocrine gland has a butterfly shape, comprising two lobes – the left lobe and the right lobe - united by a narrow isthmus. Histologically, the endocrine gland is constituted by two main types of parenchymal cells: follicular cells, which concentrate iodine and produce thyroid hormones (triiodothyronine - T_3 - and thyroxine - T_4); and parafollicular or C cells, which produce the hormone calcitonin[1]. The hormones produced by thyroid cells play relevant roles in human homeostasis. T_3 and T_4 hormones are regulators of metabolic processes crucial for normal growth and development along with regulation of metabolism in adults[2], while calcitonin is a regulator of calcium homeostasis.

Cancer is anticipated as the major cause of mortality and the barrier to increase life expectancy in the world in the 21st century[3], requiring great attention. Thyroid cancer (TC) is distinct from every other endocrine malignancy since among these malignancies TC has the highest incidence around the world. Thyroid cells can be the origin of various types of thyroid cancer: follicular cells are the origin of well differentiated thyroid cancer, which includes papillary thyroid cancer (PTC), follicular thyroid cancer (FTC) and Hürthle cell tumour (HCT), and of undifferentiated or anaplastic thyroid cancer (ATC), whereas parafollicular neuroendocrine cells give rise to medullary thyroid cancer (MTC)[1,4].

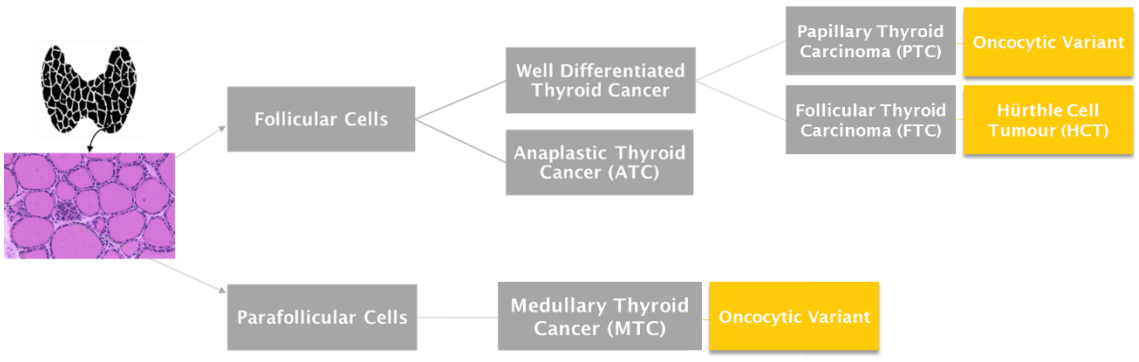

Figure 1: Thyroid cancer origin and principal histotypes scheme.

1.1 Epidemiology and Risk Factors

Cancer incidence and mortality are rapidly increasing around the world, reflecting the population growth and aging[5]. As documented by the International Agency for Research on Cancer (IARC) in 2019, cancer accounted with 18.078.957 new cases and 9.555.027 deaths worldwide in 2018, 4.229.662 (23,4%) of new cases and 1.943.478 (20,3%) of deaths occurred in Europe. Also, IARC estimated that in 2030 will be diagnosed 24.112.118 new cases and will occur 13.027.021 deaths as a result of disease around the world. During the same year, all the malignancies accounted with 58.199 new cases and 28.960 deaths, in Portugal. It is estimated that in 2030 will be diagnosed 65.356 new cases and will occur 33.935 deaths due to the disease in the country.

Thyroid cancer ranks in ninth place for cancer incidence accounting for 567.233 new cases worldwide in 2018, 1701 (2.9%) of new cases occurred in Portugal. Beyond, TC incidence is rapidly increasing. Even though most of diagnosed TCs are small PTCs, increased incidence has been observed for different tumour sizes and stages in both genders and in various ethnic groups[6]. IARC predicts that in 2030 will be diagnosed 112.882 new cases with 15.663 deaths as result of disease. The large difference between incidence and mortality demonstrates the indolent nature of this endocrine malignancy. Well-differentiated TC is the most recurrent form; PTC represents most of the cases, MTC is less common and ATC is a rare form of disease. The great number of PTC cases may be due the increase of diagnosis through detection and diagnostic improvement and perhaps through modifications in the prevalence of risk factors[7].

The principal risk factors related with thyroid cancer include ionizing radiation exposure, age and female sex[8,9]. TC is also connected to other risk factors predominantly physiological and lifestyle risk factors, as iodine intake, thyroid stimulating hormone (TSH) dysregulation, obesity and environmental pollutants[10,11].

Ionizing radiations are carcinogens that induce deoxyribonucleic acid (DNA) damage directly or through reactive oxygen species (ROS) production. Thyroid is more irradiated than other organs and tissues due to its location in the body and to its capacity to accumulate iodine[8]. In addition, the endocrine gland is more radiosensitive at early ages, children exposed to ionizing radiation commonly tend to develop PTC, the most common histotype diagnosed after radiation exposure, as seen after the Chernobyl accident when great amounts of iodine were released in the atmosphere inducing a peak of PTC cases during childhood[12]. The risk for

developing thyroid cancer after radiation exposure is also influenced by radiation doses, increasing to doses higher than 0.5-1 Gy[13].

According to IARC the global incidence of thyroid cancer in females is three times higher than in males. The less aggressive histotypes of TC – well differentiated - are more frequent in women, while the most aggressive histotypes have similar incidence in both sexes. Besides, women are diagnosed at earlier ages than men, still men reveal more aggressive disease at diagnosis. In parallel with that, men have a lower free-disease survival and a higher rate for mortility[14].

As recognised lifestyle affects cancer risk; and nutrition is a central risk factor for cancer development. Iodine intake is recognised as an influencer of thyroid cancer, but it influences the histotype rather than the incidence. In an iodine deficit diet, the capacity of thyroid gland to uptake radioactive iodine is higher, - resulting in higher radiation doses absorbed by the endocrine gland[13]. It may cause an increase of TSH - being responsible for the development of follicular carcinomas[15]. High serum TSH levels are especially associated with FTC in advanced stages[16]. On contrary, iodine excess is related with a risen risk of PTC[17]. Besides iodine, nutrients and nutrition factors that affect iodine organification can also function as thyroid carcinogens[10]. As a part of lifestyle studies, a strong relation between obesity and the risk of develop cancer and between obesity and cancer related death has been shown for various malignancies[18]. Insulin is a stimulator of thyrocyte proliferation and an expression regulator of thyroid genes expression, also the insulin resistance and hyperinsulinemia (characteristic of obesity) might be a risk factor for thyroid cancer instead of the metabolic imbalance found in obesity[19].

1.2 Diagnosis

Thyroid cancer diagnosis begins with physical examination of the neck. Additional exams are performed to define the benign or malign nature of the lesions and to evaluate the disease progress. High-resolution ultrasonography is an advantageous assistant approach to the physical examination, it allows the acquisition of images of the thyroid gland and of its nodules, the recognition of numerous nodules that would not be detected through palpation and the evaluation of suspicious cervical lymph nodes[20] for evaluation of both central and lateral lymph nodes for metastases. This exam also assists in the performance of fine needle aspiration (FNA)[20]. FNA allows the access to thyroid nodules and its

pathological evaluation. Besides FNA, laryngoscopy is relevant for assessment of thyroid nodules and for preoperative evaluation[21].

In addition, serum TSH level should be measured in order to identify underlying thyroid dysfunction[21] and serum calcitonin measurement must also be verified when MTC is suspected in nodules detection[20].

The use of molecular markers in diagnosis, including B-type Raf kinase (BRAF) and rat sarcoma virus (RAS) mutational analysis and, in a reduced extent, ret proto-oncogene rearrangement (RET/PTC), is being considered to better discriminate TC histotypes[22,23]. Currently, patients with familial MTC who are under surveillance can be identified with molecular analysis by detection of RET gene mutation[20].

1.3 Prognosis

Well-differentiated thyroid cancer is related with a long-term survival, being one of the least morbid solid carcinomas. Yet, a minor part of patients with PTC (1-6.5%) and patients with ample FTC vascular invasion die from disease-related causes[1]. Inversely to well differentiated thyroid cancer, anaplastic thyroid cancer is aggressive and is between the most deadly malignancies[1], accounting for a mortality rate higher than 90%.

Besides their role as molecular markers for diagnosis, various molecular modifications have been considered as prognostic markers in TC. Genes involved in the mitogen-activated protein kinase (MAPK) pathway are relevant, especially BRAF. Mutations in BRAF were associated, in various researches, with an increased possibility of extrathyroidal extension, lymph node metastasis, recurrence and mortality[24,25].

1.4 Treatment

1.4.1 Surgery

Surgery is always considered as treatment for thyroid cancer, but there is a controversy on how extensive a resection should be. Most surgeons defend total thyroidectomy over thyroid lobectomy[26]. Thyroidectomy is related with lower recurrence and improved survival; while thyroid lobectomy reduces the risk of increased morbidity. In some cases, especially for advanced primary tumours, it is also suggested prophylactic central-compartment neck dissection during the surgery[21,27].

1.4.2 Radioiodine Therapy

Follicular cells from thyroid gland incorporate and organify iodine in their physiological functions. For this reason, radioiodine therapy is often used in patients with well-differentiated thyroid cancer in postoperative condition in order to extinguish remaining carcinogenic thyroid tissue, avoid regional recurrence and ease surveillance with stimulated thyroglobulin measurements and whole-body iodine images. Numerous studies report declines in recurrence and mortality after iodine-131 (^{131}I) treatment[21,28], mainly in patients with big tumours (>1,5 cm), multifocality, residual disease, nodules metastasis, vascular invasion and intermediate differentiated histology[21]. However, other studies don't find this relation, especially in low-risk patients[28]. It is difficult to decide which doses of ^{131}I should be administered to patients since these doses aren't well defined. Low doses, with less than 30mCi are regularly administered on younger low-risk patients, while higher doses between 100mCi and 200mCi are applied on older high-risk patients, specifically patients with an insufficient resection of the primary tumour, aggressive primary tumour, tumours with intermediately differentiation and/or metastases[29,30].

1.4.3 External Beam Radiotherapy (EBRT), Chemotherapy

External beam radiotherapy (EBRT) and chemotherapy effect in thyroid cancer is restricted. EBRT is only performed in cases of unresectable large disease, metastases in dangerous sites that possibly will result in fracture and neurological or compressive symptoms and painful bone metastases[1]. The chemotherapeutic agent most frequently used in TC is doxorubicin (Adriamycin). Doxorubicin and cisplatin combination therapy has not demonstrated better results than single-agent therapy and gets worse toxicity. However, doxorubicin and platinum combination appears to be more effective in anaplastic thyroid cancer than doxorubicin alone[1]. Hyper fractionated radiation treatments are applied in combination with doxorubicin for unresectable disease, which is not responsive to radioiodine therapy[21].

Furthermore, new therapies are under studies. Some clinical trials are focusing on various tyrosine kinase inhibitors (TKIs), whereas others focus on inhibition of TC related molecules.

1.5 Thyroid Oncocytomas

Oncocytomas are tumours identified by cells with a huge quantity of abnormal and unfunctional mitochondria in their cytosol, regardless the benign or malignant nature of the neoplastic lesions[31]. Histopathologically, the oncocytic tumours are recognised by cells with an eosinophilic and granular cytosol, huge nuclei and protuberant nucleoli[31–33]. Oncocytomas rarely occur in most human organs, but they frequently occur in endocrine organs[33]. These tumours can be mentioned as oncocytic, oxyphilic or eosinophilic tumours. Hürthle cell tumours arise from follicular neoplasms, these tumours are commonly encapsulated and consist of a great number of oncocytic cells. Further, thyroid cancer histotypes can, also, present oncocytic variants[34]. Nevertheless, the classical therapy for TC, the radioactive iodine therapy, is often ineffective in some oncocytomas, because these tumours have less (or even lack) competence to incorporate iodine.

In oncocytic cells, the ample number of mitochondria in the cytoplasm can be observed through all the tumour (denominated "primary" oxyphilia – indicates that the carcinoma hit happened in cells that already possess mitochondrial anomalies) or in a few parts of the tumour (denominated "secondary" oxyphilia – indicates that the mitochondrial anomalies happened following the tumour initiation process)[31]. The accumulation of 20 to 50-fold more mitochondria in each oncocytic cell suggests[33,35] that this transformation can occur especially in tissues with minimal proliferative rate and decreased turnover, in reliable cells with an extended intermitotic interval[31,36]. However, the mechanisms regarding cell transformation to the oncocytic phenotype still debatable.

Oncocytic cells have reduced oxidative phosphorylation (OXPHOS) activity, which can send signals to cells to proceed into a compensation mechanism of mitochondrial super production to compensate energy deficits[37]. Probably, cellular OXPHOS activity of the new organelles is not enough to recover energy deficits, and oncocytic cells are forced to alter their metabolism to a distinct metabolic pathway for energy production to compensate the OXPHOS dysfunction[38–40]. Also, in oncocytomas the decreased recycling of abnormal organelles (autophagy) and a singular defect in mitochondria renewal (mitophagy) may concurrently occur and favour cytoplasmic mitochondrial accumulation[41,42]. The influence of each of the referred mechanism to oncocytic transformation differs in agreement with the accuracy of the carcinogenic hit and the microenvironment that involves the tumour.

Frequently, oncocytomas accumulate various mutations in genes encoding OXPHOS subunits, especially genes encoded in the mitochondrial DNA (mtDNA). mtDNA encoding complex I subunit of OXPHOS system are the most affected[43]. The high incidence of these mutations may contribute for the functional alterations observed[42–46].

Accounting for the benign nature of most oncocytic tumours, the referred modifications may be the reason for low progression and invasiveness of oncocytic tumours and may influence various cellular functions sustained by mitochondria as energy production, calcium homeostasis, macromolecule synthesis and apoptosis limiting the tumourigenic potential[44]. The particular features of oncocytomas turn them a proper model for experiments aiming to comprehend the influence of the metabolism and mitochondria in carcinogenesis.

1.6 Cellular Signalling Pathways and Thyroid Cancer

Thyroid cancer generally harbours mutations along the mitogen-activated protein kinase (MAPK) and the phosphoinositide 3-kinase (PI3K) cellular signalling pathways. MAPK pathway sends growth signals from the plasma membrane to the nucleus, modulating cell survival, differentiation and proliferation [47,48]. PI3K pathway phosphorylates various intermediates like mammalian target of rapamycin (mTOR) and forkhead box O3 (FOXO), also controlling key cellular functions as cell survival and proliferation, and protein synthesis. Mutations and genomic rearrangements involving B type Raf kinase (BRAF), rat sarcoma virus (RAS) and Ret proto-oncogene (RET) - all members of the MAPK signalling cascade – are identified in thyroid cancer as well as mutations in phosphatidylinositol-3,4,5-triphosphate 3-phosphatase (PTEN) and Akt serine/threonine kinase (AKT). The identification of these genomic alterations can be relevant for clinical management, since they can be responsible for tumour behaviour and alter responses to treatment[48].

The most common mutations found in PTC are those involving BRAF and RET. Anaplastic thyroid cancer can also be characterized by BRAF mutations. Whereas, FTC most frequent mutations are those in RAS family of oncogenes[49] and, in a smaller percentage, in the tumour suppressor gene PTEN. Medullary thyroid cancer is often related with mutations in RET, which can occur sporadically or in germline with an autosomal dominant inheritance. In MTC also occur initiating mutations in RAS[50–54].

1.6.1 B Type Raf Kinase (BRAF)

BRAF belongs to a short family of RAF proteins and functions as a cytoplasmatic threonine protein kinase in the MAPK cascade. Normally, RAS is responsible for BRAF activation[55]. When activated BRAF phosphorylates and, therefore, activates mitogen-activated protein kinases (MEK), it transduces mitogenic signals to downstream proteins as extracellular regulated kinases (ERK). BRAF gene mutations are regularly found in TC, resulting in unregulated kinase activity and increased stimulation of MAPK pathway[56]. The most common mutation in BRAF in TC is a missense mutation, with a transversion from thymine to adenine at the 1799 nucleotide position conducts to a valine to glutamate replacement at the 600 amino acid position ($BRAF^{T1799A}$ to $BRAF^{V600E}$). This mutation constitutively activates BRAF, that remains independent from RAS, and in its turn constitutively activates MEK and ERK[56,57].

BRAF mutations have been related to the aggressiveness of PTC. Numerous studies found association between BRAF mutations and tumour volume, extrathyroidal invasiveness, advanced stage at diagnosis, lymph node metastasization and risk of recurrence[58–64]. In addition, tumours harbouring BRAF mutations have a decreased responsiveness to radioiodine therapy, which limits the treatment options[64]. The responsiveness of BRAF-mutated PTCs is related with a reduced activity of proteins that participate in the incorporation and organification of iodide, for instance sodium iodide symporter (NIS), demanding a superior number of radioiodine therapy sessions and superior exposure of radioiodine refractory incidence to reach disease free status[58,65–67]. Reactivation of radioiodine activity is relevant to therapy effectiveness. It was demonstrated that BRAF and its downstream effector – MEK - inhibitors can increase NIS activity in pre-clinical models[66,68,69].

1.6.2 Rat Sarcoma Virus (RAS)

RAS proteins – that include H-RAS, N-RAS and K-RAS – are short guanosine-5´-triphosphatases (GTPases) responsible for the activation of relevant pathways, including MAPK and PI3K signalling pathways. RAS occurs in an active or inactive form reliant on a GTP-bound and, - normally its activation is promoted by exterior signals, especially signals from tyrosine kinase receptor on the cell surface. RAS constitutively activating mutations are possibly the most frequent mutations in thyroid cancer, especially mutations in N-RAS codon 61 and in H-RAS codon 61[70–72].

1.6.3 Ret Proto-Oncogene (RET)

RET is a tyrosine kinase receptor on the cell membrane that transmits signals to RAS and to the downstream proteins belonging to MAPK pathway[73]. The RET alterations found in thyroid cancer are mostly genetic rearrangements originating chimeric proteins. RET is not normally present in follicular cells, however the juxtaposition of the RET 3' kinase domain to a 5' partner and the corresponding promotor conducts to fusion oncoprotein expression and abnormal kinase activation, with downstream activity of the MAPK pathway[74,75]. RET has many fusion partners described, however the most frequent are coiled-coil domain-containing 6 (CCDC6) and non-crossover 4 (NCO4)[48,76], these fusion partners are able to constitutive dimerization, that ends in constitutive RET activation through self-phosphorylation.

1.6.4 Phosphatidylinositol-3,4,5-triphosphate 3-phosphatase (PTEN)/Akt serine/threonine kinase (AKT)

PTEN is a phosphatase that acts as an inhibitor of PI3K. Stimulated PI3K activates AKT through phosphorylation. AKT activation in cancer may be due to mutations in PTEN or to mutations in AKT itself[77,78]. Genetic alterations in PI3K and in AKT are commonly found in FTC and in ATC. Activating mutations, including amplification, in exons 9 and 20 of gene encoding for the subunit phosphatidylinositol-4,5-bisphosphate 3-kinase catalytic subunit alpha (PIK3CA) were reported in numerous cases of TC[79].

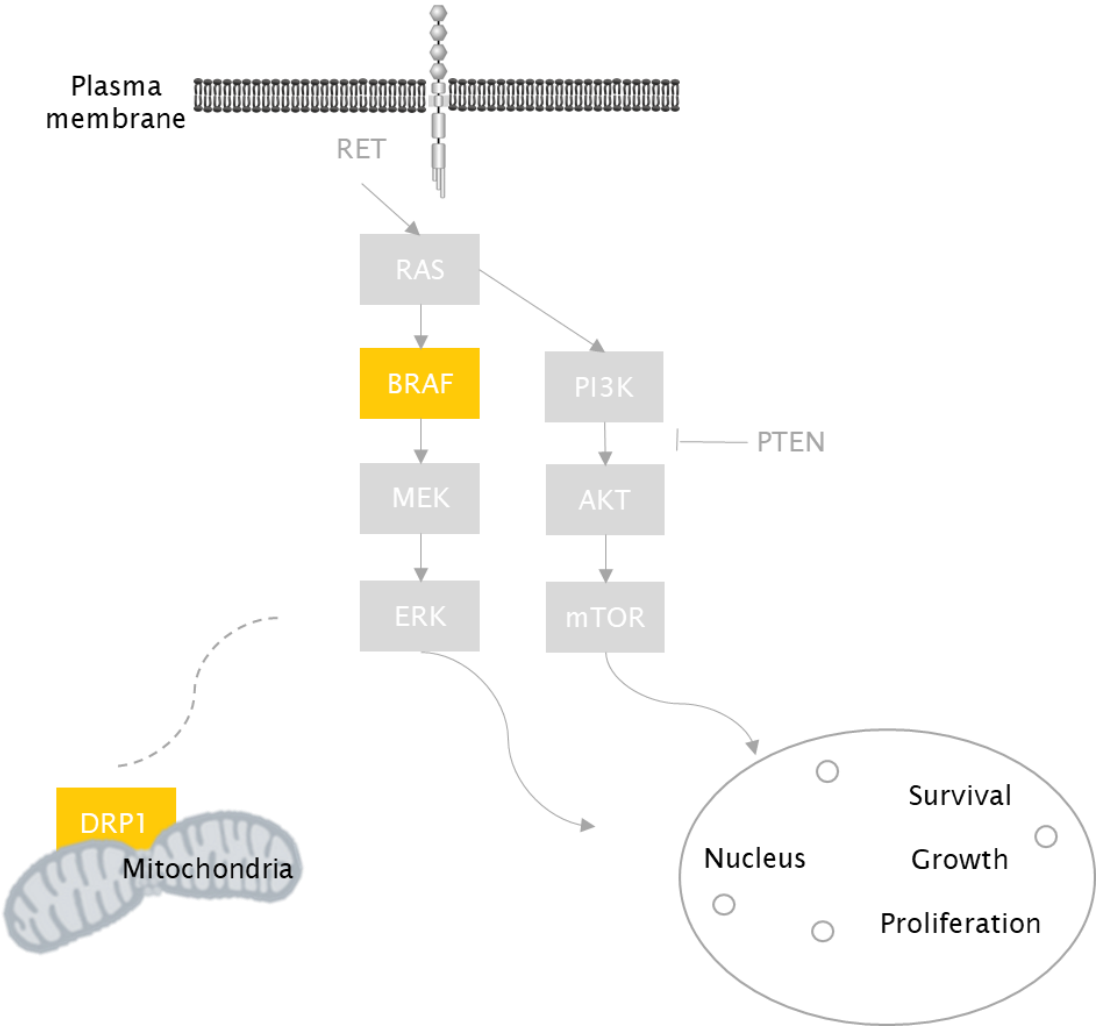

Figure 2: Thyroid cancer signalling pathways interaction and connection to DRP1.

Ret proto-oncogene (RET), rat sarcoma virus (RAS), B type Raf kinase (BRAF), mitogen-activated protein kinases (MEK), extracellular regulated kinases (ERK), phosphoinositide 3-kinase (PI3K), phosphatidylinositol-3,4,5-triphosphate 3-phosphatase (PTEN), Akt serine/threonine kinase (AKT), mammalian target of rapamycin (mTOR), dynamin-related protein 1 (DRP1).

1.7 Mitochondria

Cancer is a strongly structured, invasive, and progressive clone with origin in our tissues. It is indispensable to comprehend the cellular and molecular dynamics of cancer, to do so it is required to complement genomic and epigenomic evidence with metabolic knowledge. As Otto Warburg declared, carcinogenic agents and mutations could not sustain cancer cell transformation unless the metabolism was also modified[80]. One of the most relevant features of cancer from metabolism perspective is the excessive production of lactic acid as a result of glycolysis[80,81]. Warburg also hypothesized that tumour cells obtain their energy by fermentation instead by respiration, and damages on respiration are permanent once it never returns to normal and go on through all the subsequent divisions[80].

However, such damage on respiration is not deleterious enough to induce death in cancer cells[82,83].

Mitochondria are double-membrane dynamic organelles with their individual genome- the mitochondrial DNA (mtDNA). Even so, mitochondria are partially autonomous organelles relying on nuclear genome and not only on their own genome. The outer mitochondrial membrane (OMM) interacts with cytosol, while the inner mitochondrial membrane (IMM) projects into mitochondria matrix, and the space surrounded by the OMM and the IMM is known as intermembrane space (IMS). Mitochondria cannot be formed *de novo*; their proliferation depends on growth and division of already present organelles[84]. One somatic cell can comprehend from 200 to 2000 mitochondria; this quantity relies on the cell energy requirements[45]. Mitochondria have distinct morphological and functional purposes in a cell as cell energy production trough oxidative phosphorylation, maintenance of molecular homeostasis, reactive oxygen species (ROS) production and activation of intrinsic apoptotic cascade; but typically are known by their fundamental role in cellular metabolism[85]. Mitochondria fulfil the cell energetic requirements by adenosine-5'-triphosphate (ATP) production through an electron transport chain on their IMM - the oxidative OXPHOS system - to generate a proton gradient used in ATP synthesis in an oxygen-dependent manner[86,87], being considered the major converters of ATP and nicotinamide adenine dinucleotide phosphate (NADPH). To realize their purposes mitochondria, migrate through the cytoskeleton, through microtubules, gathering at locations where energy is required[88]. ATP production can also occur in the cytoplasm via glycolysis, in its turn in an oxygen-independent manner. Nevertheless, OXPHOS has a higher rate of production than glycolysis per glucose consumed, so usually cells prefer this via to obtain energy when there is enough oxygen (O_2). In normal cells, there is a swipe from OXPHOS to glycolysis, every time that O_2 levels reduce (Pasteur effect). However, Warburg hypothesized that cancer cells convert glucose through glycolysis, instead of OXPHOS even if there is enough O_2. The phenomenon is probably due to permanent damages of OXPHOS system in cancer cells and is referred as Warburg effect[80]. If energy production by OXPHOS is not available, glycolysis is the alternative process to produce ATP. Two main consequences of this metabolic shift create an advantageous environment for tumour cells: (1) excessive production of lactic acid and tissues acidification inducing damage to surrounding non-carcinogenic cells, and (2) growth and survival not depending on O_2 presence. Even though glycolysis

is considered a hallmark of cancer, the origin and the connection with cancer establishment and development are not clearly understood.

Furthermore, mitochondria may play a role as regulators of metabolism homeostasis, regulating the quantities of intracellular molecules[89]. One aptitude of mitochondria is calcium (Ca^{2+}) buffer role between the endoplasmic reticulum (ER) and the IMM over one mitochondrial calcium uniporter (MCU)[90,91]. Mitochondrial Ca^{2+} concentrations in their matrix are demanded for sustain ATP production[92].

An additional feature of these organelles is the production of reactive oxygen species (ROS) as products of respiration through oxidative phosphorylation, ROS in its turn can function as signalling molecules. However, they induce toxicity when produced in excess under pathological conditions.

Mitochondria are players in signalling pathways and consequently in cellular functions. For instance, mitochondria inhibit autophagy via MAPK signalling pathway suppression[93] and interfere in the intrinsic apoptotic cascade, that is stimulated in response to various stress signals. The activation of the intrinsic apoptotic pathway conducts to mitochondrial membrane permeabilization, cytochrome c liberation and consequent caspase activation, which ultimately leads to non-reversive cell death[94]. Because of their major functions in regulating key cellular processes, mitochondria are regularly in the turning point between survival and death.

Mitochondrial DNA mutations, deletions or impaired DNA replication are the principal origin of mitochondrial dysfunction. Even though most of the human genes are nuclear and are equally inherited from both progenitors, there is a group of genes located in the cytosol, within the mitochondria, that are entirely inherited from the mother – the ones encoded in mtDNA. In humans, the mtDNA encodes 37 genes: 2 ribosomal ribonucleic acid (RNAs), 22 transfer RNAs and 13 genes encoding for proteins belonging to OXPHOS chain - nicotinamide adenine nucleotide (NADH)- ubiquinone oxireductase chain 1 (ND1), ND2, ND3, ND4, ND4L, ND5, ND6, cytochrome B (CytB), cytochrome c oxidase subunit I (COI), COII, COIII, ATPase 6 and ATPase 8[86,87]. The mtDNA encodes proteins required for transcription at mitochondria and for respiratory activity.

The metabolic shift from OXPHOS to glycolysis characteristic of cancer cells in the presence of O_2 may be due to defects in OXPHOS. During the last 10 years, genetic studies for OXPHOS identified mutations on mtDNA encoding OXPHOS

genes in various forms of cancer[46]. Besides, it has been demonstrated that damage in OXPHOS cancer cells stimulate AKT pathway mechanism mediated by redox reactions[95]. Cancer can be promoted by mtDNA mutations that induce apoptosis inhibition[96] or influence the production of ROS , which stimulates cell proliferation[97]. The mutation rate in this molecule is 10 to 20 times higher than the one of nuclear DNA, this difference between both rates may be justified for mtDNA particularities: the polymerase γ does not replicate mtDNA with high fidelity; the clustering of ROS in the mitochondrial inner membrane (near to mitochondrial DNA) is high and induce mtDNA errors; mtDNA lacks competent repair mechanisms and lacks coating proteins similar to histones in the nucleus[87]. Besides, mutations in mtDNA, mutations in classical nuclear oncogenes and tumour suppressor genes from the nuclear DNA as Ras, MYC proto-oncogene (Myc), AKT and tumour protein p53 (p53) may also lead to metabolic modifications and stimulate glycolysis[83]. The changes in metabolism of cancer cells can be a gain for survival and growth in the tumour microenvironment, here the hypoxia-inducible factor (HIF) acts as protagonist[98]. Besides, mitochondrial dysfunction can also be a consequence of xenobiotics exposure and hostile environmental circumstances[82].

Imperfections in mitochondria, analogous to those observed in oncocytic tumours, where demonstrated to reduce energy generation and consequently reduce tumour growth[38]. In this angle, mitochondrial suppressors can be studied for tumours treatment.

Increased understanding of metabolic and mitochondrial faults in oncocytic cells will create chances to arrange unconventional therapeutic methods intending to modify mitochondrial activity and recover the susceptibility to conventional treatments.

1.8 Mitochondrial Dynamics

The dissemination of cytosol elements is mandatory for cell survival. Then mitochondrial delivery must guarantee that the organelles are spread to satisfy the energy demands[99]. Mitochondria structure and morphology varies according to the cell environment and differentiation and to cell energetic demands. The balance between mitochondria fission and fusion controls mitochondrial number, size and localization within the cytoplasm and is referred as “mitochondrial dynamics”[100]. Mitochondrial morphology in cells may differ from small spherical organelles

(related with fission) to elongated tubular organelles (related with fusion). Excessive fission and reduced fusion are distinctive in several tumours[101,102].

Mitochondrial fission provides a proper quantity of mitochondria to cells in growth and division sustain their cellular functions[103]. Mitochondrial division creates more organelles and contributes as a mechanism to control quality by targeting defective mitochondria for careful elimination through autophagy (denominated mitophagy in the particular case of mitochondria elimination)[104]. Alterations in mitochondrial dynamics (mostly mitochondrial fission) anticipate mitophagy[104]. Below stress stimuli or during the mitochondrial defects accumulation, mitochondrial fission is stimulated, and mitochondria recycling arises to eliminate the defective organelles in the cell[105,106]. Mitochondrial fission is regulated by different OMM proteins, that include mitochondrial fission 1 protein (FIS1), mitochondrial protein 18kDa (MTP18)[107], Endophilin B1[108] and ganglioside-induced differentiation associated protein (GDAP)[109], as well as some proteins that have been recently recognized, mitochondrial fission factor (MFF), mitochondrial dynamics protein of 49kDa (MiD49), and MiD51, every identified as cytoplasmatically-localized[110,111]. However, in mammals the major component of mitochondrial fission is the principal component of the dynamin family of GTPases, DRP1. Mitochondrial fission is regularly related to mitochondrial dysfunction as these morphological states prevail during high stress levels and cell death. However, it is not clear the conditions whether the mitochondrial morphology shaping proteins are indispensable for the regulation of apoptosis and how precisely mitochondria divide during cell death.

Mitochondrial dynamics is based on fusion when cell energy production rely on OXPHOS, as well as when cells are under stress stimuli, in this case the distribution of several components allow the non-dysfunctional mitochondria to compensate dysfunctional mitochondria[103]. Moreover, mitochondrial fusion is imperative for cell survival. Fusion is a requisite to ATP maximal production. As it happens in mitochondrial division, dynamin related GTPases play a major role in mitochondrial fusion. As mitochondria are organelles with two membranes, the synchronized fusion of IMM and OMM is a requisite, although the fusion of different membranes depends on distinct mechanisms. Two mitofusions, MFN1 and MFN2, fixed on OMM through transmembrane components, facilitate the fusion. For their activity, mitofusins dimerize and are transported to mitochondria, then GTPase hydrolysis permits mitochondria membrane gathering[112,113]. MFN1 and MFN2 are a

requisite for the fusion of OMM and IMM. MFN2 activity is stimulated by its brief interaction with the apoptosis related protein bcl-2-associated X protein (BAX), which varies its localization from cytoplasm to mitochondria in healthy cells[114]. MFN2 is concentrated at the mitochondria-ER contact sites (MAM), and is crucial for molecular stabilization of Ca^{2+} and lipids[115]. On the other side fusion of IMM is mediated via OPA1 mitochondrial dynamin like GTPase (OPA1). OPA1 genes goes through alternative splicing and produces short (s) and long (l) isoforms, essential to mitochondrial fusion. The l isoform is attached to IMM, its cleavage to the s isoform promotes the fusion of IMM, however the IMM fusion happens after the OMM fusion[116].

It has been reported that proteins coupled to mitochondrial fission (dynamin-related protein 1 (DRP1) and FIS1) and fusion (MFN1, MFN2 and OPA1) are overexpressed in Hürthle cell thyroid tumours, which is suggestive of dysregulation on mitochondrial dynamics[32,82,94].

During the last years, it was suggested that besides their implication in regulating the morphology of mitochondria, mitochondrial dynamics proteins also act in regulation of cell motility, migration and invasion[117,118]. Mitochondria shift to fusion reduces relocation of mitochondria and, therefore, cell migration velocity. So, wherever the mitochondria localize, the equilibrium between the two mechanisms of mitochondrial dynamics regulates the organelles distribution in cytoplasm, and shorter mitochondria move quicker through the microtubules. The understanding of mitochondrial dynamics participation in cell motility, migration and invasion may improve new therapeutic methodologies to supress cancer cell progression. To do that it is important to reveal the signalling pathways strictly related with mitochondria shape and the key molecules involved in this processes that appear in response to various physiological stimuli.

1.9 DRP1

Dynamin-related protein 1 (DRP1), belongs to the dynamin family of guanosine triphosphatases (GTPases) being the central element of mitochondrial fission course[119]. DRP1 has being associated with the development of various malignant tumours, as brain, lung, breast, skin and thyroid cancer[32,118,120–123]. Nevertheless, the cause of this relation is not completely understood, and several mechanisms were studied independently in different cancer cell models. It was reported that DRP1 alters energy production in melanoma, contributes to stemness in glioblastoma, associates with lymph node metastases in breast cancer, sustains

cell division and proliferation in lung cancer, and possesses a relation with the oncocytic phenotype in thyroid cancer[32,118,122,124,125].

DRP1 is mainly a cytoplasmic protein, but it has already been described to be present in both cytoplasm and mitochondria under basal conditions[32,118,122,124,125]. DRP1 moves to mitochondria depending on activation, such as mitochondrial membrane disconnection, where it connects to membrane receptors, namely MFF and FIS1, promoting the OMM constriction reliant on GTPase activity[88]. The protein gathers in spirals in locations where endoplasmic reticulum tubules limit mitochondria and consequently polymerize actin, conducting to mitochondrial fission.

Thus, by itself, DRP1 overexpression is not sufficient for mitochondrial fission alone, as DRP1 activity relies on its initiation through various post-translational alterations and on its transport from cytoplasm to mitochondria. The post-translational alterations account for phosphorylation, SUMOylation, ubiquitination, S-Nitrosylation and O-GlucNAcylation[126–128]. Numerous kinases are in charge of DRP1 activity via phosphorylation at three principal serine residues – Ser^{637}, Ser^{616}, and Ser^{693} [129,130]. The phosphorylation of the different serine residues happens through the activity of different protein kinases. $DRP1^{S616}$ is phosphorylated by protein kinases enrolled in signalling pathways, cell division, cell cytoskeleton and calcium signalling. These comprise protein kinase C (PKC), CDK1/Cyclin B in the perspective of mitosis, rho-associated coiled coil kinase (ROCK) or Ca^{2+} calmodulin depend protein kinase (CAMK-α) promoting fission[129–131]. In its turn, $DRP1^{S637}$ phosphorylation, especially by protein kinase A (PKA) supresses fission[129,132]. The dephosphorylation of the same residue is mediated by calcineurin, that is stimulated by mitochondrial depolarization and by calcium increased level in cytoplasm, particularly in nutrient privation state and under apoptosis stimuli[131]. Lastly, $DRP1^{S693}$ phosphorylation can be mediated by glycogen synthase 3β (GSK3β), an inhibitor of glycogenesis and a controller of several signalling pathways and key cellular processes, has been show to inhibit fission in apoptosis[133]. Also, various signalling pathways involving PKA, MAPK and EGFR-RAS have been related with DRP1 activation leading to mitochondrial fission[55,133–135]. Besides, the SUMO proteins may also influence DRP1 activation. DRP1 sumoylation secures the link between DRP1 and the mitochondrial membrane, depending on bcl-2-associated X protein/bcl-2 homologous antagonist killer (BAX/BAK), stimulating fission[136]. In the same way, proteins included in the E3-ubiquitin ligase family regulate DRP1 and

consequently mitochondrial fission. The cytosolic E3-ubiquitin ligase Parkin directly contacts with DRP1[137], ubiquitinating it and conducting to its proteasome-dependent elimination. Still, ubiquitination is not permanently a signal for elimination. Other E3-ubiquitin ligase, membrane associated ring-CH-type finger 5 (MARCH5)[126,127] benefits DRP1 ubiquitination[126], but does not eliminates DRP1[128]. Perhaps, MARCH5 stimulates DRP1 movement and transferring[128,138], some mitochondria morphology modifications come from MARCH5 interaction with other mitochondria-shaping proteins[126].

DRP1 is a requisite for mitophagy in response to mild oxidative stress, perhaps because of amplified ROS production and by decreased OXPHOS capacity, even with the great number of mitochondria[105,139].

Mitochondrial fission is accepted as being involved in different apoptotic models. DRP1 has been found in complexes with BAX at mitochondrial division positions, thus causing permeabilization of the outer mitochondrial membrane and promoting the cytochrome C (CytC) release[140].

All the aforementioned data point for an important role of proteins of the mitochondrial biogenesis machinery in cancer, specifically that of DRP1 protein.

Chapter 2: Objectives

DRP1 is the main element of mitochondrial fission and is associated with various cell events. The fission protein expression has been related with the progress of several human cancers, through alterations in mitochondrial metabolism, survival, growth arrest and invasion[94]. Nevertheless, the mechanisms behind this relation still unravelled.

Furthermore, activation of BRAF, one of the main proteins of MAPK signalling pathway (frequently activated in thyroid cancer) was related with an higher expression of DRP1 in melanoma – suggesting a synergistic effect of both pathways[121].

The aim of this project is to study the functional relevance of DRP1 in thyroid tumourigenesis, to understand the interplay between mitochondrial fission and MAPK signalling pathway in thyroid cancer and to explore if therapies focused on these targets would be an improvement in disease treatment.

Chapter 3: Materials and Methods

3.1 Thyroid Cell Lines and Cell Culture

Four different human thyroid carcinoma cell lines were used in this project: TPC1, C643, 8505C and XTC-1.

TPC1 cell line was obtained from a papillary thyroid carcinoma (National Cancer Center Research Intitute, Tokyo, Japan, 1989) and ceded by Dumont JE; Mareel M.[141]C643 cell line (Institute of Anatomy and Cell Biology, Goteborg University, Goteborg, Sweden) and 8505C cell line (Electro-Chemical and Cancer Institute, Chofu, Tokyo, Japan, 1993) were obtained from anaplastic thyroid carcinomas and ceded by Mareel M.[141]

XTC-1 cell line was obtained from breast metastasis of a follicular thyroid carcinoma, an oncocytic variant (Surgery Service, Veterans Affairs Medical Center, San Francisco, California, 1996) and ceded by Wong MG; Savagner F.[141]

All cell lines were maintained at 37ºC, in a humified atmosphere, 5% CO_2. TPC1, C643 and 8505C were maintained in RPMI (Roswell Park Memorial Institute) 1640 medium (RPMI-STA, Labclinics, Barcelona, Spain), supplemented with 10% fetal bovine serum (FBS) (LTI10500064, Thermo Fisher Scientific, Waltham, Massachusetts, USA) and 1% (v/v) penicillin-streptomycin (L0022100, LabClinics, Barcelona, Spain). XTC-1 was cultured in Dulbecco's modified Eagle's medium (DMEM) F12 (L0090-50, LabClinics, Barcelona, Spain) again supplemented with 10% FBS and 1% (v/v) penicillin-streptomycin.

3.2 Treatment of Thyroid Carcinoma Cell Lines with Mdivi-1 and Dabrafenib

All cell lines were treated with Mdivi-1 and Dabrafenib alone and in combination. Mitochondrial division inhibitor-1 (Mdivi-1) (M0199, Sigma-Aldrich, St. Louis, Missouri, USA) and GSK2118436 (Dabrafenib) (S2807, Selleckchen, Houston, Texas, USA) were dissolved in dimethyl sulfoxide (DMSO). Drugs were added to the cell culture media and incubated for 48 and 72 hours. DMSO was used as control.

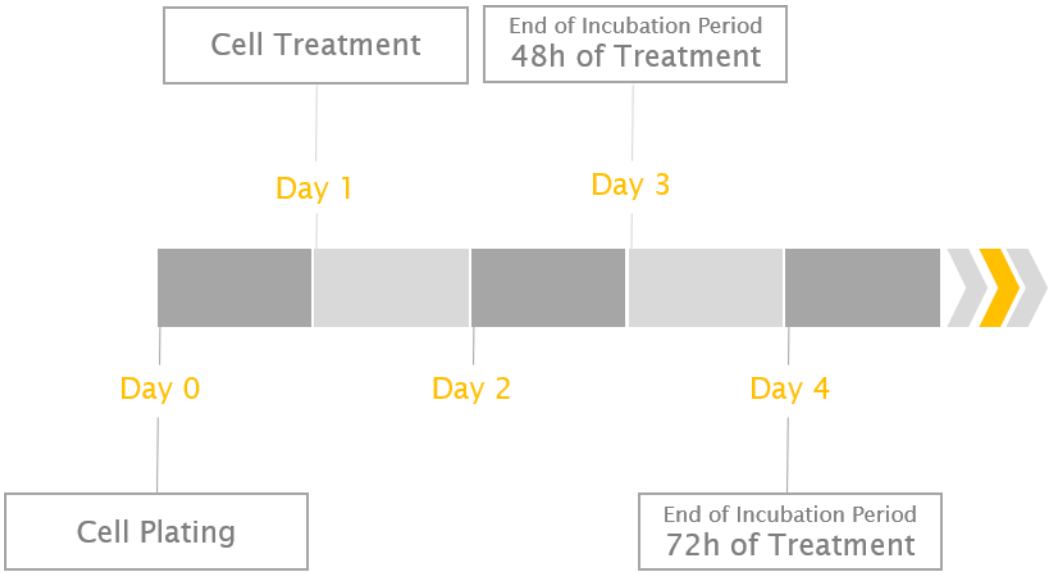

Figure 3: Treatment of thyroid cell lines timeline.

3.3 Cell Viability Assays

Cells were plated in 96-well plates with a density of 2×10^3 and $3{,}5\times10^3$ cells/well for TPC1 and XTC-1, C643 and 8505C, respectively, in 100 µL of their corresponding medium. After 24 h cells were treated, by adding 100 µL of media with dissolved drugs at the desired concentrations. For Presto Blue Assay, all cell lines were treated with Mdivi-1 in the following concentrations: 1, 2.5, 5, 10, 25, 30, 40, 50, 60, 75 and 100 µM or treated with Dabrafenib in the following concentrations: 0.1, 0.5, 1, 2.5, 5, 7.5, 10, 25, 50, 75 and 100 µM. As for Sulforhodamine B Assay all cell lines were treated with Mdivi-1 in the following concentrations: 12.5, 25 and 50 µM or with Dabrafenib in the following concentrations: 2.5,10 and 15 µM. Finally, for Sulforhodamine Assay cells were treated, for combined treatment, with Mdivi-1 25 µM plus Dabrafenib 2.5 µM and Mdivi-1 25 µM plus Dabrafenib 10 µM. Cells were incubated for 48 and 72 hours, in the culture conditions already referred.

3.3.1 Cell Viability Presto Blue Assay

Mdivi-1 and Dabrafenib treatments effects were firstly evaluated by cell viability Presto Blue assay. After the treatment period, media were removed, and cells were washed twice with 100 µL of media without supplementation (without FBS and penicillin-streptomycin). Posteriorly, 50 µL/well of medium with 10% of PrestoBlue® (PB) Reagent (A13261, Invitrogen, Thermo Fisher Scientific, Darmstadt, Germany) were added and incubated for 45 minutes. PB reagent allows the quantitative measure of cell viability through metabolically active cells power to

reduce resazurin. The fluorescence resulting from this reaction was measured by a robotic-compatible microplate reader (Synergy HT Multi-Mode Microplate Reader, Biotek Instruments Inc., Winooski, Vermont, USA) at 560 nm, for excitation wavelength, and 590 nm, for emission wavelength. Three experiments, with four replicates each, were performed to each cell line and condition. Wells without plated cells, containing only medium were used as background fluorescence control. Cell viability was analysed using GraphPadPrism 6.0 (GraphPad Software, Inc., La Jolia, California, USA).

3.3.2 Cell Viability Sulforhodamine B Assay

Sulforhodamine B (SRB) is an anionic aminoxanthrene dye that stoichiometric binds to proteins under mild acidic conditions, this method does not depend on cells metabolic activity.

For this assay, after treatment cells were fixed by adding 50 µL/well of 50% trichloroacetic acid ($C_2HCl_3O_2$) followed by incubation at 4ºC, for an hour. After, wells were rinsed with slow-running tap water and allowed to dry at room temperature. Cells were stained with 150 µL/well of 0.1% SRB in 1% acetic acid (S9012, Sigma-Aldrich, St. Louis, Missouri, USA) and incubated at room temperature for 30 minutes, washed 4 times with 1% glacial acetic acid to remove unbound dye and allowed to dry. Then, 150 µL/well of Tris-base buffer (10 mM, pH 10.5) was used to release SRB from fixed cells, the plate was incubated in a plate shaker for 30 minutes.

The absorbance resultant from this binding was read by a robotic-compatible microplate reader (Synergy HT Multi-Mode Microplate Reader, Biotek Instruments Inc., Winooski, Vermont, USA) at 560 nm. One experiment, with three replicates, was conducted to each cell line and condition. Wells without plated cells, containing only medium were used as background fluorescence controls. Cell viability was analysed using GraphPadPrism 6.0 (GraphPad Software, Inc., La Jolia, California, USA).

3.4 Growth Curves

For cellular growth curves, cells were plated in 6-well plates with a density of 1×10^5, 1.5×10^5 and 2×10^5 cells/well for TPC1, 8505C and XTC-1, and C643, respectively. Cells were treated through the conditions described in Table 2, after 24 hours. The conditions included treatments with each drug alone and their combination during 48 and 72 hours. At the end of each timepoint, cells were

collected and diluted - by a dilution factor of 200 - in Isoton II diluent (Beckman Coulter, Brea, California, USA). The number of cells in each condition was determined in the Z2 Coulter Particle Count and Syze Analyzer (Beckman Coulter, Brea, California, USA). Three experiments were performed for each cell line and condition. The growth curves were determined using GraphPadPrism 6.0 (GraphPad Software, Inc., La Jolia, California, USA).

3.5 Apoptosis and Cell Cycle

After tripsinization, cells were plated in 6-well plates with a density of 1×10^5, 1.5×10^5 and 2×10^5 cells/well for TPC1, 8505C and XTC-1, and C643, respectively. The cell treatments included those designated in Table 2, initiated 24 hours after cell seeding. The conditions comprised treatments with each drug and both drugs combined during 48 and 72 hours.

3.5.1 Apoptosis

For apoptosis analysis, the harvested cells were incubated, in the dark, with 2.5 % of annexin V (31490013x2, Immunotools,Friesoythe, Germany), for 10 minutes, and 50 µg/mL of propidium iodine (PI) (P4864, Sigma-Aldrich, St. Louis, Missouri, USA), for additional 5 minutes. Annexin V binds to the phosphatidylserine expressed on the plasma membrane of apoptotic cells, whereas PI is a dye that only penetrates the unviable membrane of necrotic cells. Cells were analysed by flow cytometry in the BD Accuri C6 flow cytometer (BD Biosciences, Franklin Lakes, New Jersey, USA), counting 20 000 events for each sample. The cells autofluorescence was also measured. Three experiments were performed for each cell line and condition. Data was obtained and analysed using the BD Accuri C6 Software (BD Biosciences, Franklin Lakes, New Jersey, USA).

3.5.2 Cell Cycle

For cell cycle analysis, the harvested cells were fixed and incubated overnight with ice-cold 70% ethanol. Fixed cells were resuspended in 200 µL of DNA staining solution comprising phosphate buffered saline (PBS) (containing 0.01 M Na_2HPO_4, 0.0018 M KH_2PO_4, 0.1370 M NaCl, 0.0027KCl, pH 7.4) 1×, 100 µg/mL of RNase A (Thermo Fisher Scientific, Darmstadt, Germany) and 5 µg/mL of PI. Cell staining was measured by the flow cytometer, counting 20 000 events per sample. Three experiments were conducted to each cell line and condition. Cell cycle results were analysed using the FlowJo 7.6.5 Software (Tree Star, Inc., Ashland USA).

3.6 Protein Expression

For protein expression, cells were plated in 6-well plates with a density of 1×10^5, 1.5×10^5 and 2×10^5 cells/well for TPC1, 8505C and XTC-1, and C643, respectively. 24 hours after seeding, cells were incubated in the conditions described in Table 2 for 48. At the end of this timepoint, cells were lysed with a reagent-based cell lysis using radioimmunoprecipitation (RIPA) buffer (50 mM Tris HCl, 150 mM NaCl, 2 mM EDTA and 1% NP-40, pH 7.5), 1% phosphatase inhibitors (P0044, Sigma-Aldrich, Darmstadt, Germany) and 4% protease inhibitors (11873580001, Roche Applied Science, Penzberg, Germany). Protein quantification for all samples was determined with the Bradford Assay Kit (Bio-Rad, Hercules, California, USA).

30 µg of protein (diluted in destilated water (dH_20) if necessary) was mixed with loading buffer (LB) (containing 5% β-mercaptoethanol and 5% bromophenol blue in Laemmli 4× with Tris-HCl, 8% sodium dodecyl sulfate (SDS) and 40% glycerol). Protein samples were denatured at 95ºC, for 5 minutes and separated by molecular masses in a 12% sodium dodecyl sulfate/polyacrylamide gel electrophoresis (SDS/PAGE). The separated proteins were transferred to a nitrocellulose membrane using iBlot 2 Dry Blotting System (Thermo Fisher Scientific, Darmstadt, Germany), according to the producer's directives, at 20 V for 1 minute, 23 V for 4 minutes and 25 V for 2 minutes. After, the membranes were stained with Ponceau S. reagent (P7170-1L, Sigma-Aldrich, St. Louis, Missouri, USA). Membranes were blocked at room temperature, for 1 hour with 5% bovine serum albumin (BSA) (12659-500MG, EMD Milipore, Burlington, Massachusetts, USA) or 5% low-fat dry milk in Tris-buffered saline 1× with 0.1% Tween 20 (P1379, Sigma-Aldrich, St. Louis, Missouri, USA) (TBS-T 0.1%), accordingly on the dilution of the primary antibodies and manufacturer's instructions.

Primary antibodies used were anti-DRP1 (1:1000, DLP1 611113, BD Biosciences, Franklin Lakes, New Jersey, USA), anti-ERK1/2 (1:1000, P44/42 MAPK (ERK1/2), 9102S, Cell Signalling Technology , Danvers, Massachusetts, USA), anti-phospho-ERK1/2 (1:1000, p-P44/42 MAPK (T20214204), 9101S, Cell Signalling Technology, Danvers, Massachusetts, USA). Membranes were incubated with the primary antibodies at 4ºC, overnight. Anti-α-tubulin (1:8000, T6074, Sigma-Aldrich, Darmstadt, Germany) was used as loading control. The membranes were incubated with anti-tubulin at 4ºC, for an hour. Peroxidase labelled secondary antibodies were used depending on the host animal species in which the primary antibody was

produced (1:2 000 GE Healthcare, Munich Germany or Santa Cruz, Heidelberg, Germany), all the secondary antibodies were diluted in 5% low-fat milk. The incubation period for the secondary antibodies was 1 hour at room temperature. Between each incubation, membranes were washed in TBS-T 0.1%. Enhanced chemiluminescence (ECL) with a 1:1 mix of Enhanced Luminol Reagent and the Oxiding Reagent (PerkinElmer, Whaltham Massachusetts, USA), and X-ray films (Amersham Hyperfilm ECL, GE Healthcare, Munich, Germany) were used for protein detection. Two protocols with different harshness were applied with the intuit to remove the previous primary and secondary antibodies. For the mild stripping, membranes remained in a solution composed by 0.2 M glycine, 1% of SDS and 10% of Tween 20, with a pH of 2.2. For the harsh stripping the membranes stayed in a buffer comprising 20% SDS 10%, 12.5% Tris-HCl 0.5M pH 6.8 and 0.8% β-mercaptoethanol, in the fume hood, at 50°C, for 45 minutes. The quantification of protein expression was obtained using the Bio-Rad Quantity One 1-D Analysis 4.6.9 Software (Bio-Rad, Hercules, California, USA).

Table 1: List of primary antibodies used for Western Blot

Primary Antibody	Reference	Host	Dilutor	Dilution	Incubation Period
Anti-DRP1	DLP1 611113, BD Biosciences	Mouse	BSA	1:1000	Overnight
Anti-ERK1/2	P44/42 MAPK (ERK1/2), 9102S, Cell Signalling Technology	Rabbit	Milk	1:1000	Overnight
Anti-phospho-ERK1/2	p-P44/42 MAPK (T20214204), 9101S, Cell Signalling Technology	Rabbit	BSA	1:1000	Overnight
Anti-α-tubulin	T6074, Sigma-Aldrich	Mouse	Milk	1:8000	1 hour

3.7 mRNA Expression

For RNA expression, cells were plated in 6-well plates with a density of 1×10^5, 1.5×10^5 and 2×10^5 cells/well for TPC1, XTC-1 and 8505C, and C643, respectively. 24 after seeding, cells were incubated in the conditions described in Table 2, except for Mdivi-1 25 and 50 μM and of Dabrafenib 15 μM, for 72h. At the

end, cells were lysed with TripleX tractor reagent (GRiSP Research Solutions, Porto, Portugal) and RNA was extracted accordingly to the manufacturer's instructions. Briefly, media was removed and 1 mL of TripleXtractor reagent was added to the top of the cells, allowed to lyse cells for 1 minute and collected to an RNAse/DNase free tube. After addition of 200 μL of chloroform, it was carried out one centrifugation at 12,000 x g for 15 minutes. After, the aqueous (upper phase containing the RNA) was collected to a new tube and RNA was recovered by isopropanol precipitation. RNA concentration was determined using the NanoDrop ND-1000 Spectrophometer (Nanodrop Technologies, Inc., DE, USA).

DNase I (ThermoScientific, USA) was used to eliminate contaminating DNA from RNA prior to qRT-PCR. Briefly, 1 mg of total RNA was incubated with 10X reaction buffer with MgCl2, 1U of DNase I and water to a final volume of 10 mL for 30 minutes at 37ºC. Later, 1 mL of 50mM EDTA was added and incubated for 10 minutes at 65ºC.

Complementary deoxyribonucleic acid (cDNA) synthesis was performed using the previous mixture where DNA was removed. 1 mL of Random Hexamer Primers was added and incubated for 5 minutes at 65ºC and immediately chilled on ice. Then, 8 μL of the following mixture were added: 4 μL of 5X Reaction Buffer, 20 U RiboLock RNase Inhibitor, 2 μL of dNTP Mix (10 mM) and 200 U of RevertAid Reverse Transcriptase (all from Thermo Scientific, USA). The reaction was incubated at 25 ºC for 10 minutes, followed by 42 ºC for 60 minutes and terminated at 70ºC for 10 minutes. The reaction was performed on Bio-Rad MyCycleTM thermal cycle (BIO RAD, CA, USA). A negative control (-RT; water) was included to later check if there was contamination during cDNA synthesis.

Real-time quantitative polymerase chain reaction (RQ-PCR) was performed to evaluate the relative mRNA expression at the different treatment conditions of NIS, TSHR and OCT4 using TBP as housekeeping gene. 100 ng of cDNA was amplified using 0.5 μL of PrimeTime® qPCR Assays for each gene of interest (IDT, USA), 5 μL of TaqMan™ Universal PCR Master Mix (ThermoScientific, USA) and water in a final volume of 10 μL. The misture was incubated at 95ºC for 10 minutes once, followed by 40 cycles of 95 ºC for 15 seconds and 60 ºC for 1 minute in the QuantStudio 5 Real-Time PCR System (ThermoScientific, USA). Triplicates were performed for each condition. -RT control, as well as a No Template Control (NTC: RT-qPCR control for contamination) were performed to check for contamination.

3.8 Colony Assay Formation

For colony assay formation, cells were plated in 6-well plates with a density of 50 cells/well and 75 cells/well for TPC1, 8505C and XTC-1, respectively. 24 hours after seeding, cells were incubated in the conditions described in Table 2 for 10 days, for TPC1 cell line, and for 14 days, for all other cell lines. After treatment cells were fixed by adding 100 % methanol (CH_3OH) followed by incubation at -20ºC, for an hour. After, the methanol was removed and wells were allowed to dry at room temperature, for at least 3 hours. Cells were stained with 2 mL/well of 0.1% SRB in 1% acetic acid (S9012, Sigma-Aldrich, St. Louis, Missouri, USA), at room temperature, for 30 minutes, washed 4 times with 1% glacial acetic acid to remove unbound dye and allowed to dry. The resulting images were obtained by a Xerox Scan, VersaLink C405 (Xerox, Norwalk, Connecticut, USA).

3.9 Statistical Analysis

The data obtained were analysed by one-way ANOVA followed by Turkey test (to correct for multiple comparisons) in GraphPadPrism 6.0 (GraphPad Software, Inc., La Jolia, California, USA). The data are presented as mean ± standard deviation (SD). A p-value equal or superior to 0.05 was statistically considered as non-significant. A p-value between 0.01 and 0.05 was considered statistically significant, between 0.005 and 0.01 was considered very significant and between 0.001 and 0.005 was considered extremely significant.

Table 2: Treatments applied to thyroid cell lines for Cell Growth, Apoptosis and Cell Cycle

One Drug Treatment	**Mdivi-1**	12.5 µM 25 µM 50 µM
	Dabrafenib	2.5 µM 10 µM 15 µM
Combined Treatment	**Mdivi-1 & Dabrafenib**	Mdivi-1 25 µM + Dabrafenib 2.5 µM Mdivi-1 25 µM + Dabrafenib 10 µM

Chapter 4: Results

Mitochondrial division inhibitor-1 is a small cell-permeable molecule derived from quinazolinone. Mdivi-1 was firstly described as a molecule binding to an allosteric site of DRP1, preventing DRP1 self-assembly into ring-like structures around mitochondria (by polymerization blockage) and reducing GTPase activity[142]. However, recently, the role of Mdivi-1 as a DRP1 inhibitor was questioned, as alternative Mdivi-1, and was hypothesised as a complex I inhibitor[143].

Dabrafenib is an ATP competitive inhibitor that inhibits $BRAF^{V600E}$ and is also able to inhibit wild type BRAF and Raf1[144].

4.1 Thyroid Cell Lines Viability

4.1.1 Determination of IC_{50} of Mdivi-1 in Thyroid Cell Lines by Cell Viability Presto Blue Assay

Thyroid cell lines – TPC1, C643, 8505C and XTC-1 – were, firstly, treated with increasing concentrations of Mdivi-1 – from 1 μM to 100 μM -, for 48h and 72h, to evaluate the drug effect on cell viability. In all thyroid cell lines, the cell viability decreases in a dose-dependent manner, as the highest doses cause more pronounced effects (Figures 4 and 5). However, the cell viability does not seem to follow the same trend in a time-dependent manner, since there are only slightly differences for the same drug concentration between the 48h and the 72h timepoints, for all cell lines except XTC-1.

For TPC1 cells (Figures 4A) the predicted IC_{50} was 30.73 μM, after 48h of treatment, and 27.13 μM, after 72h of treatment.

For C643 cells (Figures 4B) the estimated IC_{50} was 36.82 μM, after 48h of treatment, and 33.58 μM, after 72h treatment.

For 8505C cells (Figures 4C) the predicted IC_{50} was 26.60 μM, after 48h of treatment, and 22.51, after 72h of treatment.

For XTC-1 cells (Figures 4D) the estimated IC_{50} was 28.47 μM, after 48h of treatment, and 17.71 μM, after 72h of treatment. In XTC-1 cell line, Mdivi-1 induces effects in a time-dependent manner, as the same doses causes more pronounced effects in the 72h treatment, especially for doses higher than 10 μM.

For all cell lines, the cell viability decreases with statistically significant differences in relation to control – DMSO (Figure 5).

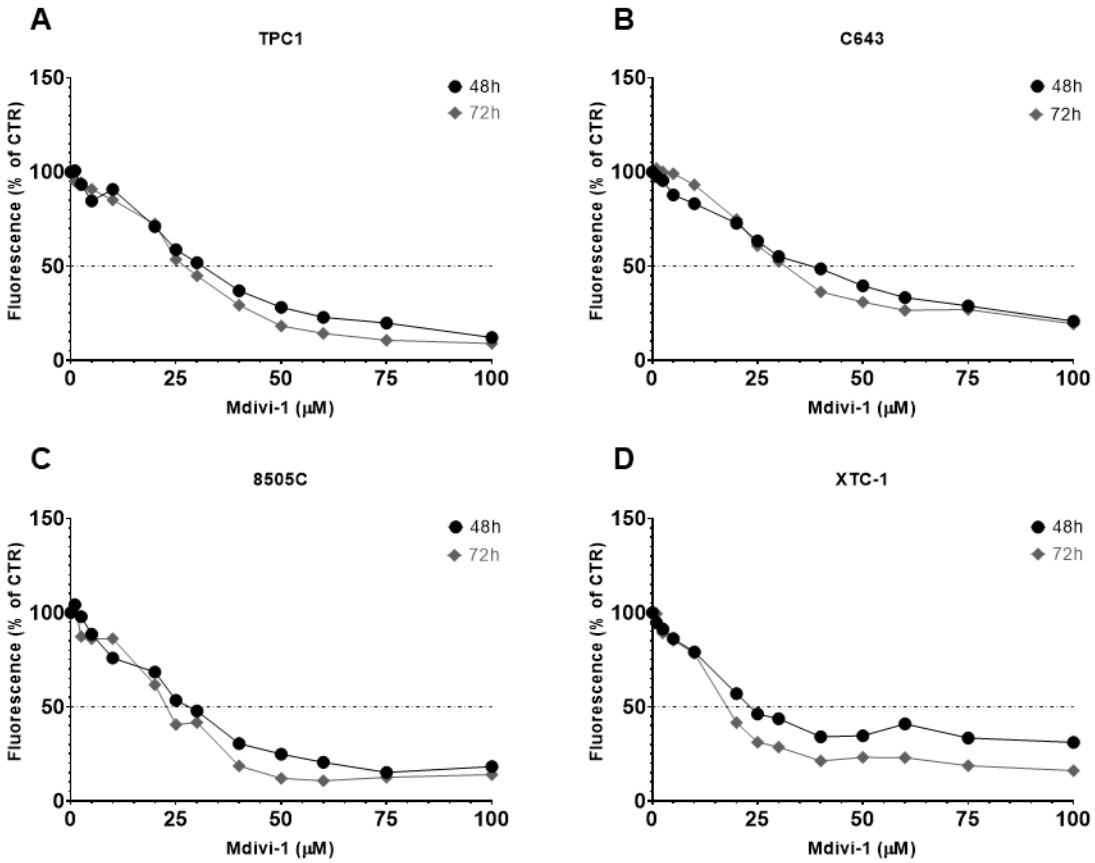

Figure 4: Mdivi-1 dose-response curves for cell viability in thyroid cell lines

Graphic representation, through a scatter plot, of cell viability after treatment with increasing concentrations of Mdivi-1 - from 1 μM to 100 μM -, during 48h and 72h, determined by cell viability Presto Blue assay, relative to control (CTR) – DMSO. A: TPC1 cell line. B: C643 cell line. C: 8505C cell line. D: XTC-1 cell line. Black dots represent the 48h treatment and gray dots represent and the 72h treatment.

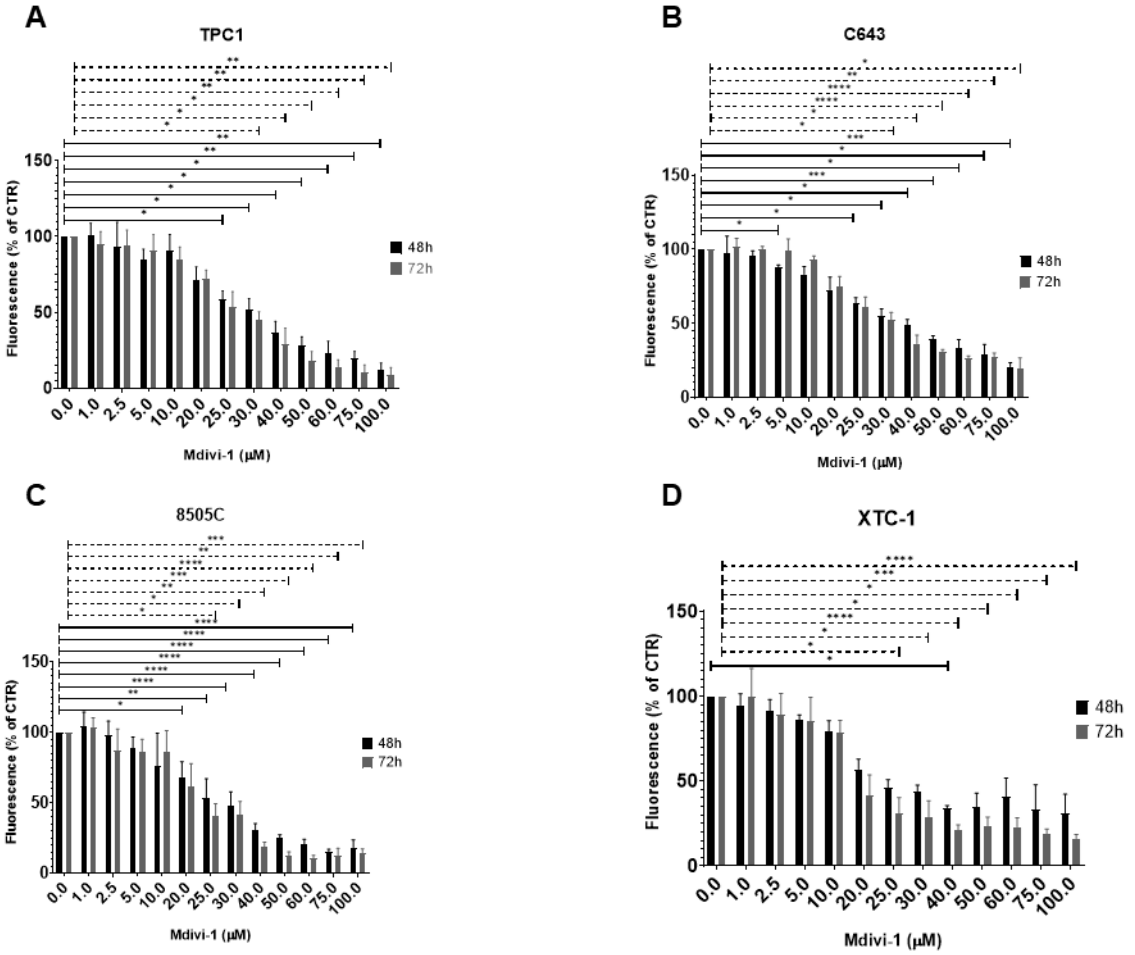

Figure 5: Effects of treatment with Mdivi-1 in thyroid cell lines viability.

Graphic representation, through a bar chart, of the percentage of TPC1 (A), C643 (B), 8505C (C) and XTC-1 (D) cell viability after treatment with increasing concentrations of Mdivi-1 - from 1 μM to 100 μM -, during 48h and 72h, determined by cell viability Presto Blue assay relative to control (CTR) – DMSO. Black bars represent the 48h treatment and gray bars represent the 72h treatment. The data are presented as mean ± SD. The continuous lines represent significant differences in the 48h treatment. The dashed line represents significant differences in the 72h treatment. Statistically significant differences were considered as * ($p \leq 0.05$), ** ($p \leq 0.005$), *** ($p \leq 0.0005$) and **** ($p < 0.0001$) when comparing each concentration with control.

4.1.2 Determination of IC_{50} of Dabrafenib in Thyroid Cell Lines by Cell Viability Presto Blue Assay

Thyroid cell lines were treated with increasing concentrations of Dabrafenib – from 0.1 μM to 100 μM -, for 48h and 72h, to evaluate the drug effect on cell viability and to determine the IC_{50}. Cell viability does not decrease in a dose-

dependent manner, as the increasing doses do not, continuously, cause more pronounced effects (Figures 6 and 7), for all cell lines expect TPC1. Cell viability does not seem to follow the same trend in a time-dependent manner, since there are differences for the same drug concentration between the 48h and the 72h timepoint, although these differences are not evident for all cell lines and for all doses.

For TPC1 cells (Figure 6A) the predicted IC_{50} was 12.96 μM, after 48h of treatment, and 8.73 μM, after 72h of treatment. In TPC1 cells, Dabrafenib reduces cell viability in a dose-dependent manner, as the highest doses cause more pronounced effects. However, the drug does not induce effects in a time-dependent manner, since there are only slightly differences for the same drug concentration between the 48h and in the 72h treatment. In TPC1 cell line, the cell viability decreases with statistically significant differences in relation to control (Figure 7A).

For C643 cells (Figure 6B) the IC_{50} could not be estimated, after 48h of treatment, since there is no reduction in cell viability below 50% of control for the range of concentrations tested. Though the estimated IC_{50} was 89.17 μM, after 72h of treatment. In C643 cells, Dabrafenib induces effects in a time-dependent manner, for doses higher than 7.5 μM. In C643 cells, the cell viability decreases with statistically significant differences in relation to control (Figure 7B).

Similarly, for 8505C cells (Figure 6C) the IC_{50} could not be predicted, after 48h of treatment, for the range of concentrations tested. Still the predicted IC_{50} was 40.65 μM, after 72h of treatment. In 8505C cells, Dabrafenib induces effects in a time-dependent manner, only for doses higher than 5 μM. In 8505C cell line, the cell viability decreases with statistically significant differences in relation to control (Figure 7C). It was not possible to apply the statistical test to 0.5 μM, 48h treatment, because the replicates do not follow a normal distribution.

Finally, for XTC-1 cells (Figure 6D) the IC_{50} estimated was 64.99 μM, after 48h of treatment, and as 32.69 μM, after 72h of treatment. In XTC-1 cells, Dabrafenib also induces effects in a time-dependent manner, only for doses higher than 25 μM. In XTC-1 cells, the cell viability decreases with statistically significant differences in relation to control. It was not possible to apply the statistical test to 2.5 μM, 48h treatment, because the replicates do not follow a normal distribution.

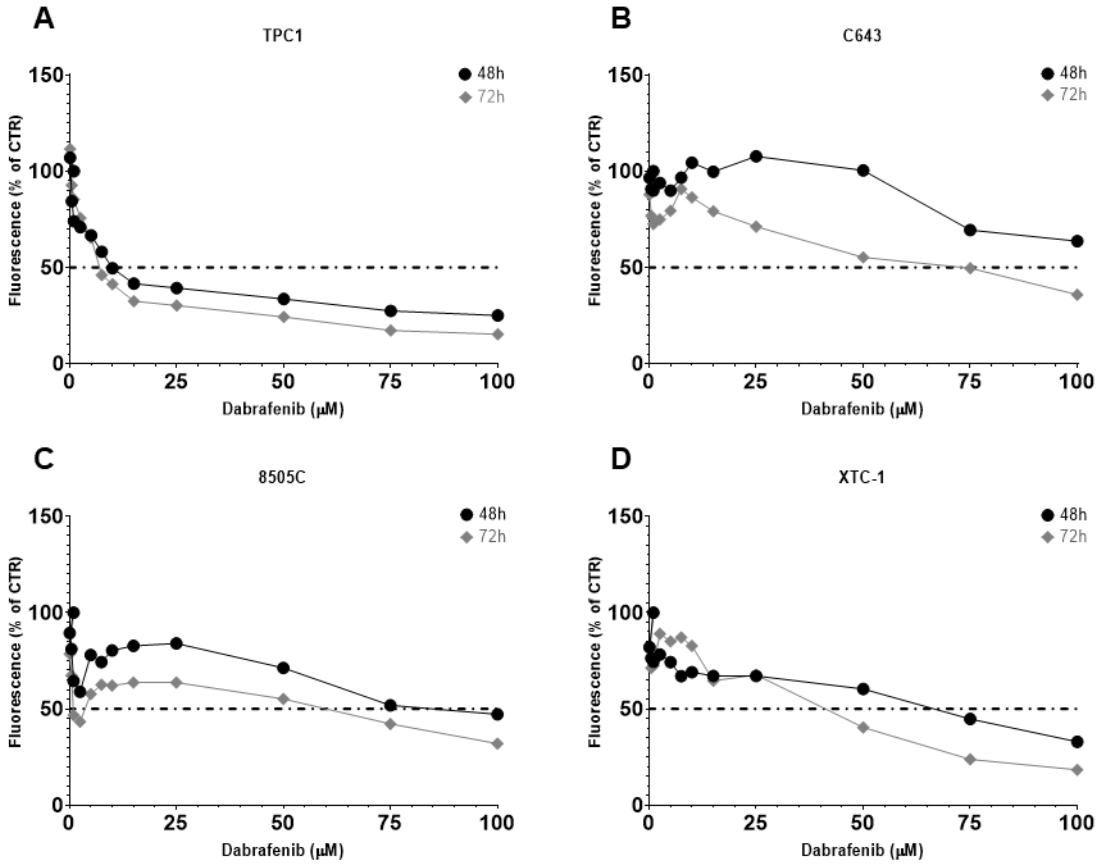

Figure 6: Dabrafenib dose-response curves for cell viability in thyroid cell lines.

Graphic representation, through a scatter plot, of cell viability after treatment with increasing concentrations of Dabrafenib - from 0.1 μM to 100 μM -, during 48h and 72h, determined by cell viability Presto Blue assay, relative to control (CTR) – DMSO. A: TPC1 cell line. B: C643 cell line. C: 8505C cell line. D: XTC-1 cell line. Black dots represent the 48h treatment and gray dots represent the 72h treatment.

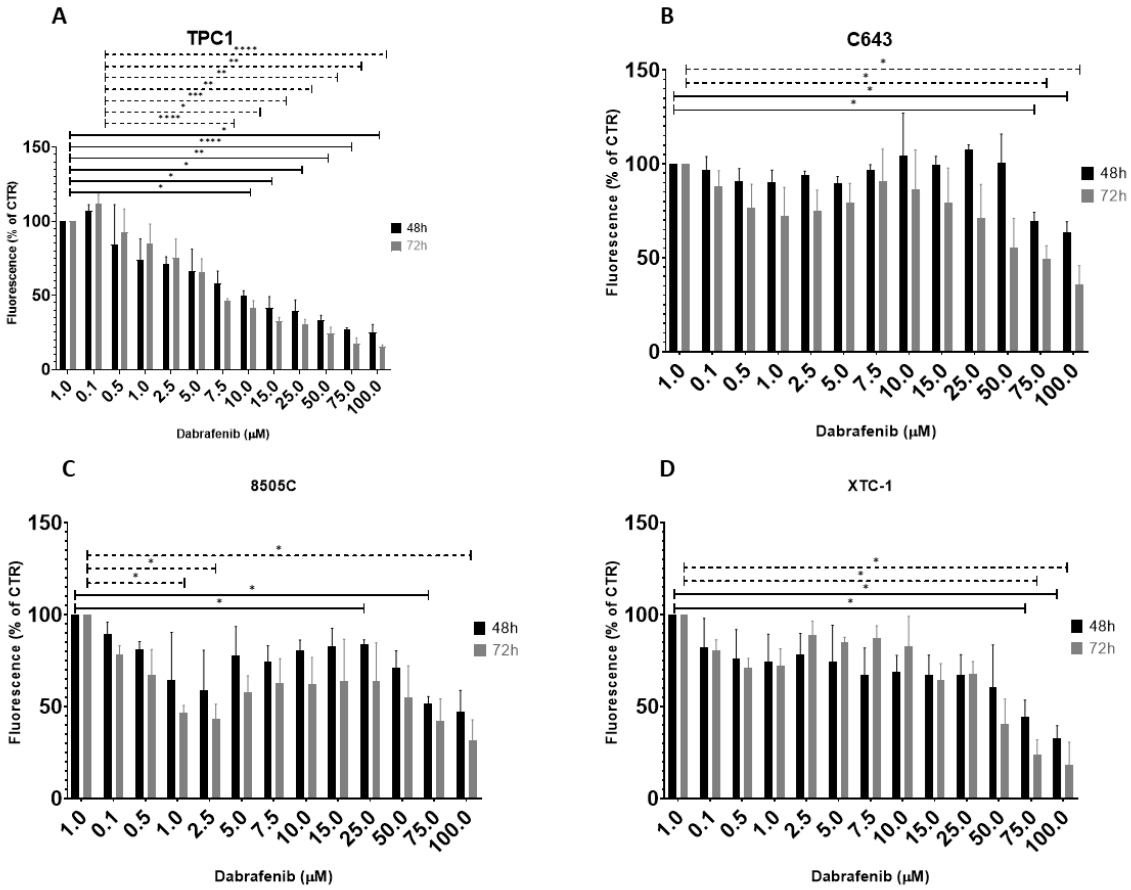

Figure 7: Effects of treatment with Dabrafenib in thyroid cell lines viability.

Graphic representation, through a bar chart, of the percentage of TPC1 (A), C643 (B), 8505C (C) and XTC-1 (D) cells viability after treatment with increasing concentrations of Dabrafenib - from 0.1 μM to 100 μM -, during 48h and 72h, determined by cell viability Presto Blue assay, relative to control (CTR) – DMSO. Black bars represent the 48h treatment and gray bars represent the 72h treatment. The data are presented as mean ± SD. The continuous lines represent significant differences in the 48h treatment. The dashed line represents significant differences in the 72h treatment. Statistically significant differences were considered as * ($p \leq 0.05$), ** ($p \leq 0.005$), *** ($p \leq 0.0005$) and **** ($p < 0.0001$) when comparing each concentration with control.

For the following experiments, in concordance with Presto Blue cell viability assay results and with the determined IC_{50} values, the concentrations applied were those indicated in Table 2.

4.1.3 Effects of Mdivi-1 and Dabrafenib on Thyroid Cell Lines on Cell Viability by Suforhodamine B Assay

Cells were treated with Mdivi-1 – 12.5 μM, 25 μM and 50 μM -, with Dabrafenib – 2.5 μM, 10 μM and 15 μM – and with combination of Mdivi-1 and

Dabrafenib – Mdivi-1 25 μM plus Dabrafenib 2.5 μM and Mdivi-1 25 μM plus Dabrafenib 10 μM -, during 48h and 72h. Drug effect on cell viability was also evaluated by Sulforhodamine B assay, to evaluate possible differences between these results and those obtained by Presto Blue assay. In all thyroid cell lines, the cell viability decreases in relation to control after one drug and combined treatment (Figure 8). For Mdivi-1 treatment, the cell viability decreases in a dose-dependent manner, as the highest doses cause more pronounced effects. However, for Dabrafenib treatment the cell viability does not decrease in a dose-dependent manner, as the highest doses do not cause more pronounced effects. In two cell lines – 8505C and XTC-1 – the cell viability is lower after treatment with Dabrafenib 2.5 μM when compared to treatment with Dabrafenib 10 μM and 15 μM (Figures 8C and 8D). The combined treatment seems to be more effective in decreasing cell viability for all cell lines, except for XTC-1 cell line (Figure 8C). In XTC-1 cell line the combined treatment produces less effects than Mdivi-1alone and Dabrafenib alone treatment. Moreover, the two-drug treatment seems to be more effective with the lowest dose of Dabrafenib – 2.5 μM. In addition, the cell viability seems to decrease in a time-dependent manner, since there are differences between the same drug concentration in the 48h and in the 72h treatment, although these differences are not evident for all cell lines and for the lowest doses.

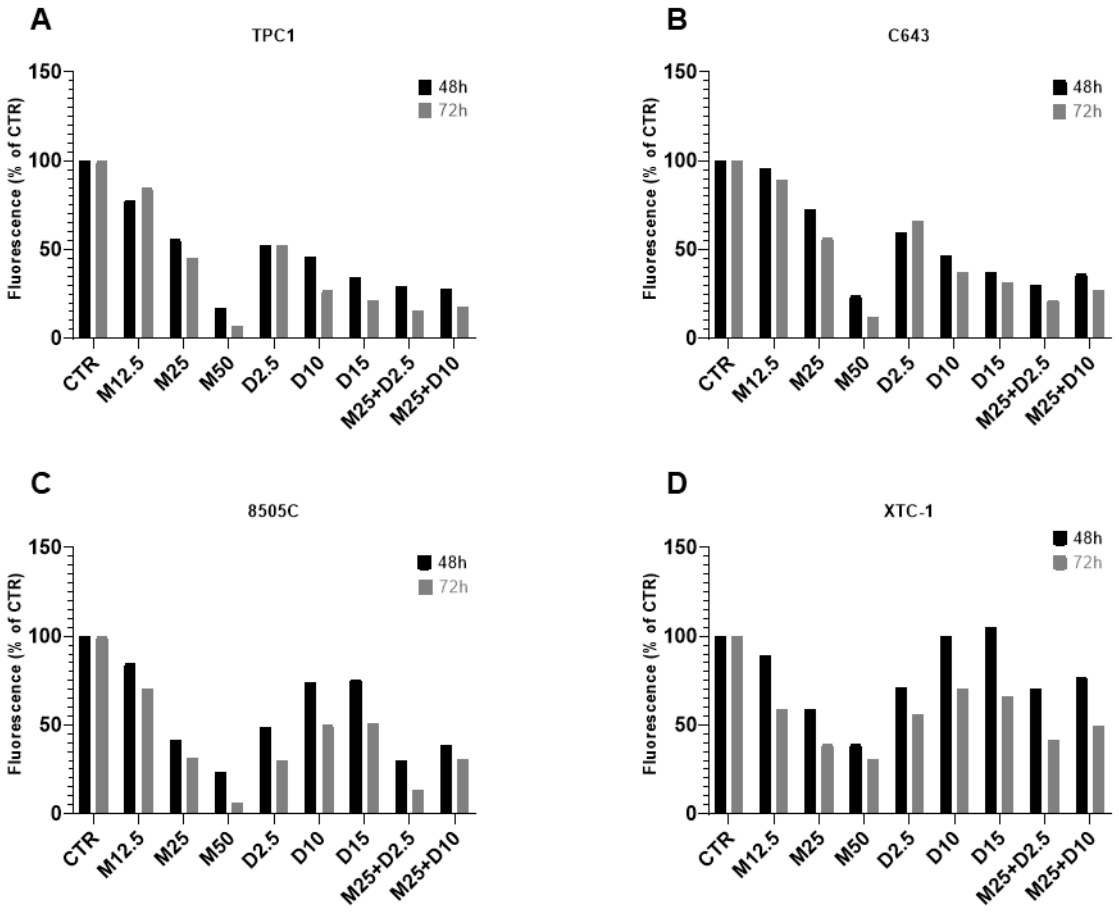

Figure 8: Comparison of effects of treatment with Mdivi-1, Dabrafenib and Mdivi-1 and Dabrafenib combinations in thyroid cell lines viability.

Graphic representation, through a bar chart, of the percentage of TPC1 (A), C643 (B), 8505C (C) and XTC-1 (D) cells emitting fluorescence after treatment with Mdivi-1 (represented as M) – 12.5 μM, 25 μM and 50 μM -, with Dabrafenib (represented as D) – 2.5 μM, 10 μM and 15 μM – and with Mdivi-1 and Dabrafenib combinations – Mdivi-1 25 μM plus Dabrafenib 2.5 μM and Mdivi-1 25 μM plus Dabrafenib 10 μM -, during 48h and 72h, determined by cell viability Sulforhodamine B assay, regarding to the cell fluorescence in the control (CTR) – DMSO added to cell culture medium. The 48h treatment is represented in black bars and the 72h treatment is represented in gray bars.

4.2 Effects of Mdivi-1 and Dabrafenib on Thyroid Cell Lines Growth

Cancer cells growth is one of the most relevant features of the disease and relies on distinct pathways. To determine the influence of DRP1 and of MAPK pathway in cells growth, thyroid cell lines were treated with Mdivi-1, with Dabrafenib and with drug combinations, during 48h and 72h, and then counted. In TPC1, C643 and 8505C cell lines, the number of cells reduces in relation to

control after treatment with DRP1 inhibitor and with BRAF inhibitor, alone and in combination (Figures 9A, 9B and 9C). In XTC-1 cell line, the treatments do not produce the same effect (Figure 9D). Also, the number of cells reduces in a dose-dependent manner after treatment with Mdivi-1, but not after treatment with Dabrafenib. The combined treatment is more effective for cell growth with the highest dose of Dabrafenib, however is not more effective than the one drug treatment. A longer period exposure to the drugs – 72h treatment -, does not seem to produce more effects on cell growth.

In TPC1 cell line (Figure 9A), the cell growth reduces with statistically significant differences in relation to control for Mdivi-1, Dabrafenib, and combined treatment and between treatments. It was not possible to apply the statistical test to Dabrafenib 15 μM, 72h treatment, because the replicates do not follow a normal distribution.

In C643 and 8505C cell line (Figures 9B and 9C), the cell growth reduces with statistically significant differences in relation to control for Mdivi-1, Dabrafenib, and combined treatment and between treatments. Also, the cell growth reduces with significant differences between treatments.

Lastly, in XTC-1 cell line (Figure 9D), the cell growth does not reduce with any statistically significant differences.

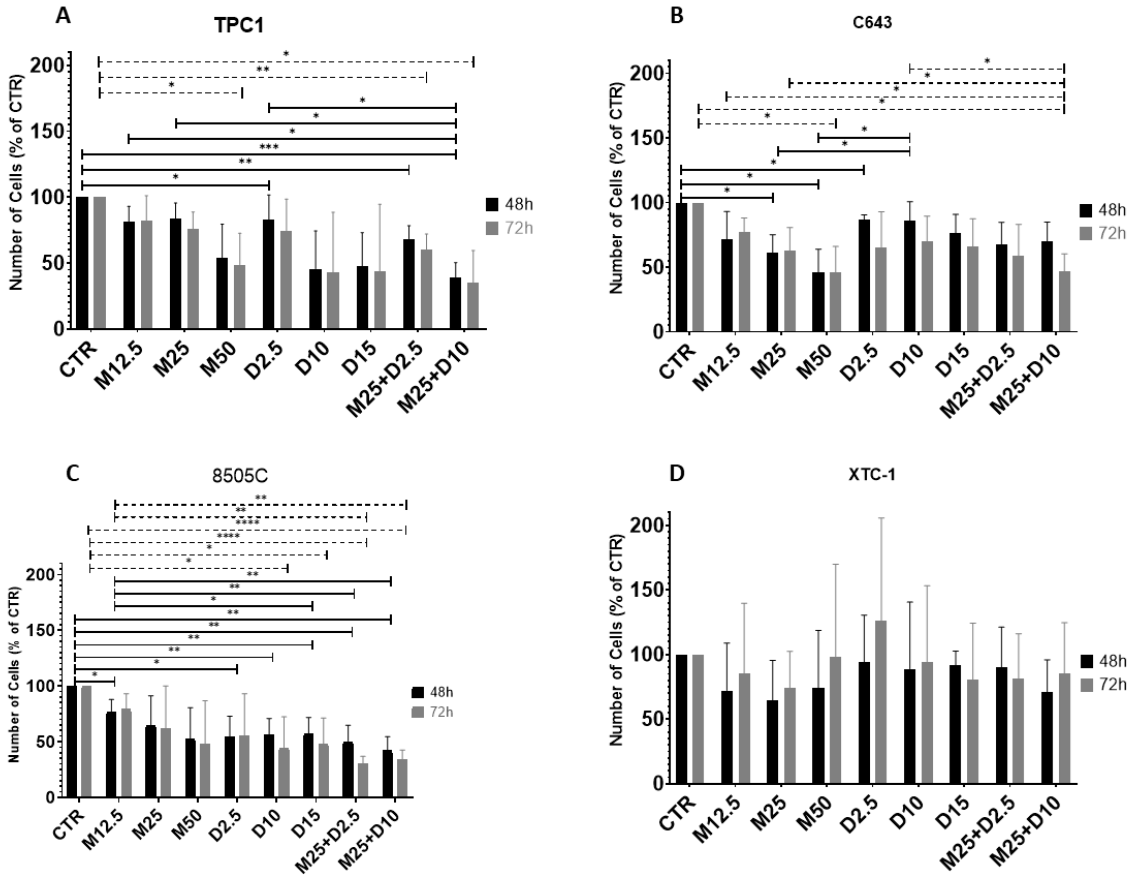

Figure 9: Effects of treatment with Mdivi-1, Dabrafenib and Mdivi-1 and Dabrafenib combinations in thyroid cell lines growth.

Graphic representation, through a bar chart, of the percentage of TPC1 (A), C643 (B), 8505C (C) and XTC-1 (D) cells counted after treatment with Mdivi-1 (represented as M) – 12.5 μM, 25 μM and 50 μM -, with Dabrafenib (represented as D) – 2.5 μM, 10 μM and 15 μM – and with Mdivi-1 and Dabrafenib combinations – Mdivi-1 25 μM plus Dabrafenib 2.5 μM and Mdivi-1 25 μM plus Dabrafenib 10 μM -, during 48h and 72h, relative to the cell number in the control (CTR) – DMSO. Black bars represent the 48h treatment and gray bars represent the 72h treatment. The data are presented as mean ± SD. The continuous lines represent significant differences in the 48h treatment. The dashed line represents significant differences in the 72h treatment. Statistically significant differences were considered as * ($p \leq 0.05$), ** ($p \leq 0.005$), *** ($p \leq 0.0005$) and **** ($p < 0.0001$) when comparing each concentration with control.

4.3 Effects of Mdivi-1 and Dabrafenib on Thyroid Cell Lines Apoptosis and Cell Cycle

4.3.1 Effects of Mdivi-1 and Dabrafenib on Thyroid Cell Lines Apoptosis

In cancer, apoptosis inhibition is frequently associated with tumour initiation, progression and invasion. The effects of Mdivi-1 and Dabrafenib alone and in combination in inducing cells apoptosis were evaluated 48h and 72h after treatment, by flow cytometry after Annexin V and PI staining. In all thyroid cell lines, the percentage of apoptotic cells increases relative to control after treatment with Mdivi-1 and Dabrafenib (Figure 10), except C643 cell line after treatment with Dabrafenib. Mdivi-1 increases apoptosis in a dose-dependent manner, especially after treatment with the highest dose (50 μM). However, Dabrafenib increases cell programmed death only slightly, also depending on doses. The drug combination seems to be slightly more effective in inducing cell death. Furthermore, the cell survival seems to decrease in a time-dependent manner, since there are differences between the same drug concentration in the 48h and in the 72h treatment. These effects are not clear for XTC-1 cell line. In XTC-1 cells, only Dabrafenib produces some effect at is lower dose and only 72h after treatment (Figure 10D). There were no found statistically significant differences.

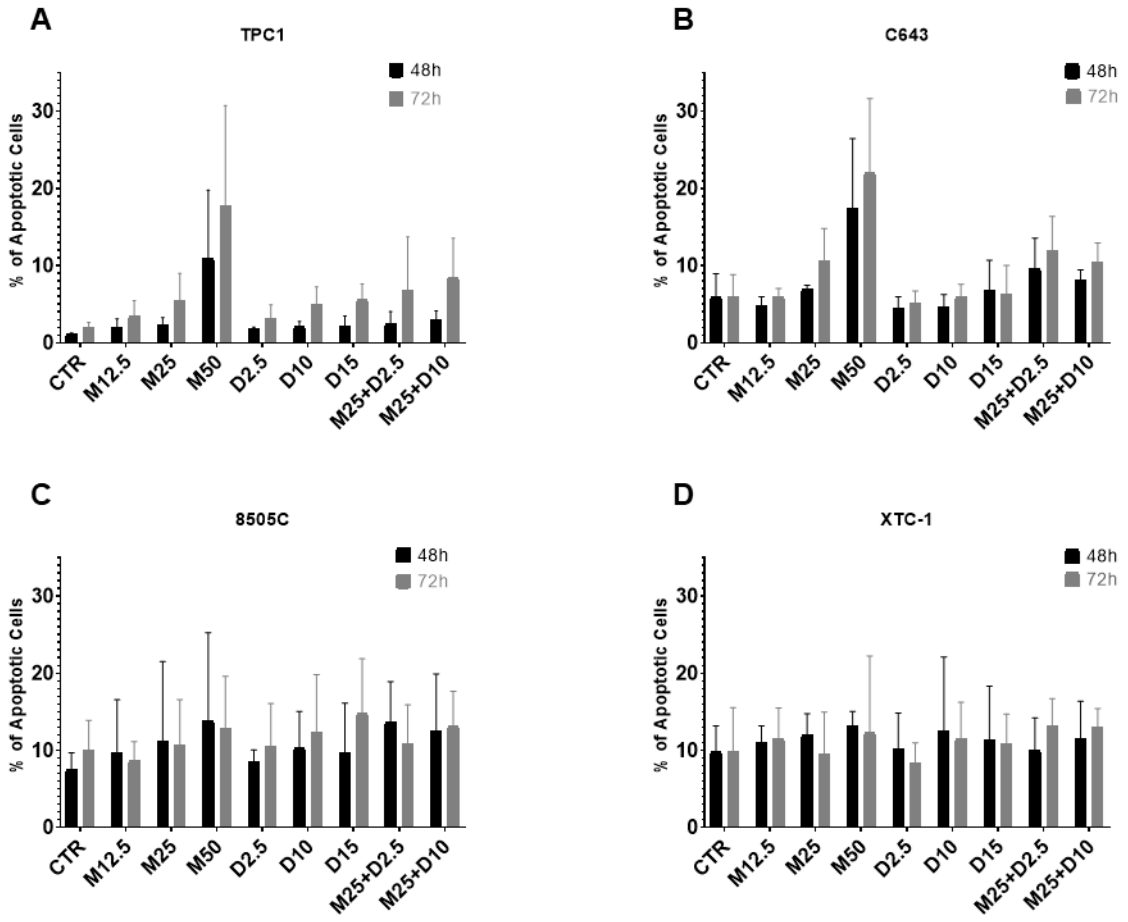

Figure 10: Effects of treatment with Mdivi-1, Dabrafenib and Mdivi-1 and Dabrafenib combinations in thyroid cell lines apoptosis.

Graphic representation, through a bar chart, of the percentage of TPC1 (A), C643 (B), 8505C (C) and XTC-1 (D) apoptotic cells after treatment with Mdivi-1 (represented as M) – 12.5 μM, 25 μM and 50 μM -, with Dabrafenib (represented as D) – 2.5 μM, 10 μM and 15 μM – and with Mdivi-1 and Dabrafenib combinations – Mdivi-1 25 μM plus Dabrafenib 2.5 μM and Mdivi-1 25 μM plus Dabrafenib 10 μM, during 48h and 72h, determined by Annexin V/PI staining and analysis by flow cytometry. The data are presented as mean ± SD. The continuous lines represent significant differences in the 48h treatment. The dashed line represents significant differences in the 72h treatment. Statistically significant differences were considered as * ($p \leq 0.05$), ** ($p \leq 0.005$), *** ($p \leq 0.0005$) and **** ($p < 0.0001$) when comparing each concentration with control.

4.3.2 Effects of Mdivi-1 and Dabrafenib on Thyroid Cell Lines Cell Cycle

Cancer progression and invasion rely on cell division. The effects of Mdivi-1 and Dabrafenib alone and in combination on cell cycle were evaluated 48h and 72h after treatment, by flow cytometry with DNA PI staining. In all thyroid cell lines, the

percentage of cells in G1, S phase or G2 is altered regarding to control after treatment with Mdivi-1 and Dabrafenib (Figures 11 and 12). Mdivi-1 slightly increases the number of cells in G1 and decreases the number of cells in S phase. Dabrafenib induces the same effect in a greater extent. also decreasing the number of cells in G2, especially for higher doses. The BRAF inhibitor seems to lose some effect 72h after treatment. Mdivi-1 and Dabrafenib combination does not seem to induce cumulative effects in cell division. Furthermore, the cell viability does not seem to decrease in a time-dependent manner, since there are only slightly differences between the same drug concentration in the 48h and in the 72h treatment. Cell cycle is altered with statistically significant differences. It was not possible to apply the statistical test to TPC1 and C643 cell lines because only two and one replicate, respectively, could be analysed by FlowJo 7.6.5 Software. Also, for Mdivi-1 50 μM the cells were to damage to perform analysis trough FlowJo 7.6.5 Software (Figure 26, Supplementary Data).

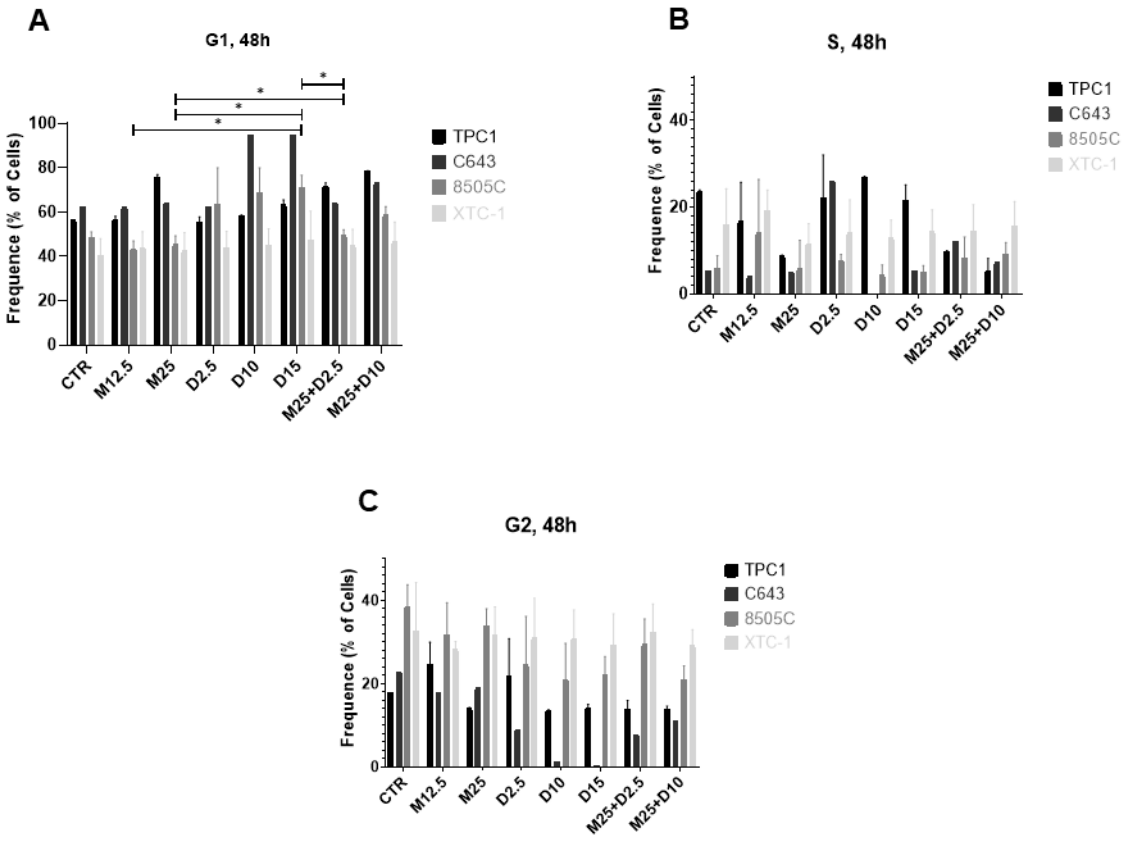

Figure 11: Effects of treatment with Mdivi-1, Dabrafenib and Mdivi-1 and Dabrafenib combinations in thyroid cell lines cell cycle (48h treatment).

Graphic representation, through a bar chart, of the percentage cells in G1 (A), S phase (B) or G2 (C) after treatment with Mdivi-1 (represented as M) – 12.5 μM, 25 μM and 50 μM -,

with Dabrafenib (represented as D) – 2.5 μM, 10 μM and 15 μM – and with Mdivi-1 and Dabrafenib combinations – Mdivi-1 25 μM plus Dabrafenib 2.5 μM and Mdivi-1 25 μM plus Dabrafenib 10 μM -, during 48h. Cell cycle was determined by DNA PI staining and analysis by flow cytometry. Black, dark gray, middle gray and light gray represent TPC1, C643, 8505C and XTC-1 cell lines, respectively. The data are presented as mean ± SD. The continuous lines represent significant differences in 8505C cell line. Statistically significant differences were considered as * ($p \leq 0.05$), ** ($p \leq 0.005$), *** ($p \leq 0.0005$) and **** ($p < 0.0001$) when comparing each concentration with control.

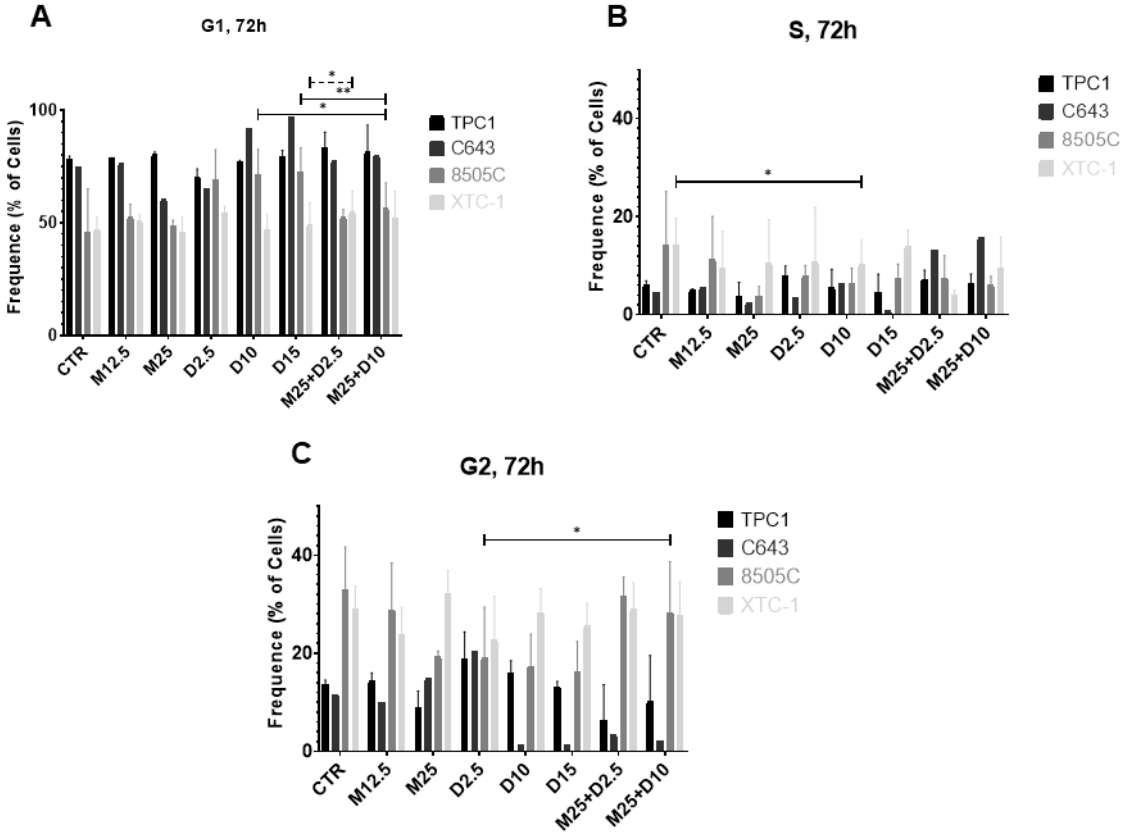

Figure 12: Effects of treatment with Mdivi-1, Dabrafenib and Mdivi-1 and Dabrafenib combinations in thyroid cell lines cell cycle (72h treatment).

Graphic representation, through a bar chart, of the percentage cells in G1 (A), S phase (B) or G2 (C) after treatment with Mdivi-1 (represented as M) – 12.5 μM, 25 μM and 50 μM -, with Dabrafenib (represented as D) – 2.5 μM, 10 μM and 15 μM – and with Mdivi-1 and Dabrafenib combinations – Mdivi-1 25 μM plus Dabrafenib 2.5 μM and Mdivi-1 25 μM plus Dabrafenib 10 μM -, during 48h. Cell cycle was determined by DNA PI staining and analysis by flow cytometry. Black, dark gray, middle gray and light gray represent TPC1, C643, 8505C and XTC-1 cell lines, respectively. The data are presented as mean ± SD. The continuous lines represent significant differences in 8505C cell line. The dashed line represents significant differences in XTC-1 cell line. Statistically significant differences were

considered as * ($p \leq 0.05$), ** ($p \leq 0.005$), *** ($p \leq 0.0005$) and **** ($p < 0.0001$) when comparing each concentration with control.

4.4 Effects of Mdivi-1 and Dabrafenib on Thyroid Cell Lines DRP1 and MAPK Pathway Proteins Expression

DRP1 is the regulator protein of mitochondrial fission and BRAF, along with all its key functions, seems to influence DRP1 activity. To evaluate the efficacy of treatments with Mdivi-1 25 μM, Dabrafenib 2.5 and 10 μM, Mdivi-1 25 μM plus Dabrafenib 2.5, and Mdivi-1 plus Dabrafenib 10 μMs the expression of DRP1, of ERK – a downstream regulator of BRAF - and of its phosphorylated form were accessed, 48h after treatment

In TPC1 cell line (Figures 13 and 14), Mdivi-1 reduces the expression of the total form of DRP1, as well as the phosphorylated form of ERK. Still, the drug does not inhibit the expression of the total form of ERK. Dabrafenib treatment produces similar effects. On its turn, the drug combination seems more powerful reducing DRP1 expression, increases of phosphorylated form of ERK and decreases the expression of the total ERK.

In C643 cell line (Figures 15 and 16), both Mdivi-1 and Dabrafenib do not seem to produce major effects on proteins expression. Dabrafenib 10 μM slightly decreases the total form of DRP1 and the phosphorylated and the total forms of ERK. On its turn, the drug combination decreases the expression of the total forms of both DRP1 and ERK and increases the expression of phospho-ERK.

In 8505C cell line (Figures 17 and 18), Mdivi-1 and Dabrafenib inhibit the total form of DRP1 and the phosphorylated form of ERK and increase the total form of ERK. Here, Dabrafenib is more effective in reducing proteins expression. On its turn, the drug combination treatment does not seem to produce different effects on protein inhibition.

Finally, in XTC-1 cell line (Figures 19 and 20) Mdivi-1 increases the protein expression levels, whereas Dabrafenib decreases it. Again, the drug combination treatment does not seem to produce a bigger effect on protein inhibition.

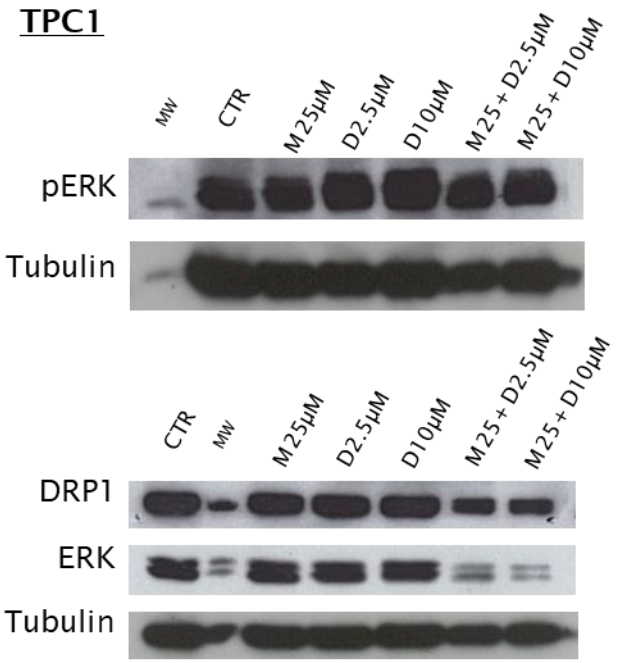

Figure 13: Effects of treatment with Mdivi-1, Dabrafenib and Mdivi-1 and Dabrafenib combinations in TPC1 cell line protein expression.

Western Blot analysis for protein expression of DRP1, phospho-ERK and ERK relative to loading control tubulin in TPC1 cell line after 48h treatment. For pERK and the respective tubulin, the molecular weight marker (MW) places in the 1st position. For DRP1, ERK and the respective tubulin, the molecular weight marker places in the 2nd position.

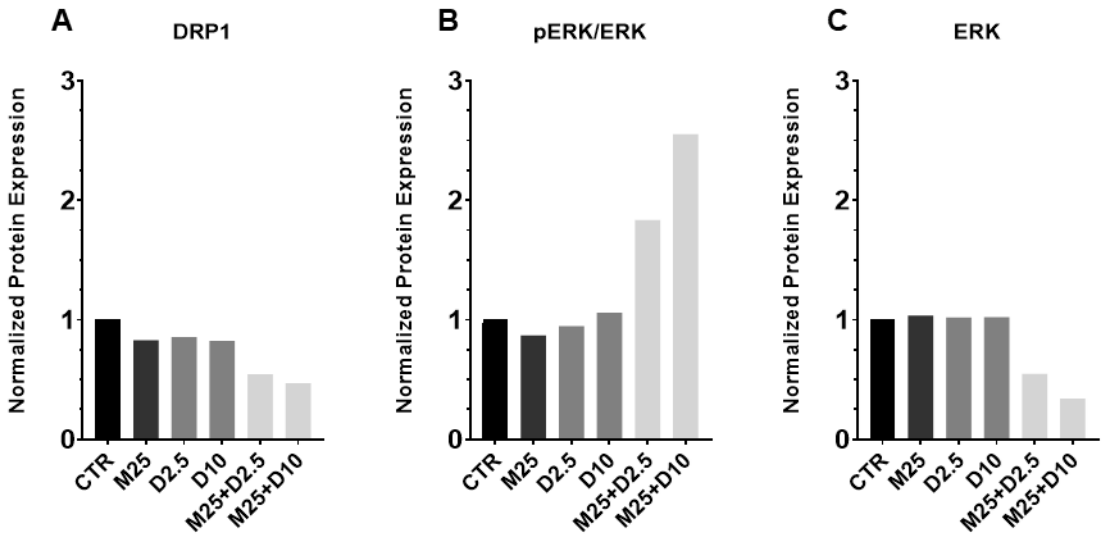

Figure 14: Effects of treatment with Mdivi-1, Dabrafenib and Mdivi-1 and Dabrafenib combinations in TPC1 cell line DRP1 and MAPK pathway proteins.

Graphic representation, through a bar chart, of the protein expression DRP1(A), phosphorylated ERK as counting part of ERK expression (B) and ERK (C) in TPC1 cells after treatment with Mdivi-1 (represented as M), – 12.5 μM, 25 μM and 50 μM - with Dabrafenib (represented as D) – 2.5 μM, 10 μM and 15 μM – and with Mdivi-1 and Dabrafenib combinations – Mdivi-1 25 μM plus Dabrafenib 2.5 μM and Mdivi-1 25 μM plus Dabrafenib 10 μM -, during 48h, determined by Western Blot analysis. The control is represented in black bars, the Mdivi-1 treatments are represented in dark gray bars, the Dabrafenib treatments are represented in middle gray bars and the combination treatments are represented in light gray bars.

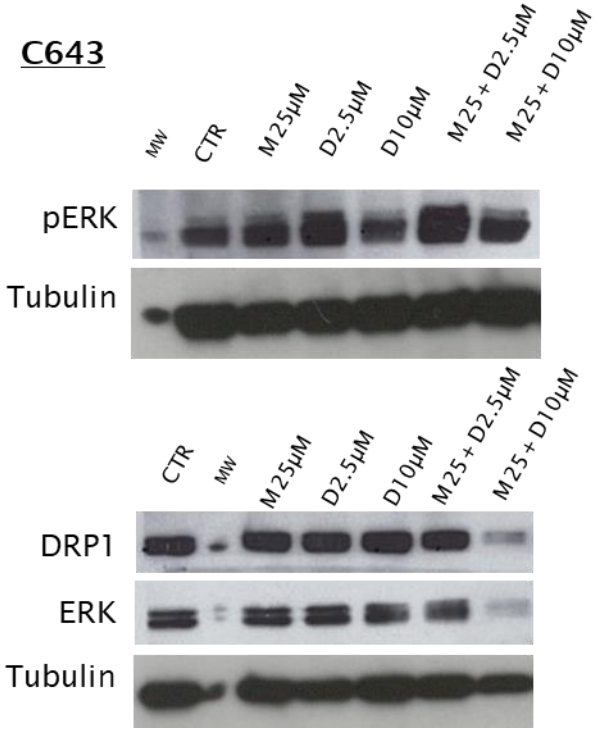

Figure 15: Effects of treatment with Mdivi-1, Dabrafenib and Mdivi-1 and Dabrafenib combinations in C643 cell line protein expression.

Western Blot analysis for protein expression of DRP1, phospho-ERK and ERK relative to loading control tubulin in C643 cell line after 48h treatment. For pERK and the respective tubulin, the molecular weight marker (MW) places in the 1st position. For DRP1, ERK and the respective tubulin, the molecular weight marker places in the 2nd position.

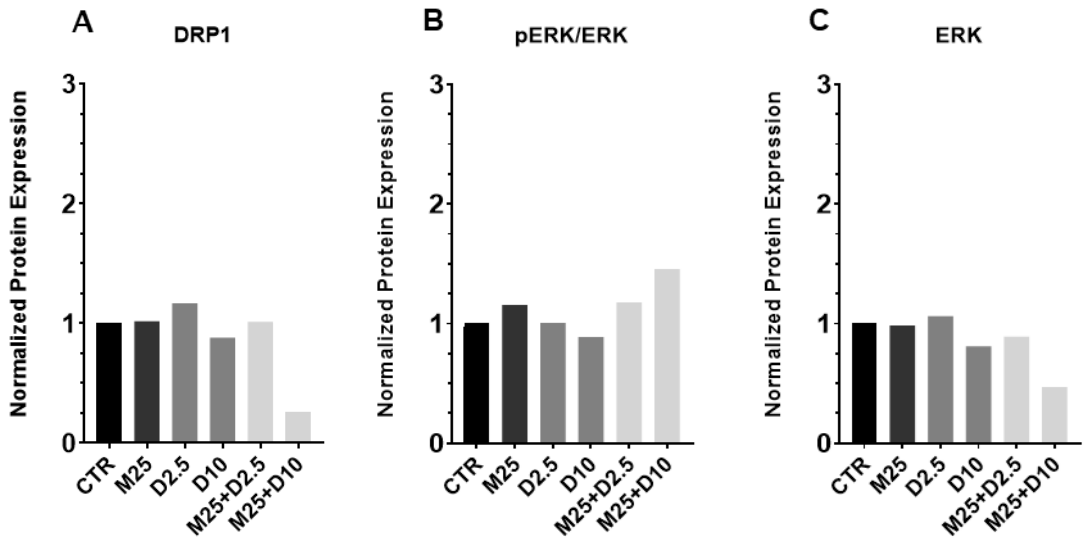

Figure 16: Effects of treatment with Mdivi-1, Dabrafenib and Mdivi-1 and Dabrafenib combinations in C643 cell line protein expression.

Graphic representation, through a bar chart, of the protein expression DRP1(A), phosphorylated ERK as counting part of ERK expression (B) and ERK (C) in C643 cells after treatment with Mdivi-1 (represented as M), – 12.5 μM, 25 μM and 50 μM -with Dabrafenib (represented as D) – 2.5 μM, 10 μM and 15 μM – and with Mdivi-1 and Dabrafenib combinations – Mdivi-1 25 μM plus Dabrafenib 2.5 μM and Mdivi-1 25 μM plus Dabrafenib 10 μM -, during 48h, determined by Western Blot analysis. The control is represented in black bars, the Mdivi-1 treatments are represented in dark gray bars, the Dabrafenib treatments are represented in middle gray bars and the combination treatments are represented in light gray bars.

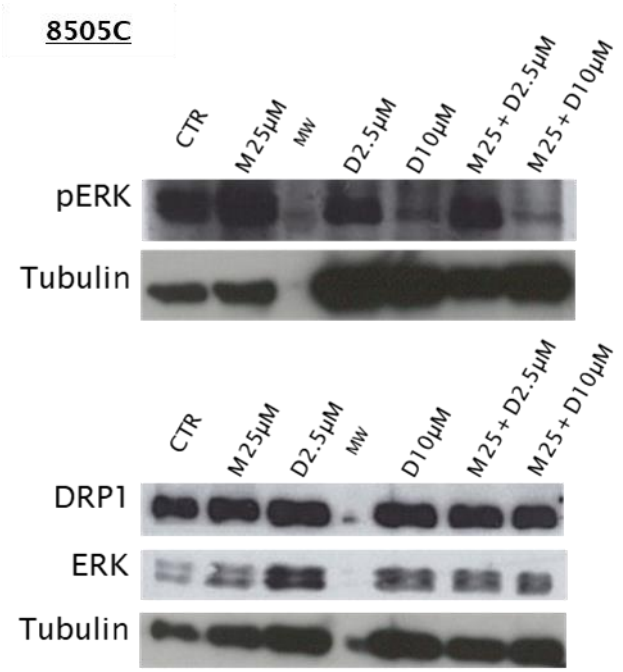

Figure 17: Effects of treatment with Mdivi-1, Dabrafenib and Mdivi-1 and Dabrafenib combinations in 8505C cell line protein expression.

Western Blot analysis for protein expression of DRP1, phospho-ERK and ERK relative to loading control tubulin in 8505C cell line after 48h treatment. For pERK and the respective tubulin, the molecular weight marker (MW) places in the 3rd position. For DRP1, ERK and the respective tubulin, the molecular weight marker places in the 4th position.

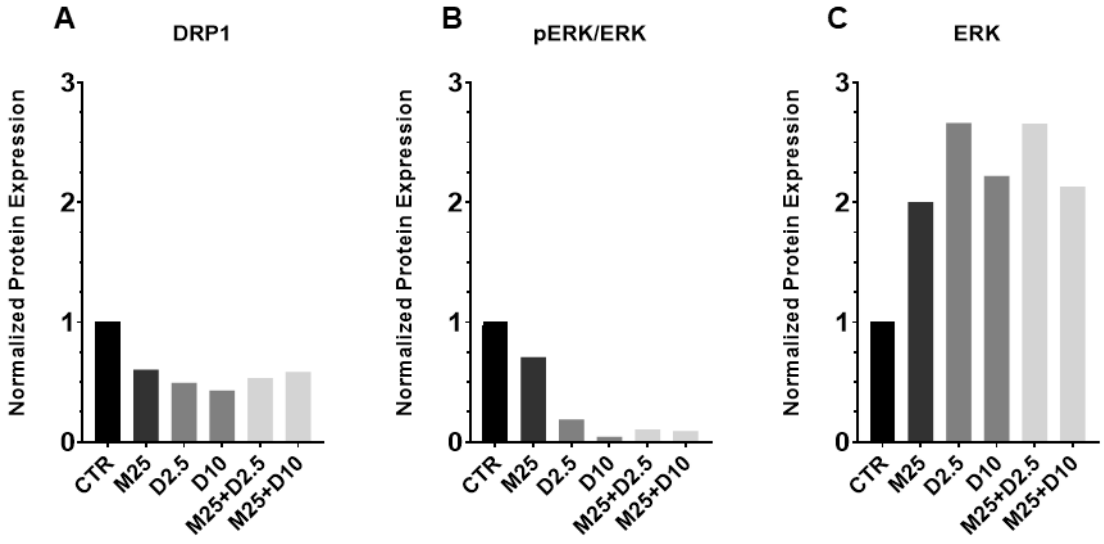

Figure 18: Effects of treatment with Mdivi-1, Dabrafenib and Mdivi-1 and Dabrafenib combinations in 8505C cell line protein expression.

Graphic representation, through a bar chart, of the protein expression DRP1(A), phosphorylated ERK as counting part of ERK expression (B) and ERK (C) in 8505C cells after

treatment with Mdivi-1 (represented as M), – 12.5 μM, 25 μM and 50 μM - with Dabrafenib (represented as D) – 2.5 μM, 10 μM and 15 μM – and with Mdivi-1 and Dabrafenib combinations – Mdivi-1 25 μM plus Dabrafenib 2.5 μM and Mdivi-1 25 μM plus Dabrafenib 10 μM -, during 48h, determined by Western Blot analysis. The control is represented in black bars, the Mdivi-1 treatments are represented in dark gray bars, the Dabrafenib treatments are represented in middle gray bars and the combination treatments are represented in light gray bars.

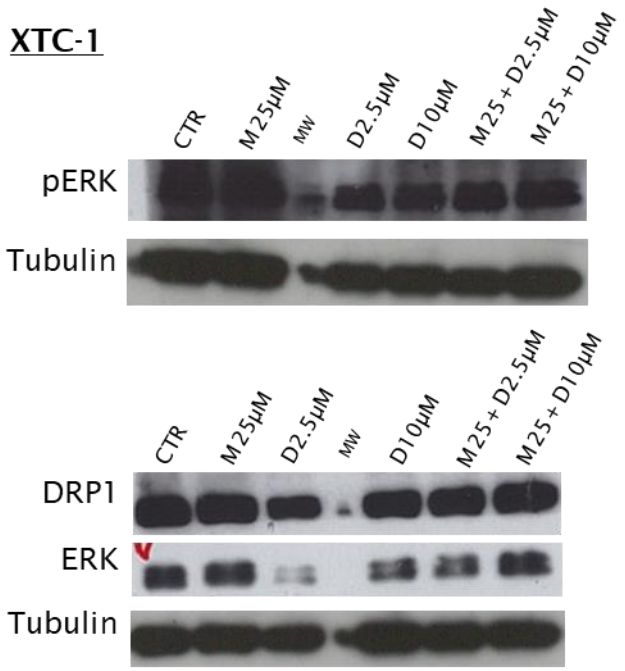

Figure 19: Effects of treatment with Mdivi-1, Dabrafenib and Mdivi-1 and Dabrafenib combinations in XTC-1 cell line protein expression.

Western Blot analysis for protein expression of DRP1, phospho-ERK and ERK relative to loading control tubulin in XTC-1 cell line after 48h treatment. For pERK and the respective tubulin, the molecular weight marker (MW) places in the 3rd position. For DRP1, ERK and the respective tubulin, the molecular weight marker places in the 4th position.

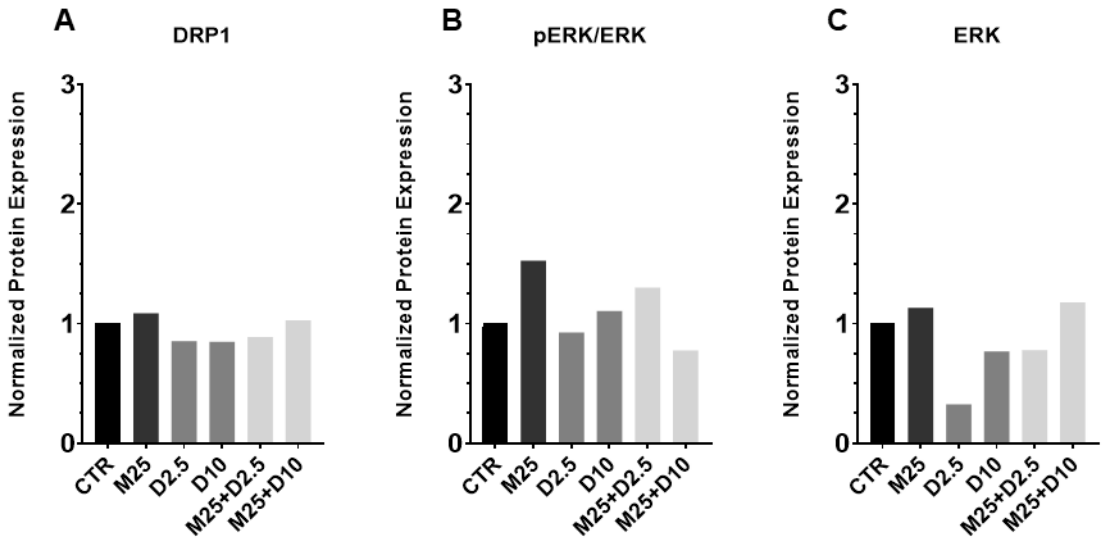

Figure 20: Effects of treatment with Mdivi-1, Dabrafenib and Mdivi-1 and Dabrafenib combinations in XTC-1 cell line protein expression.

Graphic representation, through a bar chart, of the protein expression of DRP1(A), phosphorylated ERK as counting part of ERK expression (B) and ERK (C) in XTC-1 cells after treatment with Mdivi-1 (represented as M), – 12.5 μM, 25 μM and 50 μM - with Dabrafenib (represented as D) – 2.5 μM, 10 μM and 15 μM – and with Mdivi-1 and Dabrafenib combinations – Mdivi-1 25 μM plus Dabrafenib 2.5 μM and Mdivi-1 25 μM plus Dabrafenib 10 μM -, during 48h, determined by Western Blot analysis. The control is represented in black bars, the Mdivi-1 treatments are represented in dark gray bars, the Dabrafenib treatments are represented in middle gray bars and the combination treatments are represented in light gray bars.

4.5 Effects of Mdivi-1 and Dabrafenib on Octamer-Binding Transcription Factor 4 (OCT4), Thyroid Stimulating Hormone Receptor (TSHR) and Sodium Iodide Symporter (NIS) mRNA Expression

To understand the DRP1 involvement in other cancer cell mechanisms and to evaluate the impact of a possible therapy with Mdivi-1 and Dabrafenib the OCT4, TSHR and NIS mRNA expression levels after treatment with Mdivi-125 μM, Dabrafenib 2.5 and 10 μM, Mdivi-1 25 μM plus Dabrafenib 2.5, and Mdivi-1 plus Dabrafenib 10 μM were accessed by RQ-PCR, after 72h treatment. Octamer-binding transcription factor 4 (OCT4) is a stem cell marker, related with cells self-renewal capacity, this transcription factor is expressed in thyroid tumours[145]. Moreover, thyroid stimulating hormone receptor (TSHR) and sodium iodide symporter (NIS) demonstrated relevance on radioiodine based treatment[146].

In all cell lines the mRNA levels of OCT4 was altered (Figure 13). Mdivi-1 seems to increase the expression levels of OCT4 in C643 and XTC-1 cell lines (Figures 21B and 21D) and to decrease the levels in 8505C (Figure 21C). For technical reasons, was not possible to access Mdivi-1 effects on TPC1 cell line. On its turn, Dabrafenib decreases the mRNA expression levels in all cell lines (Figure 21). The combination therapy (Mdivi-1 25 μM plus Dabrafenib 2.5 μM) decreases the OCT4 mRNA expression in TPC1 and 8505C cells (Figures 21A and 21C) and increases the mRNA expression in C643 and XTC-1 cells (Figures 21B and 21D).

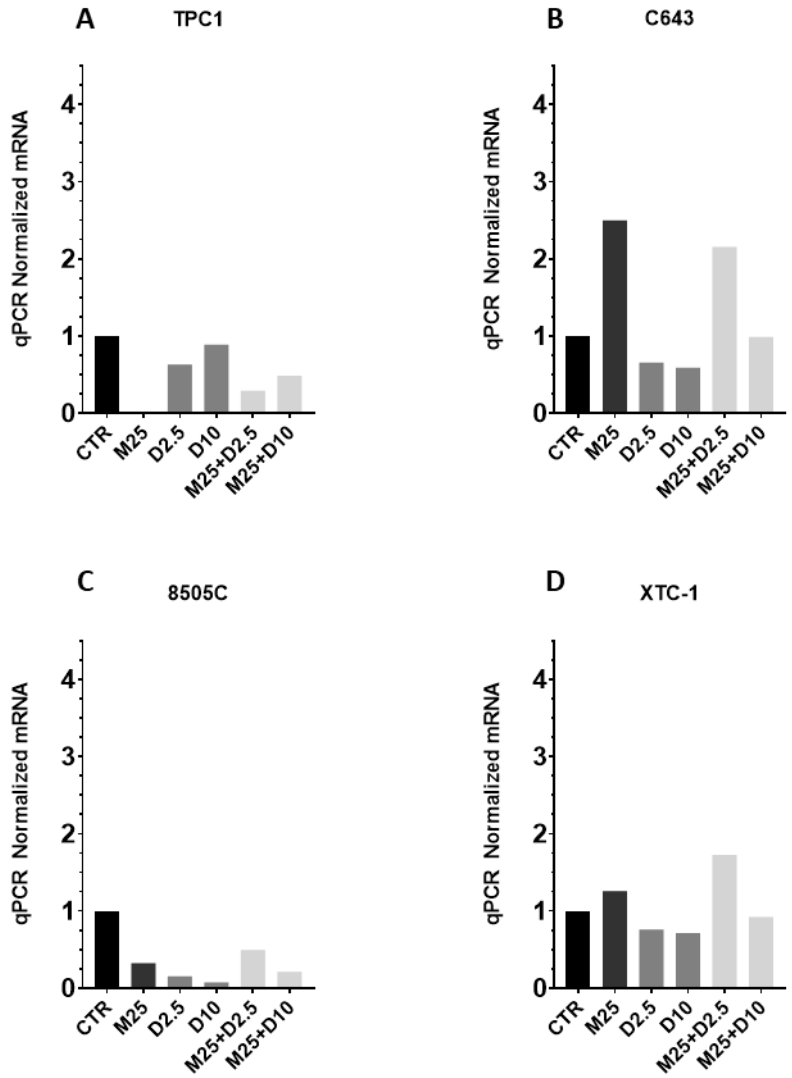

Figure 21: Effects of treatment with Mdivi-1, Dabrafenib and Mdivi-1 and Dabrafenib combinations in Thyroid Cell Lines OCT4 mRNA expression.

Graphic representation, through a bar chart, of OCT4 mRNA level in TPC1 (A), C643 (B), 8505C (C) and XTC-1 (D) cells after treatment with Mdivi-1 (represented as M) – 25 μM -, with Dabrafenib (represented as D) – 2.5 μM and 10 μM– and with Mdivi-1 and Dabrafenib

combinations – Mdivi-1 25 μM plus Dabrafenib 2.5 μM and Mdivi-1 25 μM plus Dabrafenib 10 μM -, during 72h, determined by qPCR analysis. A: TPC1 cell line, was not possible to obtain the values for M25. The control is represented in black bars, the Mdivi-1 treatment is represented in dark gray bars, the Dabrafenib treatments are represented in middle gray bars and the combination treatments are represented in light gray bars. The data are presented as mean ± SD.

Thyroid stimulating hormone receptor (TSHR) and sodium iodide symporter (NIS) mRNA levels were accessed in all cell lines. However, XTC-1 cell line is the only cell line that preserves these thyroid related genes expression[141]. Therefore, TSHR and NIS mRNA expression levels were only obtained for XTC-1 cell line.

In XTC-1 cells, Mdivi-1 and Dabrafenib decrease the thyroid stimulating hormone receptor (TSHR) mRNA expression (Figure 22). Also, the drug combination seems to produce a more accentuated reduction in the expression.

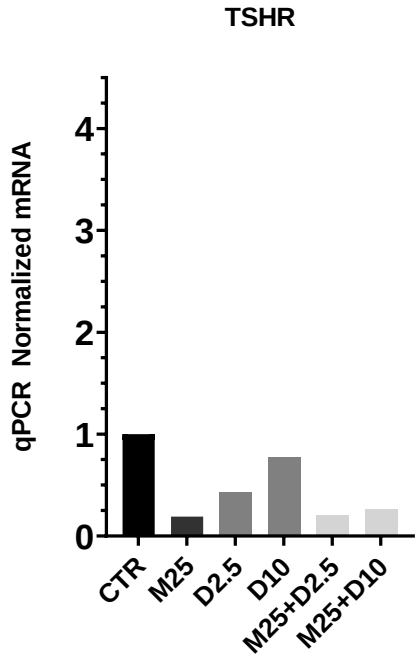

Figure 22: Effects of treatment with Mdivi-1, Dabrafenib and Mdivi-1 and Dabrafenib combinations in XTC-1 cell lines TSHR mRNA expression.

Graphic representation, through a bar chart, of TSHR mRNA level in XTC-1 cells after treatment with Mdivi-1 (represented as M) – 25 μM -, with Dabrafenib (represented as D) – 2.5 μM and 10 μM – and with Mdivi-1 and Dabrafenib combinations – Mdivi-1 25 μM plus Dabrafenib 2.5 μM and Mdivi-1 25 μM plus Dabrafenib 10 μM -, during 72h, determined by qPCR analysis. The control is represented in black bars, the Mdivi-1 treatment is represented in dark gray bars, the Dabrafenib treatments are represented in middle gray

bars and the combination treatments are represented in light gray bars. The data are presented as mean ± SD.

Moreover, in XTC-1 cells the NIS expression was decreased for all treatments except those that included Dabrafenib 10 μM. In those treatments, the expression of this transporter was increased (Figure 23).

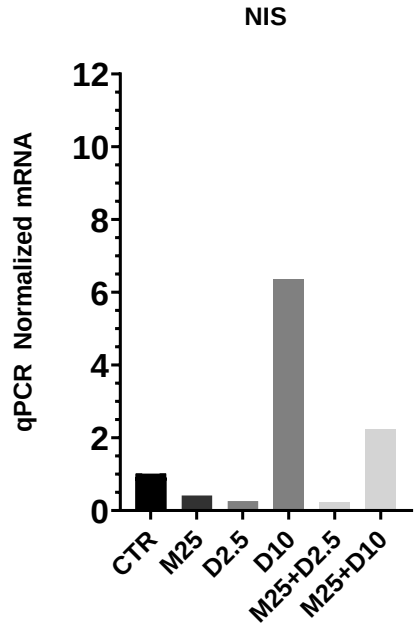

Figure 23: Effects of treatment with Mdivi-1, Dabrafenib and Mdivi-1 and Dabrafenib combinations in XTC-1 cell lines in NIS mRNA expression.
Graphic representation, through a bar chart, of NIS mRNA level in XTC-1 cells after treatment with Mdivi-1 (represented as M) – 25 μM -, with Dabrafenib (represented as D) – 2.5 μM and 10 μM – and with Mdivi-1 and Dabrafenib combinations – Mdivi-1 25 μM plus Dabrafenib 2.5 μM and Mdivi-1 25 μM plus Dabrafenib 10 μM -, during 48h, determined by qPCR analysis. The control (DMSO) is represented in black bars, the Mdivi-1 treatment is represented in dark gray bars, the Dabrafenib treatments are represented in middle gray bars and the combination treatments are represented in light gray bars. The data are presented as mean ± SD.

4.6 Effects of Treatment with Mdivi-1 and Dabrafenib in Thyroid Cell Lines Colony Formation

The invasion and progression of cancer cells are difficult to understand and to control in the disease evolution. Colony formation assay or cologenic assay is an *in vitro* cell survival assay based on the ability of a single cell to grow into a colony.

In all cell lines, Mdivi-1 diminishes the colonic potential of cells, this effect is accentuated after drug combination treatments (Figure 24). Dabrafenib does not seem to have effect in reducing the colonic potential, except in XTC-1 cell line (Figure 24D). 8505C require replicates performance, since cells did not formed colonies even in the control sample, probably the cells did not adhere to the wells.

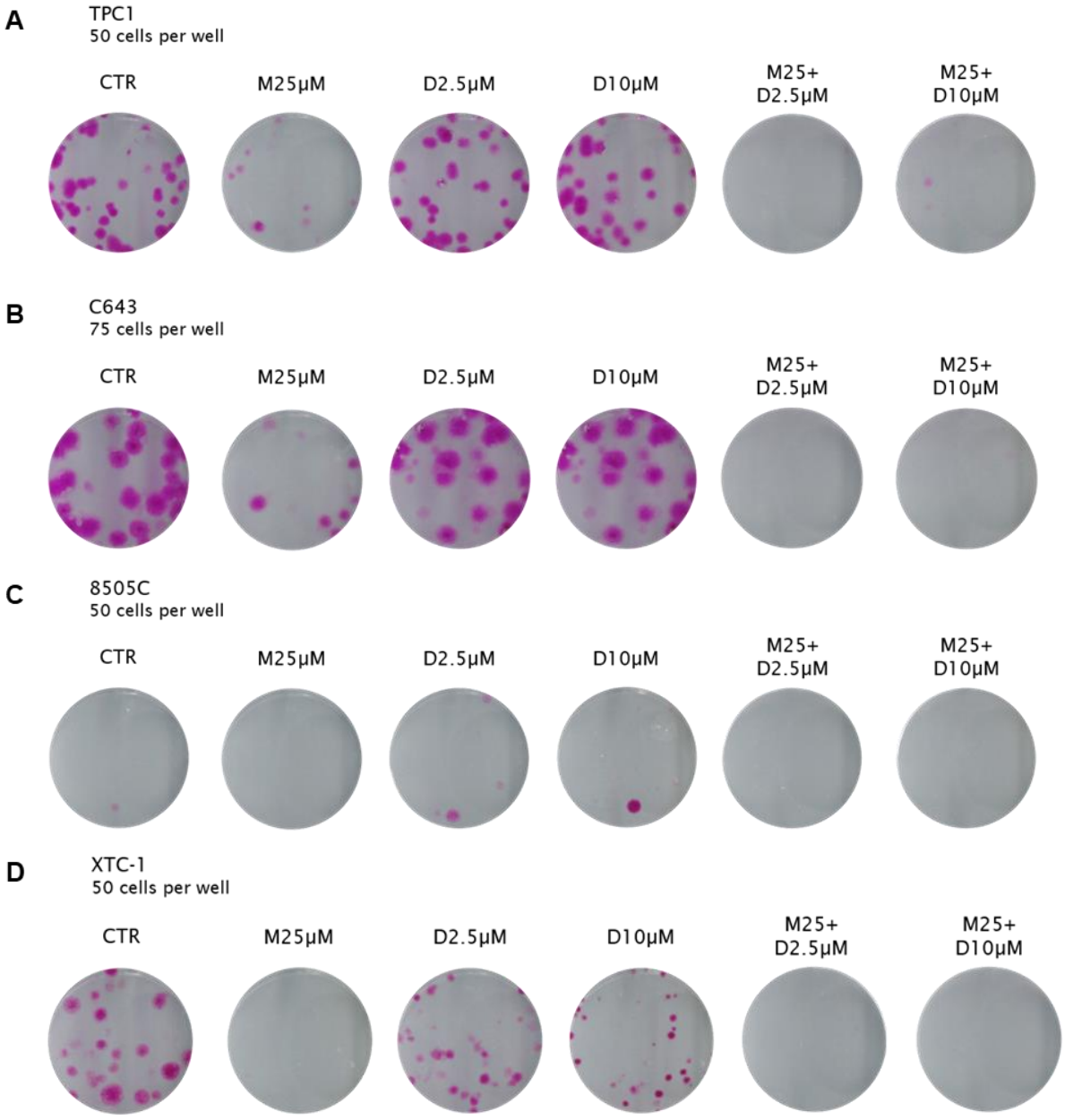

Figure 24: Effects of treatment with Mdivi-1, Dabrafenib and Mdivi-1 and Dabrafenib combinations in thyroid cell lines colony formation.

TPC1 (A), C643 (B), 8505C (C) and XTC-1 (D) cells after treatment with Mdivi-1 (represented as M) – 25 μM -, with Dabrafenib (represented as D) – 2.5 μM and 10 μM – and with Mdivi-1 and Dabrafenib combinations – Mdivi-1 25 μM plus Dabrafenib 2.5 μM and Mdivi-1 25 μM

plus Dabrafenib 10 μM -, during 10 days for TPC1 cell line, and 14, for all other cell lines, in colony assay formation.

Chapter 5: Discussion

Proteins enrolled in mechanisms related with mitochondrial dynamics regulation lead to mitochondria size and quantity adaptation to fulfil cell energetic requirements and facilitate cell division processes. In the last years, mitochondrial dynamics, particularly mitochondrial fission, have been related to cancer initiation and progression[94], however, the role of mitochondrial dynamics proteins in cancer is not yet entirely understood.

DRP1 is overexpressed in several forms of human tumour. Actually, it was demonstrated that in lung and colon cancer models, the inhibition of this fission-related protein reduces the tumour growth potential [123,147]. Moreover, DRP1 inhibition reduced the cancer cell progression in melanoma[148] and the development of metastases in breast cancer[118]. Here, we discuss the potential involvement of DRP1 in thyroid cancer tumorigenesis, also accounting for the role of MAPK pathway, that was previously referred as leading to increased mitochondrial fragmentation[121].

In this work, and in an attempt to prove our hypothesis, we used 2 drugs – Mdivi-1 and Dabrafenib, the drug concentrations used were in accordance to literature reports. Mdivi-1 has been firstly tested in concentrations between 10 and 100 μM[142] demonstrating great efficacy, further studies focused their studies on 12.5, 25 and 50 μM - Mdivi-1 50 μM is the most reported concentration in the literature- [149–151], concentrations that we also found relevant in cell viability assays. On the other side, Dabrafenib has been tested in various concentrations ranging from 3 to 10 μM or from 10 to 100 μM[152,153], as a consequence of literature incoherence, a great range of concentrations was tested on cell viability to uncover those more pertinent for the project purpose. After the Presto Blue cell viability assay, only three concentrations of each drug were selected to perform the following experiments. Mdivi-1 decreased cell viability in a dose-dependent manner. So the DRP1 inhibitor concentrations were selected as the lowest concentration producing effect on cell viability in all cell lines (12.5 μM), the concentration that produced effects in cell viability in all cell lines (25 μM) and the concentration producing major effects - and exceeding IC_{50} - on cell viability in all cell lines (50 μM). Once, Dabrafenib did not decrease cell viability in a dose-dependent manner in all cell lines, the BRAF inhibitor concentrations were selected as the concentration reducing cell viability (2.5 μM) in all cell lines, a highest

concentration not producing effect on cell viability (10 μM) and the concentration reducing, again, the cell viability in all cell lines (15 μM). Moreover, drug combination was added to cell treatments to elucidate the relation between both proteins/pathways. For Western Blot and RQ-PCR analysis, we selected a smaller range of concentrations according to the results obtained in other experiments, to fit the purpose of verify the drug effects on molecular targets and not their activity depending on doses.

Presto Blue cell viability assay results demonstrate that cell viability decreases after pharmacological inhibition of DRP1. However, different cell lines originate different responses. TPC1 cell line, derived from papillary thyroid carcinoma, is the most sensitive to DRP1 and BRAF inhibition. C643 and 8505C have analogous responses to both drugs. Whereas, XTC-1 cell line, which derives from oncocytic metastases, also demonstrates sensitivity to drug activity for cell viability. Inversely to what happens with Mdivi-1, Dabrafenib effect seems not to be dose dependent. There were found no major differences between both time points, highlighting that the drug effects depend more on doses than on exposure time. Also, Mdivi-1 reduces more powerfully cell viability than Dabrafenib, since the lowest doses cause more pronounced effects. This could probably be due to activation of cells mechanisms that could lead to Dabrafenib resistance and ERK activation as: stimulation of tyrosine kinase receptors[154,155], NRAS mutations[156], BRAF, and Raf1 overexpression[157,158], BRAF dimerization not depending on Ras[159] and activating MEK mutations[160,161].

No major differences were found between Presto Blue cell viability assay results and SRB cell viability assay results, indicating that although DRP1 is inhibited the metabolism of cells may not be altered and may truly rely on glycose instead of oxidative phosphorylation. Still, we verify alterations in cell viability, indicating that Mdivi-1 may not only affect DRP1 and mitochondria fragmentation but may also connect with thyroid tumorigenesis signalling pathways.

Even so, the cell viability decrease may not entirely correspond to cell apoptosis, but instead to a less extent of cell growth and division. Cell growth results follow an identical pattern to cell viability results. Again, Mdivi-1 treatment produces effects on cell growth indicating a possible relation with proliferation. The relation between DRP1 and MAPK signalling pathway is reinforced by the

accentuated effects produced by combination treatment compared to the one drug treatment effect. The two-drug treatment may have a cumulative or synergistic effect on thyroid cancer cell growth.

Mdivi-1 and Dabrafenib induce cell programmed death, however the differences found between control cells and treated cells are not significant and do not justify the differences found in cell viability assays. In fact, DRP1 role in cancer cells programmed death is not clear, since its activity has been related with apoptosis activation and inhibition reliant on cancer cells features and on apoptotic stimuli[32,162–166]. Moreover, BRAF is mostly connected to induction of cell growth, division and differentiation[167].

In cell cycle, it was observed that in all cell lines there is an increase of the number of cells in G1 and a reduction of the number of cells in the S phase and in G2, especially after treatment with Dabrafenib. It may lead to cell cycle blockage that prevents cell division and tumour expansion. The cell cycle blockage may also be due to DRP1 inhibition, since the expression of DRP1 is characteristic of cells in G2[168]. It was reported that when DRP1 is inhibited, cells in division do not produce the number of mitochondria required for the energetic needs of new cells[168].

TPC1, C643 and XTC-1 cell lines do not show differences in the expression of proteins of DRP1 and MAPK pathways, after treatment with Mdivi-1 and Dabrafenib alone. Although, the proteins levels are not altered in these cell lines the drugs produce effects on their viability, growth and cell cycle, indicating that both drugs may play a role in proteins activity or actuate trough unspecific mechanisms, as toxicity. All three cell lines were more sensitive to combination treatment. Inversely, 8505C cell line was sensitive to Mdivi-1 and Dabrafenib in what concerns to protein expression levels. Western Blot results must be confirmed, since the experiment was performed only one time and in some cases the tubulin is overexposed.

RQ-PCR results demonstrate that the inhibition of BRAF may reduce the cells stemness potential through inhibition of OCT4 mRNA expression in all cell lines. Further studies must confirm and explore these results. Moreover, Dabrafenib treatment increases the TSHR mRNA expression in XTC-1 cell line. Dabrafenib increases NIS mRNA expression in the XTC-1 cell line. XTC-1 cell line is an HCT cell

line that, as referred before, commonly is not sensitive to radioiodine therapy. Based on our results, HCT patients can benefit of Dabrafenib as a therapeutic approach. Further studies must be conducted to validate or exclude this hypothesis.

Dabrafenib (and Selumetinib, another MPAK signalling pathway inhibitor) have been described as capable of recover radioactive iodine intake *in vivo*[169]. NIS is accountable for thyroid cells iodine intake[170], the increased expression of NIS after Dabrafenib treatment may explain the referred recovery[169]. In 8505C cell line was not possible to access NIS expression, since the NIS mRNA levels were too low. However, XTC-1 cell line increased NIS expression after treatment with Dabrafenib 10 μM. In further experiments, other thyroid cell lines harbouring $BRAF^{V600E}$ mutation (namely BCPAP, KI and WRO cell lines) must be considered for mRNA NIS expression evaluation to access Dabrafenib potential in therapeutics.

Finally, the colony formation assay suggests that the inhibition of DRP1 alone and of DRP1 and BRAF together decrease cells colonic potential, since after treatment these cells can no longer form colonies. These results came in agreement with those obtained for cell growth and for cell cycle.

Cell lines genotypic and molecular profiles can explain, in part, some of our results. TPC1 cell line harbours a RET/PTC1 rearrangement[141], this rearrangement regularly conducts to phosphorylation of numerous residues and consequent activation of signalling pathways that promote cancer progression. MAPK signalling pathway, one of the most relevant pathways in TC, can be activated through the constitutive activity of RET/PTC1. Therefore, TPC1 cell line susceptibility to Dabrafenib can be explained by the drug ability to inhibit MAPK signalling through BRAF inhibition. Nevertheless, in this cell line ERK phosphorylation does not demonstrate major alterations after treatment with Dabrafenib, limiting this hypothesis and suggesting that, probably, Dabrafenib can target unidentified molecular targets. Also, TPC1 sensitivity to Mdivi-1 can be justified by the crosstalk between the MAPK signalling pathway and DRP1. ERK2, a downstream protein of BRAF belonging to MAPK signalling pathway has been described as being responsible for DRP1 phosphorylation on the Serine 616 residue[135]. To confirm this hypothesis a study focusing on DRP1 phosphorylation after Mdivi-1 and Dabrafenib treatment must be performed.

Moreover, C643 and 8505C present mutations on TP53[141]. As recognized the genome guardian arrests cell cycle and induces apoptosis, mutations on this tumour suppressor gene do not initiate these processes and even after MAPK signalling inhibition cells survive and grow. Also, C643 cell line harbours a mutation on HRAS[141] that might contribute to development of resistance mechanisms to Mdivi-1 and Dabrafenib.

8505C cell line is the only cell line, among the studied cell lines, that harbours the $BRAF^{V600E}$, explaining its unique response in protein expression and elucidating the selective activity of Dabrafenib. The high levels of ERK, in this anaplastic cell line, may be an attempt of cells to recover from MAPK signalling inhibition.

Lastly, the low response of XTC-1 cell line can be explained through the cell line origin, this particular cell line was established from a metastases of a Hürthle cell tumour, as referred before Hürthle cell tumours are benign tumours that rarely metastasize, the original tumour should attain much more aggressiveness features than those currently found in clinic. Also, XTC-1 cell line has been described as a cell line with low and inefficient metabolism[171], which can leads to slower incorporation of drugs.

DRP1 function is not only important for mitochondria fragmentation but also to thyroid tumorigenesis, especially for processes related to tumour progression, as the fission protein inhibition prevents cells growth and division. MAPK signalling function is recognized as also promoting cell proliferation, and the direct inhibition of BRAF produced similar effects to those obtained with Mdivi-1 treatments, suggesting that DRP1 and MAPK signalling pathway, particularly BRAF can be are related in thyroid cancer.

Mdivi-1 and Dabrafenib demonstrated some potential as adjuvant therapeutics, to control tumour progression and, in case of Dabrafenib, to overcome some conventional therapies issues, as the low radioiodine intake in oncocytomas. Actuality, Dabrafenib already showed its potential in various clinical trials and in clinics[172,173].

Chapter 6: Conclusion and Future Perspectives

Together, our results indicate that mitochondrial dynamics, particularly mitochondrial fission, control thyroid cancer growth, proliferation and invasion, therefore DRP1 is not only relevant for mitochondrial fragmentation.

Furthermore, DRP1 and MAPK signalling pathway play overlapping roles on TC. However, additional studies are required to better understand how DRP1 and MAPK signalling pathway activity is regulated in the cancer context.

Mdivi-1 and Dabrafenib should be considered for thyroid cancer therapy as additional therapies, especially oncocytomas, a rare and particular form of disease with no personalized treatment.

To improve of our results the number of experiments must be increased. We also aim to address the mitochondrial morphology and the ROS production in order to better understand the role of mitochondrial dynamics, particularly fission, in thyroid cancer; to consider other cell lines (as the already referred BCPAP, KI and WRO cell lines) and more proteins activity (as DRP1^{S616}).

Chapter 7: References

1. Carling T, Udelsman R. Thyroid Cancer. *Annu Rev Med*. 2014;65(1):125-137. doi:10.1146/annurev-med-061512-105739

2. Mullur R, Liu Y-Y, Brent GA. Thyroid Hormone Regulation of Metabolism. *Physiol Rev*. 2014;94(2):355-382. doi:10.1152/physrev.00030.2013

3. F. Bray, J. Ferlay, I. Soerjomataram, R. L. Siegel, L. A. Torre AJ. Global Cancer Statistics 2018: GLOBOCAN Estimates of Incidence and Mortality Worldwide for 36 Cancers in 185 Countries. *Cancer J Clin*. 2018;68:394-424. doi:10.3322/caac.21492

4. Cabanillas ME, McFadden DG, Durante C. Thyroid Cancer. *Lancet*. 2016;388(10061):2783-2795. doi:10.1016/S0140-6736(16)30172-6

5. ABDEL R. OMRAN. The Epidemiologic Transition: A Theory of the Epidemiology of Population Change. *Milbank Q*. 2005;83(4):731-757. doi:10.1111/j.1468-0009.2005.00398.x

6. Zhu C, Zheng T, Kilfoy BA, et al. A birth cohort analysis of the incidence of papillary thyroid cancer in the United States, 1973-2004. *Thyroid Off J Am Thyroid Assoc*. 2009;19(10):1061-1066. doi:10.1089/thy.2008.0342

7. Kitahara CM, Sosa JA. The changing incidence of thyroid cancer. *Nat Rev Endocrinol*. 2016;12(11):646-653. doi:10.1038/nrendo.2016.110

8. G. P, F. F, C. R, S. S, R. V. Worldwide increasing incidence of thyroid cancer: Update on epidemiology and risk factors. *J Cancer Epidemiol*. 2013;2013. doi:10.1155/2013/965212

9. Sipos JA, Mazzaferri EL. Thyroid cancer epidemiology and prognostic variables. *Clin Oncol*. 2010;22(6):395-404. doi:10.1016/j.clon.2010.05.004

10. Peterson E, De P, Nuttall R. BMI, diet and female reproductive factors as risks for thyroid cancer: A systematic review. *PLoS One*.

2012;7(1):1-10. doi:10.1371/journal.pone.0029177

11. Zimmermann MB, Galetti V. Iodine intake as a risk factor for thyroid cancer: A comprehensive review of animal and human studies. *Thyroid Res*. 2015;8(1):1-21. doi:10.1186/s13044-015-0020-8

12. Williams D. Radiation carcinogenesis: Lessons from Chernobyl. *Oncogene*. 2008;27(S2):S9-S18. doi:10.1038/onc.2009.349

13. Iglesias, M. L.; Schmidt, A.; Ghuzlan, A. A.; Lacroix, L.; de Vathaire, F.; Chevillard, S.; Schlumberger M. Radiation Exposure and Thyroid Cancer. *J Clin Endocrinol Metab*. 2017;61(2):180-187. doi:10.1001/jama.1977.03270460075025

14. Kilfoy, B. A.; Devesa, S. S.; Ward, M. H; Zhang, Y.; Rosenberg, P. S.; Holford, T. R.; Andreson WF. Gender is an Age-Specific Effect Modifier for Papillary Cancers of the Thyroid Gland. *Cancer Epidemiol Biomarkers*. 2009;18(4):1092-1100. doi:10.1017/cbo9780511575747.091

15. Feldt-Rasmussen U. Iodine and Cancer. *Thyroid*. 2002;11(5):483-486. doi:10.1089/105072501300176435

16. Haymart MR, Repplinger DJ, Leverson GE, et al. Higher serum thyroid stimulating hormone level in thyroid nodule patients is associated with greater risks of differentiated thyroid cancer and advanced tumor stage. *J Clin Endocrinol Metab*. 2008;93(3):809-814. doi:10.1210/jc.2007-2215

17. Delange F, Lecomte P. Iodine supplementation. Benefits outweigh risks. *Drug Saf*. 2000;22(2):89-95. doi:10.2165/00002018-200022020-00001

18. Ungefroren H, Gieseler F, Fliedner S, Lehnert H. Obesity and cancer. *Horm Mol Biol Clin Investig*. 2015;21(1):5-15. doi:10.1515/hmbci-2014-0046

19. Almquist M, Johansen D, Björge T, et al. Metabolic factors and risk of

thyroid cancer in the Metabolic syndrome and Cancer project (Me-Can). *Cancer Causes Control*. 2011;22(5):743-751. doi:10.1007/s10552-011-9747-2

20. Kloos (Chair) RT, Eng C, Evans DB, et al. Medullary Thyroid Cancer: Management Guidelines of the American Thyroid Association. *Thyroid*. 2009;19(6):565-612. doi:10.1089/thy.2008.0403

21. Cooper DS, Doherty GM, Haugen BR, et al. Revised American Thyroid Association Management Guidelines for Patients with Thyroid Nodules and Differentiated Thyroid Cancer. *Thyroid*. 2009;19(11):1167-1214. doi:10.1089/thy.2009.0110

22. Nikiforov YE, Steward DL, Robinson-Smith TM, et al. Molecular testing for mutations in improving the fine-needle aspiration diagnosis of thyroid nodules. *J Clin Endocrinol Metab*. 2009;94(6):2092-2098. doi:10.1210/jc.2009-0247

23. Xing M. Prognostic Utility of BRAF Mutation in Papillary Thyroid Cancer. *Mol Cell Endocrinol*. 2010;93(0 1):321-386. doi:10.1016/j.neuroimage.2013.08.045.The

24. Xing M, Clark D, Guan H, et al. BRAF mutation testing of thyroid fine-needle aspiration biopsy specimens for preoperative risk stratification in papillary thyroid cancer. *J Clin Oncol*. 2009;27(18):2977-2982. doi:10.1200/JCO.2008.20.1426

25. Xing MM, Alzahrani AS, Carson KA, et al. Association between BRAF V600E mutation and mortality in patients with papillary thyroid cancer. *JAMA - J Am Med Assoc*. 2013;309(14):1493-1501. doi:10.1001/jama.2013.3190

26. Bilimoria KY, Bentrem DJ, Ko CY, et al. Extent of surgery affects survival for papillary thyroid cancer. *Ann Surg*. 2007;246(3):375-381. doi:10.1097/SLA.0b013e31814697d9

27. Shirley LA, Jones NB, Phay JE. The Role of Central Neck Lymph Node Dissection in the Management of Papillary Thyroid Cancer. *Front*

Oncol. 2017;7(June):1-7. doi:10.3389/fonc.2017.00122

28. Sawka AM, Thephamongkhol K, Brouwers M, Thabane L, Browman G, Gerstein HC. A systematic review and metaanalysis of the effectiveness of radioactive iodine remnant ablation for well-differentiated thyroid cancer. *J Clin Endocrinol Metab*. 2004;89(8):3668-3676. doi:10.1210/jc.2003-031167

29. Mallick U, Harmer C, Yap B, et al. Ablation with Low-Dose Radioiodine and Thyrotropin Alfa in Thyroid Cancer. *N Engl J Med*. 2012;366(18):1674-1685. doi:10.1056/NEJMoa1109589

30. Mallick U, Harmer C, Yap B et al. Strategies of Radioiodine Ablation in Patients with Low-Risk Thyroid Cancer. *N Engl J Med*. 2012;85:366-1674. doi:10.1056/NEJMoa1203165

31. Máximo V, Sobrinho-Simões M. Hurthle cell tumours of the thyroid. A review with emphasis on mitochondrial abnormalities with clinical relevance. *Virchows Arch*. 2000;437(2):107-115. doi:10.1007/s004280000219

32. Ferreira-da-Silva A, Valacca C, Rios E, et al. Mitochondrial Dynamics Protein Drp1 is Overexpressed in Oncocytic Thyroid Tumors and Regulates Cancer Cell Migration. *PLoS One*. 2015;10(3):1-17. doi:10.1371/journal.pone.0122308

33. Máximo V, Rios E, Sobrinho-Simões M. Oncocytic lesions of the thyroid, kidney, salivary glands, adrenal cortex, and parathyroid glands. *Int J Surg Pathol*. 2014;22(1):33-36. doi:10.1177/1066896913517938

34. Lloyd, RV; Osamura, RY; Klöppel GRJ. *WHO Classification of Tumours of Endocrine Organs 2017; Vol. 10.*; 2017.

35. Sobrinho-simoes M, Maximo V, Castro IV De, Fonseca E, Soares P, Garcia-rostan G. Hurthle (Oncocytic) Cell Tumors of Thyroid : Etiopathogenesis , Diagnosis and Clinical Significance. 2005;13(1):29-35.

36. Tumors C, Ma V, Soares P, Lima J, Sobrinho-simo M. Mitochondrial DNA Somatic Mutations (Point Mutations and Large Deletions) and Mitochondrial DNA Variants in Human Thyroid Pathology A Study with Emphasis on Hu. 2002;160(5):1857-1865. doi:10.1016/S0002-9440(10)61132-7

37. Malthiery Y, S IEF, Biochimie L De. Defective Mitochondrial ATP Synthesis in Oxyphilic. 2015;86(May):4920-4925.

38. Xiwei Zheng, Cong Bi, Marissa Brooks and DSH. The Genomic Landscape of Renal Oncocytoma Identifies a Metabolic Barrier to Tumorigenesis. *Anal Chem*. 2015;25(4):368-379. doi:10.1016/j.cogdev.2010.08.003.Personal

39. Baris O, Savagner F, Nasser V, et al. Transcriptional Profiling Reveals Coordinated Up-Regulation of Oxidative Metabolism Genes in Thyroid Oncocytic Tumors. *J Clin Endocrinol Metab*. 2004;89(2):994-1005. doi:10.1210/jc.2003-031238

40. Pereira SL, Rodrigues AS, Sousa MI, Correia M, Perestrelo T, Ramalho-Santos J. From gametogenesis and stem cells to cancer: Common metabolic themes. *Hum Reprod Update*. 2014;20(6):924-943. doi:10.1093/humupd/dmu034

41. Ham S, Lee MH, Kim SJ, et al. Dysregulation of Parkin-mediated mitophagy in thyroid Hürthle cell tumors. *Carcinogenesis*. 2015;36(11):1407-1418. doi:10.1093/carcin/bgv122

42. Cavadas B, Pereira JB, Correia M, et al. Genomic and Transcriptomic Characterization of the Mitochondrial-Rich Oncocytic Phenotype on a Thyroid Carcinoma Background. *Mitochondrion*. 2018;(October 2017):0-1. doi:10.1016/j.mito.2018.04.001

43. Máximo V, Soares P, Lima J, Cameselle-Teijeiro J, Sobrinho-Simões M. Mitochondrial DNA Somatic Mutations (Point Mutations and Large Deletions) and Mitochondrial DNA Variants in Human Thyroid Pathology. *Am J Pathol*. 2011;160(5):1857-1865. doi:10.1016/s0002-

9440(10)61132-7

44. Correia M, Pinheiro P, Batista R, Soares P, Sobrinho-Simões M, Máximo V. Etiopathogenesis of Oncocytomas. *Semin Cancer Biol*. 2017;47(June):82-94. doi:10.1016/j.semcancer.2017.06.014

45. Pereira L, Soares P, Máximo V, Samuels DC. Somatic mitochondrial DNA mutations in cancer escape purifying selection and high pathogenicity mutations lead to the oncocytic phenotype : pathogenicity analysis of reported somatic mtDNA mutations in tumors. *BMC Cancer*. 2012;12(1):53. doi:10.1186/1471-2407-12-53

46. Gasparre G, Porcelli AM, Bonora E, et al. Disruptive mitochondrial DNA mutations in complex I subunits are markers of oncocytic phenotype in thyroid tumors. *Proc Natl Acad Sci*. 2007;104(21):9001-9006. doi:10.1073/pnas.0703056104

47. Hanahan, D; Weinberg RA. Hallmarks of Cancer: The Next Generation. *Cell*. 2011;144(1):646-674. doi:10.1016/j.cell.2011.02.013

48. Vu-Phan D, Koenig RJ. Genetics and Epigenetics of Sporadic Thyroid Cancer. *Mol Cell Endocrinol*. 2013;386(1-2):55-66. doi:10.1016/j.mce.2013.07.030

49. Nikiforov YE, Nikiforova MN. Molecular genetics and diagnosis of thyroid cancer. *Nat Rev Endocrinol*. 2011;7(10):569-580. doi:10.1038/nrendo.2011.142

50. Xing M, Alzahrani AS, Carson KA, et al. Association between BRAF V600E mutation and recurrence of papillary thyroid cancer. *J Clin Oncol*. 2015;33(1):42-50. doi:10.1200/JCO.2014.56.8253

51. Hou P, Liu D, Shan Y, et al. Genetic alterations and their relationship in the phosphatidylinositol 3-kinase/Akt pathway in thyroid cancer. *Clin Cancer Res*. 2007;13(4):1161-1170. doi:10.1158/1078-0432.CCR-06-1125

52. Ciampi R, mian caterina, Fugazzola L, et al. Evidence of a Low

Prevalence of Ras Mutations in a Large Medullary Thyroid Cancer Series. *Thyroid*. 2012;23(1):120822105920003. doi:10.1089/thy.2012-0207

53. Romei C, Tacito A, Molinaro E, et al. Twenty years of lesson learning: How does the RET genetic screening test impact the clinical management of medullary thyroid cancer? *Clin Endocrinol (Oxf)*. 2015;82(6):892-899. doi:10.1111/cen.12686

54. Romei C, Cosci B, Renzini G, et al. RET genetic screening of sporadic medullary thyroid cancer (MTC) allows the preclinical diagnosis of unsuspected gene carriers and the identification of a relevant percentage of hidden familial MTC (FMTC). *Clin Endocrinol (Oxf)*. 2011;74(2):241-247. doi:10.1111/j.1365-2265.2010.03900.x

55. Avruch J. Ras Activation of the Raf Kinase: Tyrosine Kinase Recruitment of the MAP Kinase Cascade. *Recent Prog Horm Res*. 2004;56(1):127-156. doi:10.1210/rp.56.1.127

56. Wan PTC, Garnett MJ, Roe SM, et al. Mechanism of activation of the RAF-ERK signaling pathway by oncogenic mutations of B-RAF. *Cell*. 2004;116(6):855-867. doi:10.1016/S0092-8674(04)00215-6

57. Cantwell-Dorris ER, O'Leary JJ, Sheils OM. BRAFV600E: Implications for Carcinogenesis and Molecular Therapy. *Mol Cancer Ther*. 2011;10(3):385-394. doi:10.1158/1535-7163.MCT-10-0799

58. Elisei R, Viola D, Torregrossa L, et al. The BRAFV600E mutation is an independent, poor prognostic factor for the outcome of patients with low-risk intrathyroid papillary thyroid carcinoma: Single-institution results from a large cohort study. *J Clin Endocrinol Metab*. 2012;97(12):4390-4398. doi:10.1210/jc.2012-1775

59. Fernandez IJ, Piccin O, Sciascia S, et al. Clinical significance of braf mutation in thyroid papillary cancer. *Otolaryngol - Head Neck Surg (United States)*. 2013;148(6):919-925. doi:10.1177/0194599813481942

60. Young SJ, Li S, Jung HS, et al. Influence of the BRAF V600E mutation on expression of vascular endothelial growth factor in papillary thyroid cancer. *J Clin Endocrinol Metab*. 2006;91(9):3667-3670. doi:10.1210/jc.2005-2836

61. Kim TH, Park YJ, Lim JA, et al. The association of the BRAF V600E mutation with prognostic factors and poor clinical outcome in papillary thyroid cancer: A meta-analysis. *Cancer*. 2012;118(7):1764-1773. doi:10.1002/cncr.26500

62. Namba H, Nakashima M, Hayashi T, et al. Clinical implication of hot spot BRAF mutation, V599E, in papillary thyroid cancers. *J Clin Endocrinol Metab*. 2003;88(9):4393-4397. doi:10.1210/jc.2003-030305

63. Nikiforova MN, Kimura ET, Gandhi M, et al. BRAF Mutations in Thyroid Tumors Are Restricted to Papillary Carcinomas and Anaplastic or Poorly Differentiated Carcinomas Arising from Papillary Carcinomas. *J Clin Endocrinol Metab*. 2003;88(11):5399-5404. doi:10.1210/jc.2003-030838

64. Xing M, Westra WH, Tufano RP, et al. BRAF mutation predicts a poorer clinical prognosis for papillary thyroid cancer. *J Clin Endocrinol Metab*. 2005;90(12):6373-6379. doi:10.1210/jc.2005-0987

65. Barollo S, Pennelli G, Vianello F, et al. BRAF in primary and recurrent papillary thyroid cancers: The relationship with 131I and 2-[18F]fluoro-2-deoxy-D-glucose uptake ability. *Eur J Endocrinol*. 2010;163(4):659-663. doi:10.1530/EJE-10-0290

66. Durante C, Puxeddu E, Ferretti E, et al. Brief report: BRAF mutations in papillary thyroid carcinomas inhibit genes involved in iodine metabolism. *J Clin Endocrinol Metab*. 2007;92(7):2840-2843. doi:10.1210/jc.2006-2707

67. Riesco-Eizaguirre G, Gutiérrez-Martínez P, García-Cabezas MA, Nistal M, Santisteban P. The oncogene BRAFV600E is associated with a high

risk of recurrence and less differentiated papillary thyroid carcinoma due to the impairment of Na+/I- targeting to the membrane. *Endocr Relat Cancer*. 2006;13(1):257-269. doi:10.1677/erc.1.01119

68. Liu D, Hu S, Hou P, Jiang D, Condouris S, Xing M. Suppression of BRAF/MEK/MAP kinase pathway restores expression of iodide-metabolizing genes in thyroid cells expressing the V600E BRAF mutant. *Clin Cancer Res*. 2007;13(4):1341-1349. doi:10.1158/1078-0432.CCR-06-1753

69. Nucera C, Goldfarb M, Hodin R, Parangi S. Role of B-RafV600Ein differentiated thyroid cancer and preclinical validation of compounds against B-RafV600E. *Biochim Biophys Acta - Rev Cancer*. 2009;1795(2):152-161. doi:10.1016/j.bbcan.2009.01.003

70. Bamford S, Dawson E, Forbes S, et al. The COSMIC (Catalogue of Somatic Mutations in Cancer) database and website. *Br J Cancer*. 2004;91(2):355-358. doi:10.1038/sj.bjc.6601894

71. Namba H, Rubin SA, Fagin JA. Point Mutations of Ras Oncogenes are an Early Event in Thyroid Tumorigenesis. *Mol Endocrinol*. 1990;4(10):1474-1479. doi:10.1210/mend-4-10-1474

72. Volante M, Rapa I, Gandhi M, et al. RAS mutations are the predominant molecular alteration in poorly differentiated thyroid carcinomas and bear prognostic impact. *J Clin Endocrinol Metab*. 2009;94(12):4735-4741. doi:10.1210/jc.2009-1233

73. Marotta V, Guerra A, Sapio MR, Vitale M. RET/PTC rearrangement in benign and malignant thyroid diseases: a clinical standpoint. *Eur J Endocrinol*. 2011;165(4):499-507. doi:10.1530/eje-11-0499

74. Melillo RM, Fusco A, Santoro M, et al. The RET / PTC-RAS-BRAF linear signaling cascade mediates the motile and mitogenic phenotype of thyroid cancer cells Find the latest version : The RET / PTC-RAS-BRAF linear signaling cascade mediates the motile and mitogenic phenotype of thyroid cancer cel. *J Clin Investgation*.

2005;115(April):1068-1081. doi:10.1172/JCI200522758.1068

75. Miyagi E, Braga-Basaria M, Hardy E, et al. Chronic expression of RET/PTC 3 enhances basal and insulin-stimulated PI3 kinase/AKT signaling and increases IRS-2 expression in FRTL-5 thyroid cells. *Mol Carcinog*. 2004;41(2):98-107. doi:10.1002/mc.20042

76. Greco A, Mariani C, Miranda C, et al. The DNA rearrangement that generates the TRK-T3 oncogene involves a novel gene on chromosome 3 whose product has a potential coiled-coil domain. *Mol Cell Biol*. 1995;15(11):6118-6127. doi:10.1128/mcb.15.11.6118

77. Orloff MS, He X, Peterson C, et al. Germline PIK3CA and AKT1 mutations in cowden and cowden-like syndromes. *Am J Hum Genet*. 2013;92(1):76-80. doi:10.1016/j.ajhg.2012.10.021

78. Paes JE, Ringel MD. Dysregulation of the Phosphatidylinositol 3-Kinase Pathway in Thyroid Neoplasia. *Endocrinol Metab Clin North Am*. 2008;37(2):375-387. doi:10.1016/j.ecl.2008.01.001

79. Xing M. Genetic alterations in the phosphatidylinositol-3 kinase/Akt pathway in thyroid cancer. *Thyroid*. 2010;20(7):697-706. doi:10.1089/thy.2010.1646

80. O W. On the origin of cancer cells. *Science (80-)*. 1956;123(3191):309-314.

81. Warburg Berlin-Dahlem O. The Metabolism of Carcinoma Cells. *J Cancer Res*. 1925;9(1):148 LP - 163. doi:10.1158/jcr.1925.148

82. Srinivasan S, Guha M, Kashina A, Avadhani NG. Mitochondrial Dysfunction and Mitochondrial Dynamics-The Cancer Connection. *Biochim Biophys Acta - Bioenerg*. 2017;1858(8):602-614. doi:10.1016/j.bbabio.2017.01.004

83. Máximo, V; Lima, J; Soares, P.; Sobrinho-Simões M. Mitochondria and Cancer. *Virchow Arch*. 2009;454:481-495. doi:10.1016/j.bbabio.2017.01.012

84. Westermann B. Mitochondrial fusion and fission in cell life and death. *Nat Rev Mol Cell Biol*. 2010;11(12):872-884. doi:10.1038/nrm3013

85. Lewis PD, Baxter P, Griffiths AP, Parry JM, Skibinski DOF. Detection of damage to the mitochondrial genome in the oncocytic cells of Warthin's tumour. *J Pathol*. 2000;191(3):274-281. doi:10.1002/1096-9896(2000)9999:9999<::AID-PATH634>3.0.CO;2-U

86. Wallace D. Mitochondrial Disease in Man and Mouse. *Science (80-)*. 1999;283(March):1482-1488.

87. Wallace D. A Mitochondrial Paradigm of Metabolic and Degenerative Diseases, Aging and Cancer. *Annu Rev Genet*. 2005;(39):359. doi:10.1146/annurev.genet.39.110304.095751.A

88. Ferreira A, Romana F, Máximo V, Campello S, Ring M. Mitochondria dynamism : of shape , transport and cell migration. 2014:2313-2324. doi:10.1007/s00018-014-1557-8

89. Tait SWG, Green DR. Mitochondria and cell signalling. *J Cell Sci*. 2012;125(4):807-815. doi:10.1242/jcs.099234

90. Baughman JM, Perocchi F, Girgis HS, et al. Integrative genomics identifies MCU as an essential component of the mitochondrial calcium uniporter. *Nature*. 2011;476(7360):341-345. doi:10.1038/nature10234

91. Stefani D De, Raffaello A, Teardo E, Szabò I, Rizzuto R. A 40 kDa protein of the inner membrane is the mitochondrial calcium uniporter. *Nature*. 2013;476(7360):336-340. doi:10.1038/nature10230.A

92. Pizzo P, Drago I, Filadi R, Pozzan T. Mitochondrial Ca 2+ homeostasis: Mechanism, role, and tissue specificities. *Pflugers Arch Eur J Physiol*. 2012;464(1):3-17. doi:10.1007/s00424-012-1122-y

93. Cárdenas, C.; Miller, R.; Smith, I.; Bui, T.; Molgó, J.; Müler, M.; Vais, H.; Cheung, K.; Yang, J.; Parker, I.; Thompson, C.; Birnbaum, M.;

Hallows, K.; Foskett J. Essential Regulation of Cell Bioenergetics By Constitutive InsP3 Recepetor Ca2+ Transfer to Mitochondria. *Cell*. 2010;142(2):270-283. doi:10.1371/journal.pone.0178059

94. Lima AR, Santos L, Correia M, et al. Dynamin-Related Protein 1 at the Crossroads of Cancer. *Genes (Basel)*. 2018;9(2). doi:10.3390/genes9020115

95. Pelicano H, Xu RH, Du M, et al. Mitochondrial respiration defects in cancer cells cause activation of Akt survival pathway through a redox-mediated mechanism. *J Cell Biol*. 2006;175(6):913-923. doi:10.1083/jcb.200512100

96. Shidara Y, Yamagata K, Kanamori T, et al. Positive contribution of pathogenic mutations in the mitochondrial genome to the promotion of cancer by prevention from apoptosis. *Cancer Res*. 2005;65(5):1655-1663. doi:10.1158/0008-5472.CAN-04-2012

97. Petros, J; Baumann, A; Ruiz-Pesini, E.; Amin, M.; Qi Sun, C.; Hall, J.; Lim, S.; Issa, M.; Flanders, W.; Hosseini, S.; Marshall, F.; Wallace D. mtDNA Mutations Increase Tumorigenecity in Prostate Cancer. *PNAS*. 2005;102(3):719-724.

98. Hsu PP, Sabatini DM. Cancer cell metabolism: Warburg and beyond. *Cell*. 2008;134(5):703-707. doi:10.1016/j.cell.2008.08.021

99. Chang DTW. Mitochondrial trafficking in healthy and injured neurons. 2005:1-15. http://d-scholarship.pitt.edu/10356/.

100. Liesa M, Palacín M, Zorzano A. Mitochondrial Dynamics in Mammalian Health and Disease. *Physiol Rev*. 2009;89(3):799-845. doi:10.1152/physrev.00030.2008

101. Vance JE. Phospholipid Synthesis and Transport in Mammalian Cells. *Traffic*. 2015;16(1):1-18. doi:10.1111/tra.12230

102. Huang, H.; Gao, Q.; Peng, X.; Choi, S.; Sarma, K.; Ren, H.; Morris, A.; Frohman M. piRNA-associated germline nuage formation and

spermatogenesis require MitoPLD pro-fusogenic mitochondrial-surface lipid signaling. *Dev Cell*. 2011;20(3):376-387. doi:10.1371/journal.pone.0178059

103. Youle RJ, Van Der Bliek AM. Mitochondrial Fission, Fusion, and Stress. *Science (80-)*. 2012;337(6098):1062-1065. doi:10.1126/science.1219855

104. Shirihai, O.; Song, M.; Dorn II G. How mitochondrial dynamism orchestrates mitophagy. *Circ Res*. 2015;116(11):1835-1849. doi:10.1002/cncr.27633.Percutaneous

105. Frank M, Duvezin-Caubet S, Koob S, et al. Mitophagy is triggered by mild oxidative stress in a mitochondrial fission dependent manner. *Biochim Biophys Acta - Mol Cell Res*. 2012;1823(12):2297-2310. doi:10.1016/j.bbamcr.2012.08.007

106. Song, M.; Mihara, K.; Chen, Y.; Scorrano, L.; Dorn II G. Mitochondrial fission and fusion factors reciprocally orchestrate mitophagic culling in mouse hearts and cultered fibroblasts. *Cell Metab*. 2015;21(2):273-285. doi:10.1038/mp.2011.182.doi

107. Tondera D. The mitochondrial protein MTP18 contributes to mitochondrial fission in mammalian cells. *J Cell Sci*. 2005;118(14):3049-3059. doi:10.1242/jcs.02415

108. Karbowski M, Jeong SY, Youle RJ. Endophilin B1 is required for the maintenance of mitochondrial morphology. *J Cell Biol*. 2004;166(7):1027-1039. doi:10.1083/jcb.200407046

109. Barneo-Muñoz M, Juárez P, Civera-Tregón A, et al. Lack of GDAP1 Induces Neuronal Calcium and Mitochondrial Defects in a Knockout Mouse Model of Charcot-Marie-Tooth Neuropathy. *PLoS Genet*. 2015;11(4):1-27. doi:10.1371/journal.pgen.1005115

110. Otera H, Wang C, Cleland MM, et al. Mff is an essential factor for mitochondrial recruitment of Drp1 during mitochondrial fission in mammalian cells. *J Cell Biol*. 2010;191(6):1141-1158.

doi:10.1083/jcb.201007152

111. Zhao J, Liu T, Jin S, et al. Human MIEF1 recruits Drp1 to mitochondrial outer membranes and promotes mitochondrial fusion rather than fission. *EMBO J*. 2011;30(14):2762-2778. doi:10.1038/emboj.2011.198

112. Rojo, M.; Legros, F.; Chateau, D.; Lombés A. Membrane Topology and Mitochondrial Targeting of Mitofusins, Ubiquitous Mammalian Homologs of the Transmembrane GTPase Fzo. *J Cell Sci*. 2002;115:1663-1674. doi:10.1111/j.1467-968X.1858.tb01122.x

113. Ishihara N. Mitofusin 1 and 2 play distinct roles in mitochondrial fusion reactions via GTPase activity. *J Cell Sci*. 2004;117(26):6535-6546. doi:10.1242/jcs.01565

114. Hoppins, S.; Edlich, F.; Clealand, M.; Banerjee, S.; McCaffery, J.; Youle, R.; Nunnari J. The soluble form of Bax regulates mitochondrial fusion via MFN2 homotypic complexes. *Mol Cell*. 2011;41(2):150-160. doi:10.1371/journal.pone.0178059

115. de Brito OM, Scorrano L. Mitofusin-2 regulates mitochondrial and endoplasmic reticulum morphology and tethering: The role of Ras. *Mitochondrion*. 2009;9(3):222-226. doi:10.1016/j.mito.2009.02.005

116. Song Z, Chen H, Fiket M, Alexander C, Chan DC. OPA1 processing controls mitochondrial fusion and is regulated by mRNA splicing, membrane potential, and Yme1L. *J Cell Biol*. 2007;178(5):749-755. doi:10.1083/jcb.200704110

117. Campello S, Lacalle RA, Bettella M, Mañes S, Scorrano L, Viola A. Orchestration of lymphocyte chemotaxis by mitochondrial dynamics. *J Exp Med*. 2006;203(13):2879-2886. doi:10.1084/jem.20061877

118. Zhao J, Zhang J, Yu M, et al. Mitochondrial dynamics regulates migration and invasion of breast cancer cells HHS Public Access. *Oncogene*. 2013;32(40):4814-4824. doi:10.1038/onc.2012.494

119. Kageyama, Y.; Zhang, Z.; Sesaki H. Mitochondrial division: molecular machinery and physiological functions. *Curr Opin Cell Biol*. 2011;23(4):427-434. doi:10.1038/mp.2011.182.doi

120. Kitamura S, Yanagi T, Imafuku K, Hata H, Abe R, Shimizu H. Drp1 Regulates Mitochondrial Morphology and Cell Proliferation in Cutaneous Squamous Cell Carcinoma. *J Dermatol Sci*. 2017;88(3):298-307. doi:10.1016/j.jdermsci.2017.08.004

121. Wieder, S; Serasinghe, M.; Sung, J.; Choi, D.; Birge, M.; Yao, J.; Bernstein, E; Celebi, J.; Chipuk J. Activation of the Mitochondrial Fragmentation Protein DRP1 Correlates with BRAFV600E Melanoma. *J Investig Dermatology*. 2015;135(10):2544-2547. doi:10.1016/j.physbeh.2017.03.040

122. Xiwei Zheng, Cong Bi, Marissa Brooks and DSH. Mitochondrial Control by DRP1 in Brain Tumor Initiating Cells. *Anal Chem*. 2015;25(4):368-379. doi:10.1016/j.cogdev.2010.08.003.Personal

123. Ma J-T, Zhang X-Y, Cao R, et al. Effects of Dynamin-related Protein 1 Regulated Mitochondrial Dynamic Changes on Invasion and Metastasis of Lung Cancer Cells. *J Cancer*. 2019;10(17):4045-4053. doi:10.7150/jca.29756

124. Serasinghe MN, Wieder SY, Renault TT, et al. Mitochondrial division is requisite to RAS-induced transformation and targeted by oncogenic MAPK pathway inhibitors. *Mol Cell*. 2015;57(3):521-537. doi:10.1016/j.molcel.2015.01.003

125. Guerra F, Kurelac I, Cormio A, et al. Placing mitochondrial DNA mutations within the progression model of type I endometrial carcinoma. *Hum Mol Genet*. 2011;20(12):2394-2405. doi:10.1093/hmg/ddr146

126. Nakamura N, Kimura Y, Tokuda M, Honda S, Hirose S. MARCH-V is a novel mitofusin 2- and Drp1-binding protein able to change mitochondrial morphology. *EMBO Rep*. 2006;7(10):1019-1022.

doi:10.1038/sj.embor.7400790

127. Yonashiro R, Ishido S, Kyo S, et al. A novel mitochondrial ubiquitin ligase plays a critical role in mitochondrial dynamics. *EMBO J*. 2006;25(15):3618-3626. doi:10.1038/sj.emboj.7601249

128. Karbowski M, Neutzner A, Youle RJ. The mitochondrial E3 ubiquitin ligase MARCH5 is required for Drp1 dependent mitochondrial division. *J Cell Biol*. 2007;178(1):71-84. doi:10.1083/jcb.200611064

129. Qi X, Disatnik M-H, Shen N, Sobel RA, Mochly-Rosen D. Aberrant mitochondrial fission in neurons induced by protein kinase C under oxidative stress conditions in vivo. *Mol Biol Cell*. 2011;22(2):256-265. doi:10.1091/mbc.e10-06-0551

130. Taguchi N, Ishihara N, Jofuku A, Oka T, Mihara K. Mitotic phosphorylation of dynamin-related GTPase Drp1 participates in mitochondrial fission. *J Biol Chem*. 2007;282(15):11521-11529. doi:10.1074/jbc.M607279200

131. Han XJ, Lu YF, Li SA, et al. CaM kinase Iα-induced phosphorylation of Drp1 regulates mitochondrial morphology. *J Cell Biol*. 2008;182(3):573-585. doi:10.1083/jcb.200802164

132. Cribbs JT, Strack S. Reversible phosphorylation of Drp1 by cyclic AMP-dependent protein kinase and calcineurin regulates mitochondrial fission and cell death. *EMBO Rep*. 2007;8(10):939-944. doi:10.1038/sj.embor.7401062

133. Chou CH, Lin CC, Yang MC, et al. GSK3beta-Mediated Drp1 Phosphorylation Induced Elongated Mitochondrial Morphology against Oxidative Stress. *PLoS One*. 2012;7(11). doi:10.1371/journal.pone.0049112

134. Son D, Le NT, Pannacciulli N, et al. Mitochondrial Division is Requisite to RAS-Induced Transformation and Targeted by Oncogenic MAPK Pathway Inhibitors. 2015;86(3):573-579. doi:10.1109/TMI.2012.2196707.Separate

135. Kashatus JA, Nascimento A, Myers LJ, et al. ERK2 Phosphorylation of DRP1 Promotes Mitochondrial Fission and MAPK-Driven Tumor Growth. 2016;57(3):537-551. doi:10.1016/j.molcel.2015.01.002.Erk2

136. Wasiak S, Zunino R, McBride HM. Bax/Bak promote sumoylation of DRP1 and its stable association with mitochondria during apoptotic cell death. *J Cell Biol*. 2007;177(3):439-450. doi:10.1083/jcb.200610042

137. Wang H, Song P, Du L, et al. Parkin Ubiquitinates Drp1 for Proteasome-dependent Degradation. *J Biol Chem*. 2011;286(13):11649-11658. doi:10.1074/jbc.m110.144238

138. Fang L, Hemion C, Goldblum D, et al. Inactivation of MARCH5 Prevents Mitochondrial Fragmentation and Interferes with Cell Death in a Neuronal Cell Model. *PLoS One*. 2012;7(12):1-8. doi:10.1371/journal.pone.0052637

139. Kageyama Y, Hoshijima M, Seo K, et al. Parkin-independent mitophagy requires Drp1 and maintains the integrity of mammalian heart and brain. *EMBO J*. 2014;33(23):2798-2813. doi:10.15252/embj.201488658

140. Harris MH, Thompson CB. The role of the Bcl-2 family in the regulation of outer mitochondrial membrane permeability. *Cell Death Differ*. 2000;7(12):1182-1191. doi:10.1038/sj.cdd.4400781

141. Follicular T, Carcinoma C, Cell D, et al. Molecular and Genotypic Characterization of Human. 2007;17(8).

142. Cassidy-stone A, Chipuk JE, Ingerman E, et al. Chemical Inhibition of the Mitochondrial Divison Dynamin Reveals its Role in Bax/Bak-Depedent Mitochndrial Outer Membrane Permeabilization. 2008;14(2):193-204. doi:10.1016/j.devcel.2007.11.019.Chemical

143. Bordt EA, Clerc P, Roelofs BA, et al. The Putative DRP1 Inhibitor Mdivi-1 is a Reversible Mitochondrial Complex I Inhibitor that Modulates

Reactive Oxygen Species. 2017;40(6):583-594. doi:10.1016/j.devcel.2017.02.020.The

144. Johnson GL, Stuhlmiller TJ, Angus SP, Zawistowski JS, Lee M. Molecular Pathways: Adaptive Kinome Reprogramming in Response to Targeted Inhibition of the BRAF-MEK-ERK Pathway in Cancer. 2015;20(10):2516-2522. doi:10.1158/1078-0432.CCR-13-1081.Molecular

145. Nagayama Y, Shimamura M, Mitsutake N. Cancer stem cells in the thyroid. *Front Endocrinol (Lausanne)*. 2016;7(FEB):1-7. doi:10.3389/fendo.2016.00020

146. Liu T, Men Q, Su X, et al. Downregulated expression of TSHR is associated with distant metastasis in thyroid cancer. *Oncol Lett*. 2017;14(6):7506-7512. doi:10.3892/ol.2017.7122

147. Inoue-Yamauchi A, Oda H. Depletion of mitochondrial fission factor DRP1 causes increased apoptosis in human colon cancer cells. *Biochem Biophys Res Commun*. 2012;421(1):81-85. doi:10.1016/j.bbrc.2012.03.118

148. Dal Yontem F, Kim S-H, Ding Z, Grimm E, Ekmekcioglu S, Akcakaya H. Mitochondrial dynamic alterations regulate melanoma cell progression. *J Cell Biochem*. 2018. doi:10.1002/jcb.27518

149. Manczak M, Kandimalla R, Yin X, Reddy PH. Mitochondrial division inhibitor 1 reduces dynamin-related protein 1 and mitochondrial fission activity. 2019;28(2):177-199. doi:10.1093/hmg/ddy335

150. Akita M, Suzuki-karasaki M, Fujiwara K, Nakagawa C. Mitochondrial division inhibitor-1 induces mitochondrial hyperfusion and sensitizes human cancer cells to TRAIL-induced apoptosis. 2014:1901-1912. doi:10.3892/ijo.2014.2608

151. Wang J, Mirzapoiazova T, Tan YC, Ming K, Pozhitkov A, Wang Y. Inhibiting crosstalk between MET signaling and mitochondrial dynamics and morphology : a novel therapeutic approach for lung

cancer and mesothelioma. *Cancer Biol Ther*. 2018;19(11):1023-1032. doi:10.1080/15384047.2018.1472193

152. Gentilcore G, Madonna G, Mozzillo N, et al. Effect of dabrafenib on melanoma cell lines harbouring the BRAFV600D/Rmutations. *BMC Cancer*. 2013;13(1):1. doi:10.1186/1471-2407-13-17

153. Kurata K, Onoda N, Noda S, et al. Growth arrest by activated BRAF and MEK inhibition in human anaplastic thyroid cancer cells. *Int J Oncol*. 2016;49(6):2303-2308. doi:10.3892/ijo.2016.3723

154. Villanueva J, Vultur A, Lee JT, et al. Acquired resistance to BRAF inhibitors mediated by a RAF kinase switch in melanoma can be overcome by co-targeting MEK and IGF-1R/PI3K. 2011;18(6):683-695. doi:10.1016/j.ccr.2010.11.023.Acquired

155. Girotti MR, Pedersen M, Sanchez-Laorden B, et al. Inhibiting EGF receptor or SRC family kinase signaling overcomes BRAF inhibitor resistance in melanoma. *Cancer Discov*. 2013;3(2):158-167. doi:10.1158/2159-8290.CD-12-0386

156. Nazarian R, Shi H, Wang Q, et al. Melanomas acquire resistance to B-RAF(V600E) inhibition by RTK or N-RAS upregulation. 2011;468(7326):973-977. doi:10.1038/nature09626.Melanomas

157. Shi, H.; Moriceu, G.; Kong, X.; Lee, M.; Lee, H.; Koya, R.; Ng, C.; Chodon, T.; Scolyer, R.; Dahlman, K.; Sosman, J.; Kefford, R.; Long, G.; Nelson S.; Ribas, A.; Lo R. Melanoma whole exome sequencing identifies V600E B-RAF amplification-mediated acquired B-RAF inhibitor resistance. *Physiol Behav*. 2017;176(5):139-148. doi:10.1016/j.physbeh.2017.03.040

158. Montagut C, Sharma S V, Shioda T, et al. Elevated CRAF as a potential mechanism of acquired resistance to BRAF inhibition in melanoma. 2008;68(12):4853-4861. doi:10.1158/0008-5472.CAN-07-6787.Elevated

159. Poulikakos PI, Persaud Y, Janakiraman M, et al. RAF inhibitor

resistance is mediated by dimerization of aberrantly spliced BRAF(V600E). 2012;480(7377):387-390. doi:10.1038/nature10662.RAF

160. Wagle N, Emery C, Berger MF, et al. Dissecting therapeutic resistance to RAF inhibition in melanoma by tumor genomic profiling. *J Clin Oncol*. 2011;29(22):3085-3096. doi:10.1200/JCO.2010.33.2312

161. Shi, H.; Moriceau, G.; Kong, X.; Koya, R.; Nazarian, R.; Pupo, G.; Bacchiocchi, A.; Dahlman, K.; Chmielowski, B.; Sosman, J.; Halaban, R.; Kefford, R.; Long, G.; Ribas, A.; Lo R. Preexisting MEK1 Exon 3 Mutations in V600E/K BRAF Melanomas Do Not Confer Resistance to BRAF Inhibitors. *Bone*. 2013;23(1):1-7. doi:10.1038/jid.2014.371

162. Suen, D.; Norris, K.; Youle R. Mitochondrial Dynamics and Apoptosis. *Genes Dev*. 2008;22:1577-1590. doi:10.1101/gad.1658508.GENES

163. Frank S, Gaume B, Bergmann-Leitner ES, et al. The Role of Dynamin-Related Protein 1, a Mediator of Mitochondrial Fission, in Apoptosis. *Dev Cell*. 2001;1(4):515-525. doi:10.1016/S1534-5807(01)00055-7

164. Estaquier J, Arnoult D. Inhibiting Drp1-mediated mitochondrial fission selectively prevents the release of cytochrome c during apoptosis. *Cell Death Differ*. 2007;14(6):1086-1094. doi:10.1038/sj.cdd.4402107

165. Sheridan C, Delivani P, Cullen SP, Martin SJ. Bax- or Bak-Induced Mitochondrial Fission Can Be Uncoupled from Cytochrome c Release. *Mol Cell*. 2008;31(4):570-585. doi:10.1016/j.molcel.2008.08.002

166. Lee, Y.; Jeong, S.; Karbowski, M.; Smith, C.; Youle R. Roles of the Mammalian Mitochondrial Fission and Fusion Mediators Fis1, Drp1, and Opa1 in Apoptosis. *Mol Biol Cell*. 2004;15:5001-5011. doi:10.1091/mbc.E04

167. Hong S, Hong S. Overcoming Metastatic Melanoma with BRAF Inhibitors. 2011;34(5):699-701. doi:10.1007/s12272-011-0521-5

168. Mishra P CD. Mitochondrial Dynamics and Inheritance During Cell Division, Development and Disease. *Mol Biol*. 2014;15(10):643-646. doi:10.1038/embor.2009.147

169. Rothenberg SM, McFadden DG, Palmer EL, Daniels GH, Wirth LJ. Redifferentiation of iodine-refractory BRAF V600E-mutant metastatic papillary thyroid cancer with dabrafenib. *Clin Cancer Res*. 2015;21(5):1028-1035. doi:10.1158/1078-0432.CCR-14-2915

170. Tavares C, Coelho MJ, Eloy C, et al. NIS expression in thyroid tumors, relation with prognosis clinicopathological and molecular features. *Endocr Connect*. 2018;7(1):78-90. doi:10.1530/EC-17-0302

171. Stankov K, Biondi A, Aurelio MD, et al. Mitochondrial Activities of a Cell Line Derived from Thyroid Hürthle Cell Tumors. 2006;16(4).

172. Subbiah V, Kreitman RJ, Wainberg ZA, et al. Dabrafenib and Trametinib Treatment in Patients With Locally Advanced or Metastatic *BRAF* V600–Mutant Anaplastic Thyroid Cancer. *J Clin Oncol*. 2017;36(1):JCO.2017.73.678. doi:10.1200/JCO.2017.73.6785

173. Food US, Spring S, Food US. FDA Approval Summary : Dabrafenib and Trametinib for the Treatment of Metastatic Non-Small Cell Lung Cancers Harboring BRAF V600E Mutations. 2018:740-745. doi:10.1634/theoncologist.2017-0642

Chapter 8: Supplementary Data

8.1 Effects of Mdivi-1 and Dabrafenib on Thyroid Cell Lines on Cell Viability by Sulfohordamine B Assay

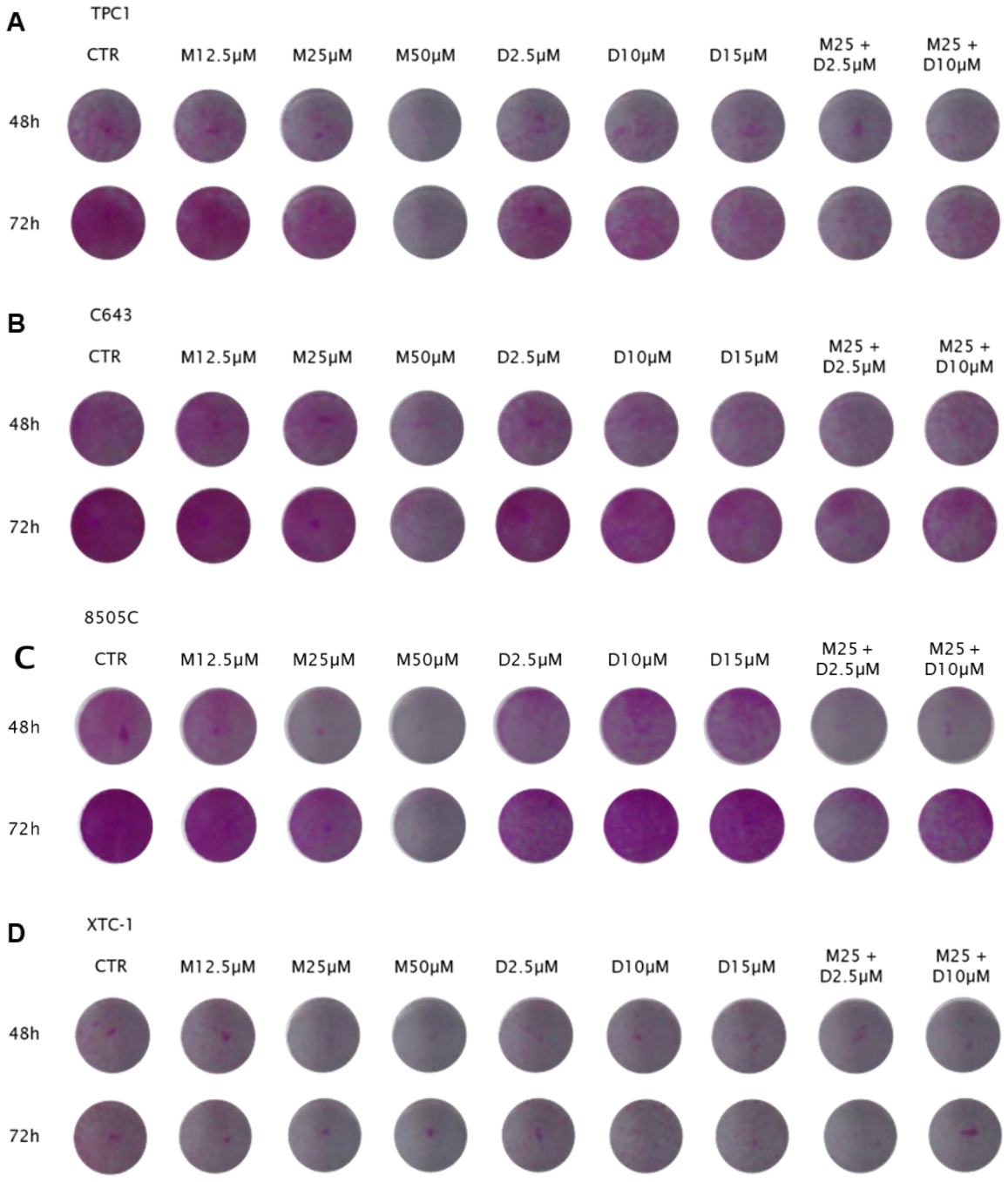

Figure 25: Effects of treatment with Mdivi-1, Dabrafenib and Mdivi-1 and Dabrafenib combinations in thyroid cell lines viability, SRB assay images.

TPC1 (A), C643 (B), 8505C (C) and XTC-1 (D) cells after treatment with Mdivi-1 (represented as M) – 12.5 μM, 25 μM and 50 μM -, with Dabrafenib (represented as D) – 2.5 μM, 10 μM and 15 μM – and with Mdivi-1 and Dabrafenib combinations – Mdivi-1 25 μM plus Dabrafenib 2.5 μM and Mdivi-1 25 μM plus Dabrafenib 10 μM -, during 48h and 72h, in the

Sulforhodamine B assay. The resulting images were obtained by a Xerox Scan, Versa Link C405 (Xerox, Norwalk, Connecticut, USA).

8.2 Effects of Mdivi-1 and Dabrafenib on Thyroid Cell Lines Cell Cycle

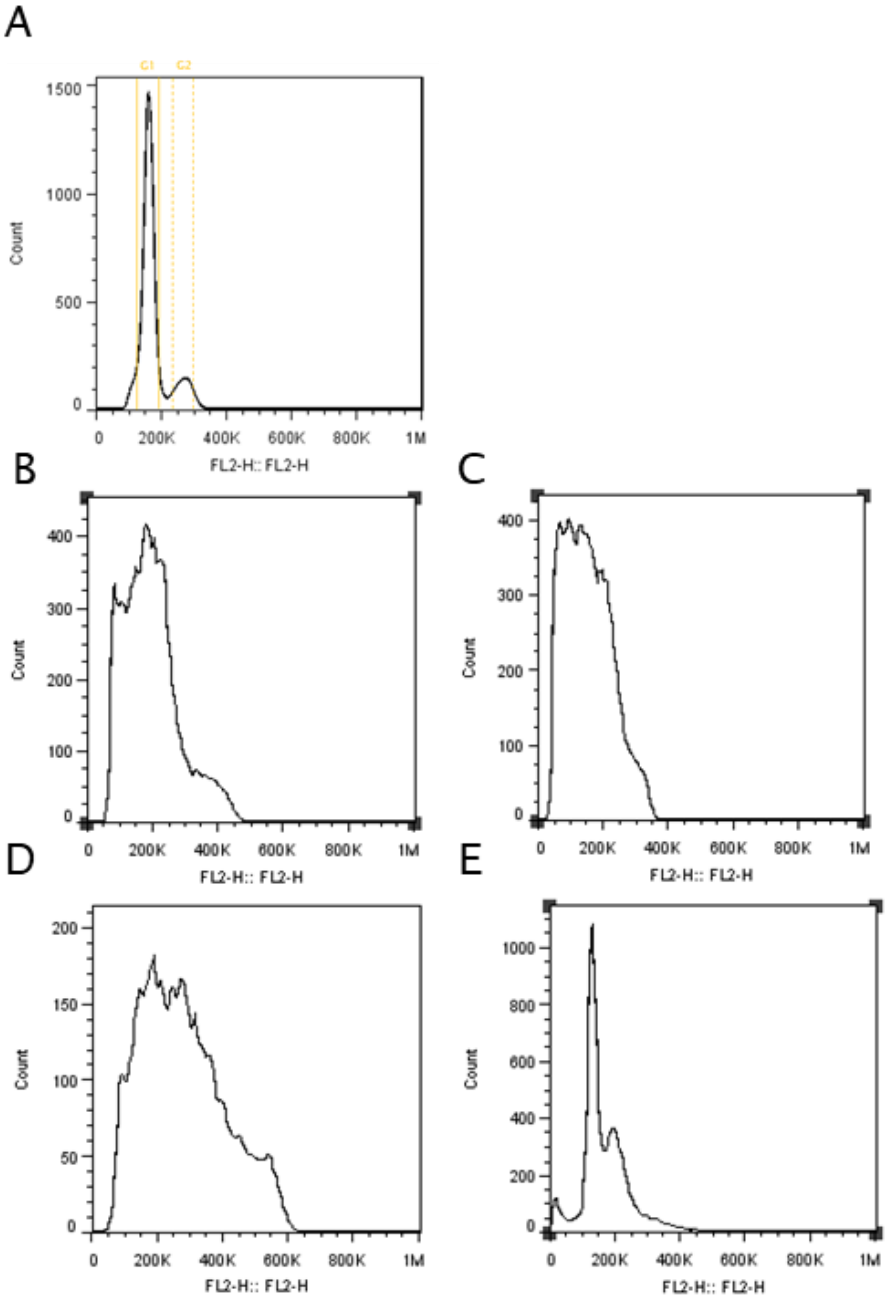

Figure 26: Effects of treatment with Mdivi-1, Dabrafenib and Mdivi-1 and Dabrafenib combinations in thyroid cell lines cell cycle (72h treatment).

Control (CTR) – DMSO example (A), TPC1 (B), C643 (C), 8505C (D) and XTC-1 (E) cell lines after treatment with Mdivi-1 50 μM, during 72h.

8.3 Effects of Mdivi-1 and Dabrafenib on Thyroid Cell Lines Colony Formation

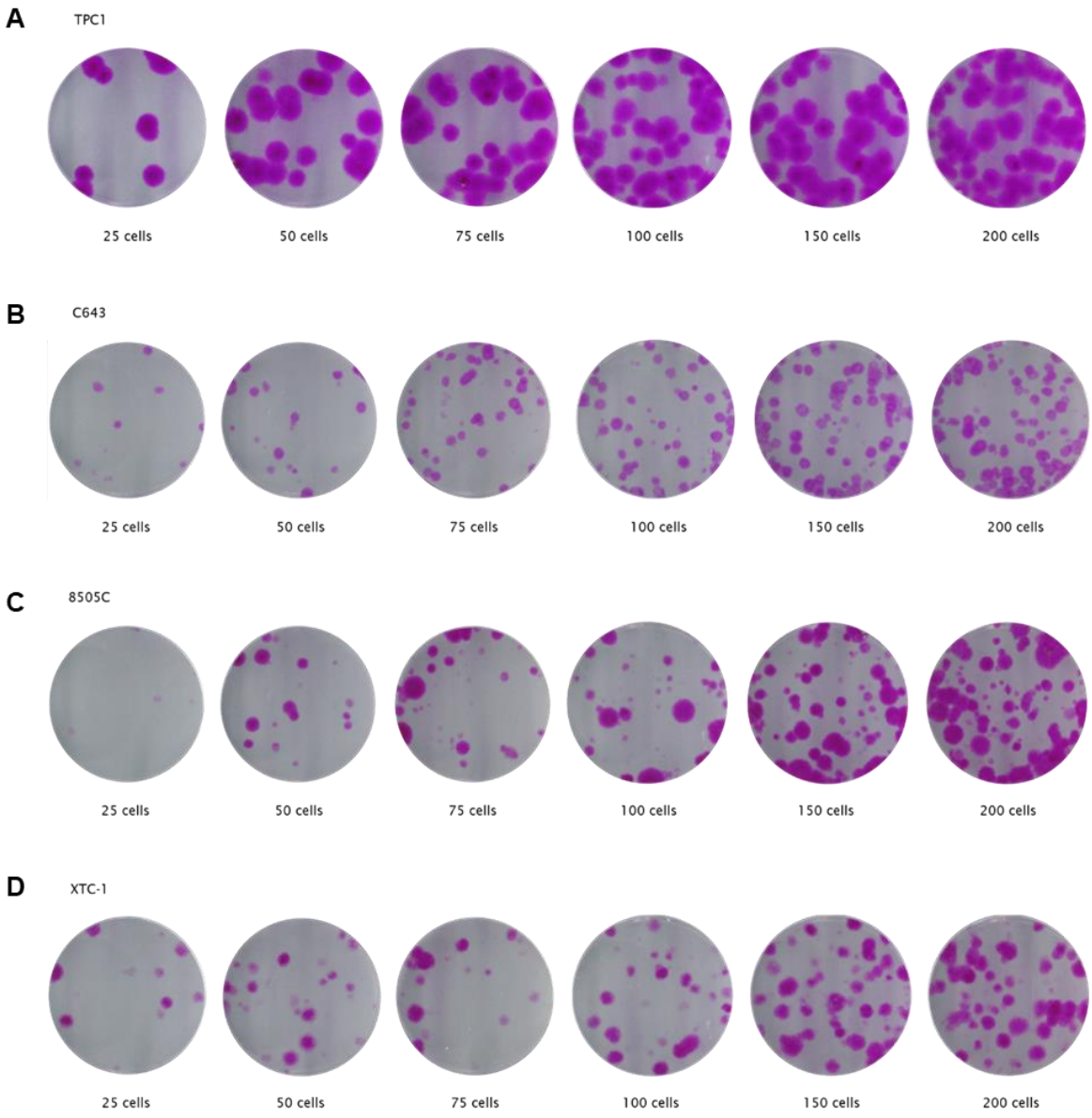

Figure 27: Thyroid cell lines colony assay formation.

TPC1 (A), C643 (B), 8505C (C) and XTC-1 (D) cells growing with no treatment, during 14 days in colony assay formation. The resulting images were obtained by a Xerox Scan, Versa Link C405 (Xerox, Norwalk, Connecticut, USA).